universität wien

MASTERARBEIT

Titel der Masterarbeit

Investigation of the N-terminal domain of the vaccinia virus protein A46

verfasst von

Katharina Radakovics, BSc

angestrebter akademischer Grad

Master of Science (MSc)

Wien, 2015

Studienkennzahl lt. Studienblatt:	A 066 830
Studienrichtung lt. Studienblatt:	Masterstudium Molekulare Mikrobiologie und Immunbiologie
Betreut von:	Ao. Univ.-Prof. Dr. Timothy Skern

Acknowledgements

First of all, I want to thank my supervisor Tim Skern for giving me the chance to work on this interesting project and for always encouraging me to believe in myself.
Moreover, I thank Sofiya Fedosyuk for sharing her knowledge of and experience in protein expression and purification with me, for teaching me new techniques and for patiently answering all of my questions.
Many thanks also to my colleague Martina Aumayr for her advice and help with any problems that occurred in the course of my project.

In addition, I am grateful that I had the chance to participate in the GEN-AU summer school. I want to thank J. Andrew Pospisilik, the supervisor of my first internship, for giving me the opportunity to gain insights into the life of a researcher. The experiences I have made during those three weeks have aroused my wish to become a molecular biologist.

Special thanks goes to my parents for the endless support they are giving me, for encouraging me to do what makes me happy and for believing in me.
Thanks also to my friends: Thank you for listening to my work-related and –unrelated problems, for studying together and for always being there when I need you. I would have never come that far without you.
Last but not least, thanks to Patrick Ranz for transforming my scribbles into a beautiful individualized graph of TLR signaling and for changing and optimizing it until it was exactly what I have wanted. Thank you for your patience.

Table of contents

Abstract

Vaccinia virus (VACV), a member of the *Orthopoxviridae*, was used as vaccine in the worldwide campaign against smallpox, a disease caused by the closely related variola virus. VACV is a large virus with a linear double-stranded DNA genome and an exclusively cytoplasmic life cycle. Eukaryotes have developed several mechanisms to detect invading viruses and to prevent their successful replication and spread. One of the most important signaling pathways of the innate immune system is mediated by Toll-like receptors (TRLs). These receptors detect pathogen-associated molecular patterns and activate a phosphorylation cascade that leads to the activation of transcription factors, for example NF-κB and interferon regulatory factors. The transcription factors induce the expression of, among others, pro-inflammatory signaling molecules and protein kinase R to establish an antiviral state. However, during the co-evolution with their hosts, viruses have developed strategies to evade the host immune responses. Therefore, VACV codes not only for several enzymes involved in genome transcription and replication, but also for a wide range of immune evasion proteins. One of these proteins is A46, an inhibitor of TLR-mediated signaling pathways. A46 binds to the TIR domains of TLR adapter proteins and prevents the activation of the phosphorylation cascade. The structure of the C-terminal part of A46 has been solved and it was shown that it is sufficient for the binding of TLR adapter proteins. In contrast, little is known about the structure and function of the N-terminal part (residues 1 to 90) of A46. Therefore, one aim of my Master's thesis was to further investigate this domain. I expressed and purified A46(6M1-T83), covering the amino acids M1 to T83. Using SEC-MALLS, I showed that under different conditions this domain can form trimers as well as tetramers. The N-terminal part of A46 might, therefore, facilitate oligomerization of the full-length protein. In addition, I used microscale thermophoresis to quantify the interaction between A46(6M1-T83) and TLR adapter proteins. A46(6M1-T83) binds MyD88, but neither MAL nor TRAM. Therefore, the N-terminal domain appears to add specificity to the interaction of A46 with its biologic target proteins. Another aim of this thesis was to investigate whether an intact BB loop in the TLR adapter protein TRAM is necessary for the interaction with A46. I constructed mutant TRAM proteins with one or three mutations in their BB loops and tested whether the mutant proteins interacted with A46 by microscale thermophoresis. In contrast to the findings of Stack & Bowie (2012), I observed an interaction between A46 and the single mutants TRAM F112A and P116H, as well as the triple mutant TRAM F112A P116H C117H.

Zusammenfassung

Vaccinia Virus (VACV), ein Mitglied der Familie *Orthopoxviridae*, wurde als Impfstoff während der weltweiten Kampagne zur Ausrottung der Pocken verwendet. Die Pocken sind eine gefährliche Krankheit, die durch das nah verwandte Variola Virus ausgelöst wird. VACV ist ein großes Virus mit einem Genom aus doppelsträngiger DNA und einem vollständig cytoplasmatischen Lebenslauf. Höhere Eukaryoten können eindringende Viren durch verschiedenste Mechanismen erkennen und deren Replikation und Ausbreitung verhindern. Einer der wichtigsten Signalwege des angeborenen Immunsystems basiert auf Toll-ähnlichen Rezeptoren (TLRs). Diese erkennen Pathogen-assoziierte molekulare Muster und aktivieren eine Phosphorylierungs-Kaskade, die zur Aktivierung von Transkriptionsfaktoren, zum Beispiel NF-κB, führt. Diese induzieren die Expression von, unter anderem, pro-inflammatorischen Signalmolekülen und Protein Kinase R um die Zelle in einen antiviralen Zustand zu versetzen. Allerdings entwickelten Viren im Laufe der Co-Evolution Strategien, um die Immunabwehr ihrer Wirte zu umgehen. Auch VACV codiert nicht nur für Enzyme zur Replikation und Transkription des viralen Genoms, sondern auch für eine Vielzahl an immunsupprimierenden Proteinen. Eines davon ist A46, welches die Signalübertragung von TLRs verhindert. A46 bindet die TIR-Domänen von TLR-Adapterproteinen und verhindert dadurch die Aktivierung der Phosphorylierungs-Kaskade. Die Struktur des C-terminalen Teils von A46 wurde bereits entschlüsselt. Außerdem wurde gezeigt, dass diese Domäne für die Interaktion mit den Adapterproteinen ausreicht. Im Gegensatz dazu ist erst wenig über die Funktion der N-terminalen 90 Aminosäuren von A46 bekannt. Daher war das Ziel meiner Masterarbeit, diesen Teil des Proteins zu untersuchen. Ich exprimierte und isolierte das Protein A46(6M1-T83), welches die Aminosäuren M1 bis T83 von A46 umfasst. Mittels SEC-MALLS zeigte ich, dass A46(6M1-T83), abhängig von den Bedingungen, sowohl Trimere als auch Tetramere bilden kann. Eine Funktion der N-terminalen Domäne könnte daher sein, die Oligomerisierung von A46 zu ermöglichen. Außerdem verwendete ich MST, um die Interaktion zwischen A46(6M1-T83) und TLR-Adapterproteinen zu quantifizieren. A46(6M1-T83) bindet MyD88, aber weder MAL noch TRAM. Die N-terminale Domäne von A46 scheint also für Spezifität in der Interaktion mit biologischen Bindungspartnern zu sorgen. Ein weiteres Ziel dieser Arbeit war, zu untersuchen, ob ein intaker BB-Loop im TLR-Adapterprotein TRAM für die Bindung an A46 notwendig ist. Ich konstruierte Varianten von TRAM mit einer oder drei Mutationen im BB-Loop. Im Gegensatz zu den Resultaten von Stack & Bowie (2012) beobachtete ich trotz der Mutationen eine Interaktion mit A46.

1 Introduction

Smallpox was a devastating disease that emerged in Asia in the 1st century AD and was endemic in most countries from the late 18th to the early 20th century. A worldwide vaccination campaign resulted in the eradication of smallpox in 1979. The vaccine consisted of live vaccinia virus (VACV), a close relative to the smallpox-causing variola virus (VARV). Much remains to be learned about VARV. However, research on VARV itself is possible in only two institutions. Therefore, most research on the family of *Orthopoxviridae* to which VARV and VACV belong is performed on the latter (Fenner et al., 1988; Moss, 2001). In this introduction, I will highlight the significance of research on VACV and subsequently summarize the VACV life cycle, some of the most important innate immune signaling pathways of animals and the mechanisms VACV has evolved to evade them.

1.1 Significance of Research on Vaccinia Virus

VACV is a close relative of the smallpox-causing variola virus (VARV). Therefore, immunization with VACV causes cross-immunity against VARV. Despite its eradication in 1979, VARV might still be a threat for humanity, due to its potential as bioterroristic agent. The origin of VARV is uncertain. One theory is that it co-evolved with humans from an ancestor that infected the ancestors of humans without causing a disease as severe as smallpox until about 3000 years ago. An alternative theory is the evolution from a closely related orthopox-species, for example monkeypox virus. If the latter is the case, a virus with similar characteristics as VARV could emerge again. Smallpox was characterized by fever as the first symptom, occurring after an incubation time of usually ten to fourteen days. The fever was often accompanied by a headache and vomiting and followed by a serious rash one to four days later. The rash first appeared in the respiratory tract, for example on the tongue, and the face and covered the whole body shortly after. The mortality of the disease was about 30 %, although there were geographical differences and also differences between distinct outbreaks. In survivors, the rash healed out after about three weeks, but permanent facial pockmarks were seen in about 65 to 80 %. Although rare, encephalitis and blindness were also complications associated with smallpox (Fenner et al., 1988). Due to its high transmissibility and mortality, VARV would cause a serious threat if it is re-introduced by bioterrorists. Moreover, after smallpox had been declared eradicated, vaccination was stopped. This renders a high percentage of the current world population susceptible to the

virus (Mahy, 2003). Stocks of the live VACV used during the WHO eradication campaign as vaccine are stored to be immediately availaible if VARV is re-introduced. However, the original vaccine caused rare but serious complications, for example encephalomyelitis. Therefore, it is important to better understand the immune reactions it elicits and to develop safer vaccines, such as NYVAC, which was created by the specific deletion of open reading frames from VACV of the Copenhagen strain (Fenner et al., 1988; Mahy et al., 2003; Tartaglia et al., 1992).

In addition, VACV cannot only be used as vaccine against VARV, but also as anti-tumour vaccine or as recombinant vaccine against pathogens other than VARV (Verardi et al. 2012). Even the highly attenuated modified vaccinia virus Ankara (MVA) strain that cannot replicate in most mammalian hosts is able to express recombinant proteins in human cells (Sutter & Moss, 1992).

An example for an MVA-based anti-tumour vaccine is TroVax, which codes for the tumour antigen 5T4. 5T4 is a glycoprotein with similar characteristics in humans and mice. It is hardly expressed by normal cells but upregulated in several cancers (Hole & Stern, 1988; Woods et al., 2002). Vaccination of mice with MVA coding for human 5T4 inhibited the growth of human-derived tumour cells expressing 5T4 (Mulryan et al., 2002). First clinical trials showed that Trovax induces antibody formation against the tumour antigen with associated prolonged survival (Harrop et al., 2006). However, although no adverse effects have been reported, only a subgroup of patients seems to benefit from TroVax (Kim et al., 2010). Moreover, immune evasion or suppression caused by regulatory T cells was shown to dampen the efficacy of TroVax (Elkord et al., 2009).

Vaccination against, for example, influenza virus (Kreijtz et al., 2007; Smith et al., 1983b), malaria (Smith et al., 1984), herpes simplex virus (Paoletti et al., 1984) or hepatitis B virus (Paoletti et al., 1984; Smith et al., 1983a) using recombinant MVA expressing according antigens has also shown promising results in rodents and even chimpanzees in the case of hepatits B virus (Moss et al., 1984). Trials in humans with an MVA-based vaccine against *Mycobacterium tuberculosis* showed at least a boost of pre-existing immunity (McShane et al., 2004). Moreover, the efficacy of plasmid DNA vaccines can be enhanced by simultaneous infection with recombinant MVA coding for the same protein as the plasmid (McConkey et al., 2003).

In summary, VACV can be of great use for the human population and it is therefore desirable to learn more about this virus.

1.2 Introduction to Vaccinia Virus

VACV is the best characterized member of the orthopoxviruses, one of the nine genera of the sub-family *Chordopoxvirinae* in the family *Chordopoxviridae* (King et al., 2011; Moss, 2001). It was used as vaccine against the closely related smallpox-causing VARV in the WHO eradication program (World Health Organization, 1980). In the late 19th century, Edward Jenner introduced vaccination against smallpox with samples from pox lesions on bovine or human skin (Riedel, 2005; Willis, 1997). Subsequently, many natural scientists were interested in the nature of the agent providing immunity. Soon, they found out that not bacteria, but smaller particles, later identified to be VACV, are responsible for the development of pox lesions (Negri, 1906).

1.2.1 Vaccinia Virus Structure

VACV is, with a cross section of about 350 x 270 nm, one of the biggest animal viruses and thus visible by light microscopy (Dubochet et al., 1994; Moss, 2001). The VACV genome consists of a double stranded (ds), linear DNA with inverted terminal repeats and hairpin loops at each end that covalently link the two strands (Garon et al., 1978; Geshelin & Berns, 1974; Wittek et al., 1978). The whole genome sequences of several VACV strains are available. The VACV genome is about 190 kbp long and encodes more than 200 possible open reading frames (Goebel et al., 1990; Zhang et al., 2013). The DNA is associated with proteins and packaged into a brick-shaped core containing 75 (Chung et al., 2006) to 80 (Resch et al., 2007) VACV proteins and more than 20 host proteins (Chung et al., 2006; Resch et al., 2007). The nucleoprotein core and two attached proteinaceous lateral bodies are coated by a 20 – 40 nm thick layer of proteins (see Fig. 1) (Kuznetsov, et al., 2008; Moss, 2001).

Despite the size and early discovery of VACV, the number of membranes surrounding the core and two lateral bodies as well as their origin are still under debate. Some authors report a single membrane that might be synthesized de *novo* (Carter et al., 2005; Dales & Mosbach, 1968; Heuser, 2005; Hollinshead et al., 1999) whereas others observed multiple, tightly apposed membranes derived from intracellular membranes, for example from the

intermediate compartment or the endoplasmic reticulum (ER) (Chlanda et al., 2009; Maruri-Avidal et al., 2013a; Sodeik et al., 1993). The simplest form of infectious VACV is composed of the core and lateral bodies, surrounded by one or more membranes. This form is called the mature virus (MV). Another form of infectious VACV is called the extracellular virus (EV). A subset of MVs acquires an additional double membrane as the viruses are enwrapped into intracytoplasmic membranes, forming wrapped viruses (WVs). They exit the host cell by fusion of the outer membrane with the host cell membrane, and are released with one more membrane than MVs (Payne & Kristenson, 1979). MVs and EVs are antigenically different, explaining why antibodies against MVs cannot inhibit the spread of the virus that is mainly performed by EVs (Appleyard et al., 1971; Boulter, 1969; Boulter et al., 1971; Payne, 1979; Turner & Squires, 1971). The amount of EV that is released depends on the host cell type as well as on the virus strain and correlates with the virulence of distinct vaccinia strains (Payne, 1980). Nine glycosylated proteins, including the vaccinia virus hemagglutinin A56 as well as one non-glycosylated but acylated protein are present in the EV membrane (DeHaven et al., 2011; Hiller & Weber, 1985; Payne, 1979). Some of them, like the products of the A33R (Roper et al., 1996), SalL4R (Duncan & Smith, 1992) and B5R (Engelstad et al., 1992; Isaacs et al., 1992) genes and the vaccinia virus hemagglutinin (Payne, 1979, Payne & Norrby, 1976), are specific for the EV membrane and not found on MVs, accounting for the antigenic difference.

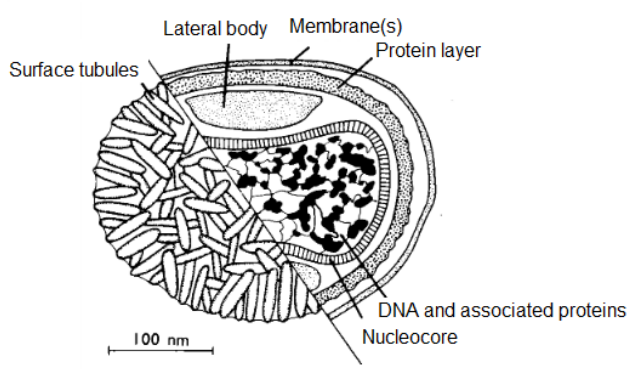

Fig. 1: Structure of VACV MV. This cartoon, adapted from Fenner et al. (1988) shows the structure of an MV. The DNA is together with associated proteins packaged into a core. The nucleocore and two lateral bodies are surrounded by a layer of proteins. The MV single membrane or double membranes is/are coated by viral proteins.

1.2.2 Vaccinia Virus Life Cycle

1.2.2.1 Vaccinia Virus Host Cell Entry

As with the number of MV membranes, the entry mechanism of VACV into host cells is not yet fully understood. Studies on the entry mechanism are complicated by the existence of two infectious forms of virus that may have different entry mechanisms (Vanderplasschen et

al., 1998; Vanderplasschen & Smith, 1997). For example, the entry of MV cores is associated with signaling cascades, whereas the entry of EV is not (Locker et al., 2000). Moreover, the mechanism for cell attachment and entry exploited by VACV seems to depend at least partly on the host cell (Shitbeck et al., 2009). Evidence exists for fusion of the virus with the host plasma membrane as well as for endocytic entry mechanisms. For example, Dales and Siminovitch (1961) and later Vanderplasschen et al. (1998) demonstrated that EV enters the host cell by endocytosis. The outer membrane is destroyed by the low pH in endosomes and the MV can subsequently fuse with the endosomal membrane. Accordingly, Townsley et al. (2006) and Townsley and Moss (2007) found the VACV entry mechanism to be dependent on low pH. The hypothesis of endocytic entry could be verified and extended by various studies. Recent publications suggest that VACV mimics apoptotic bodies to actively trigger its uptake by macropinocytosis (Mercer & Helenius, 2009; Mercer & Helenius, 2010; Schmidt et al., 2011). Fluid phase endocytosis, dependent on the cellular protein VPEC, has also been suggested (Huang et al., 2008). In addition, binding of VACV to β1 integrin and subsequent phosphatidylinositol 3-kinase (PI3K)/Akt signaling can promote host cell entry (Izmailyan et al., 2012).

In contrast, also direct fusion of VACV with the host cell plasma membrane has been observed (Armstrong et al., 1973; Carter et al., 2005; Chang & Metz, 1976; Vanderpasschen et al., 1998). Law et al. (2006) showed that cellular polyanions induce disruption of the outer membrane of EV, allowing the release of the core into the cytoplasm upon fusion of the MV membrane with the host cell plasma membrane.

So far, no specific cellular proteins have been found to be necessary and sufficient for VACV entry. Glycosaminoglycans seem to play a role in VACV attachment to the host cells. The VACV protein D8 binds chondroitin sulfate and antibodies against D8 or a soluble form of the viral protein can neutralize VACV infection of BSC40 cells. However, this is only the case if the WR32-7/Ind14K strain is used, which has genomic deletions compared to wild-type VACV strains. This indicates that other proteins can complement for the loss of D8 in the wild-type virus (Hsiao et al., 1999). The positively charged N-terminus of A27 binds heparan sulfate. Soluble A27 can reduce, but not inhibit VACV infectivity (Chung et al., 1998; Hsiao et al., 1998; Vázquez & Esteban, 1999). The H3L gene product binds heparan sulfate as well. As it is also involved in virion assembly, its necessity for virus attachment is hard to assess (Lin et al., 2000). VACV infectivity is reduced by soluble glycosaminoglycans, but not completely abolished. Moreover, the extent of inhibition is cell-type specific. Therefore, other cellular proteins must exist that allow attachment of VACV to its host (Carter et al., 2005).

One of those proteins might be laminin, which is bound by A26 (Chiu et al., 2007). In addition, a glycosamin-independent way of attachment exists that is inhibited by a soluble form of the VACV protein L1 (Foo et al., 2009).

Although cellular receptors remain to be discovered, several VACV proteins have been identified to mediate host cell entry. An entry fusion complex is formed by the MV proteins A16, A21, A28, G3, G9, H2, I5, J5 and L5. They are conserved in all poxviruses and have non-redundant functions. Although virions with deletions of entry fusion complex proteins can still attach to host cells, penetration does not occur (Bisht et al., 2008; Ojeda et al., 2006; Moss, 2006; Senkevich et al., 2004; Senkevich et al., 2005; Senkevich & Moss, 2005; Townsley et al., 2005a, Townsley et al., 2005b;).

The super-infection of already infected host cells is prevented by two mechanisms. One mechanism is mediated by a complex of the transmembrane viral hemagglutinin A56 and the serine protease inhibitor (SPI)-3, also called K2, which can directly bind at least two proteins of the entry fusion complex (DeHaven et al., 2011; Wagenaar & Moss, 2007; Wagenaar et al. 2008). The A56/K2 complex is present on the plasma membrane of infected cells and can therefore prevent superinfection with newly released virions (Turner & Moyer, 2008; Wagenaar & Moss, 2007; Wagenaar & Moss, 2009).

The second mechanism is mediated by the viral early proteins A33 and A36. They reside in the host cell membrane and induce the formation of actin tails upon contact with EVs. The forming actin tails repel the viruses from already infected cells and therefore facilitate fast and efficient spread (Doceul et al., 2010). In contrast to the A56/K2-mediated mechanism that targets proteins of the MV membrane, the A33/A36-mediated mechanism targets EVs, highlighting the importance of both viral forms for infection.

1.2.2.2 Vaccinia Virus Transcription

Already in 1905, Prowazek stated that VACV is present in the cytoplasm, but not in the nucleus of infected cells (Prowazek, 1905). It is now known that the complete VACV life cycle, including replication and transcription of its DNA genome, takes place in the cytoplasm (Moss, 2001). Its cytoplasmic life cycle forces VACV to introduce its own enzymes for DNA and RNA biosynthesis into the host cell cytoplasm. VACV codes for a DNA polymerase (Challberg & Englund, 1979; Citarella et al., 1972; Jungwirth & Joklik, 1965), a multi-subunit DNA-dependent RNA polymerase (Baroudy & Moss, 1980; Jones et al., 1987; Kates &

McAusland, 1967a; Kates & McAusland, 1967b; Munyon et al., 1967; Nevins & Joklik, 1977a; Spencer et al., 1980) as well as other enzymes involved in replication and transcription, for example a poly(A) polymerase (Brakel & Kates, 1974; Nevins & Joklik, 1977b) and a DNA ligase (Kerr & Smith, 1989). The viral DNA is transcribed as well as replicated in so-called "viral factories" that were first described in the early 1960s (Cairns, 1960; Dales & Siminovitch, 1961). VACV mRNAs have a 5' cap of 7-methylguanosine and a 2'-O-methyladenosine or 2'-O-methylguanosine (Wei & Moss, 1975). Capping and poly-adenylation are performed by the same, virally encoded enzyme that is packaged into the virus core (Morgan et al., 1984; Niles et al., 1989; Schnierle et al., 1992).

The transcription of viral genes is regulated in time by a cascade model. Transcription factors for early genes are expressed late in infection and packaged into the virion, whereas transcription factors for intermediate genes are expressed early in infection and transcription factors for late genes are intermediate gene products (Broyles, 2003; Gershon & Moss, 1990). Early genes can be further distinguished into immediate early and early genes (Assarsson et al., 2007; Cooper & Moss, 1979). The VACV RNA polymerase consists of two large and several small subunits, which are encoded by the virus itself and are mostly expressed continuously during infection (Ahn et al., 1990a; Ahn et al., 1990b; Amegadzie et al., 1991a; Amegadzie et al., 1991b; Amegadzie et al., 1992; Broyles & Moss, 1986; Broyles & Pennington, 1990; Quick & Broyles, 1990). The two large and the smallest subunits share sequence similarity with the largest and smallest subunits of eukaryotic RNA polymerase II (Amegadzie et al., 1991b; Amegadzie et al., 1992; Broyles & Moss, 1986; Patel & Pickup, 1989). A 30-kDa subunit of the viral RNA polymerase shares homology with the eukaryotic transcription elongation factor SII (TFIIS) (Ahn et al., 1990a).

In addition to the RNA polymerase, the RNA polymerase-associated gene Rap94, which is associated with 30 – 40 % of viral RNA polymerases, and the heterodimeric ATPase vaccinia virus early transcription factor (VETF) are necessary and sufficient for the transcription of early genes (Ahn et al., 1994; Ahn & Moss, 1992; Broyles et al., 1988; Broyles & Fesler, 1990; Broyles & Moss, 1988; Gershon & Moss, 1990). Early mRNAs are produced inside the core immediately after infection and are released into the cytoplasm (Kates & Beeson, 1970; Kates & McAuslan, 1967b; Mallardo et al., 2002). The released mRNAs are transported on microtubules to their site of translation at some distance to the cores, where they are translated by cellular ribosomes (Mallardo et al., 2001; Mallardo et al., 2002; Metz et al., 1975).

The transcription of intermediate genes starts after DNA replication (Vos & Stunnenberg, 1988). In contrast to the transcription of early genes, the transcription of intermediate genes depends on cellular proteins, namely G3BP and p137, which together form the vaccinia virus intermediate transcription factor (VITF)-2 (Katsafanas & Moss, 2004; Rosales et al., 1994b). Two more VITFs and a capping enzyme, all virally encoded, are necessary for intermediate gene transcription (Sanz & Moss, 1998; Vos et al., 1991). VITF-1 is a free form of the 30-kDa subunit of the RNA polymerase that shares homologies to the eukaryotic TFIIS (Rosales et al., 1994a).

The transcription of late genes takes place only after three vaccinia virus late transcription factors (VLTFs) have been expressed as intermediate genes from newly synthesized DNA (Hubbs & Wright, 1996; Keck et al., 1990; Keck et al., 1993; Passarelli et al., 1996; Wright et al., 1991; Zhang et al., 1992). In contrast to the cascade model of regulation of transcription, another factor necessary for the transcription of late genes, VLTF-4, is expressed early in infection (Kovacs et al., 1994; Kovacs & Moss, 1996; Wright & Coroneos, 1993). As intermediate gene expression, also late gene expression is stimulated by cellular proteins, namely hnRNP A2 and RMB3 (Dellis et al., 2004; Wright et al., 2001).

1.2.2.3 Vaccinia Virus Replication

Upon its release from the viral core, the genomic DNA associates with the endoplasmic reticulum (ER) and is subsequently replicated in factories enclosed by membranes derived from this organelle (Mallardo et al., 2002; Tolonen et al., 2001). Like transcription, DNA replication is also performed by virus-encoded proteins. The DNA polymerase holoenzyme is composed of three proteins, which are necessary and sufficient for DNA replication *in vitro*: a 110 kDa enzyme with polymerase and 3'-5'-exonuclease activity (Challberg & Englund, 1979; Earl et al., 1986; Jones & Moss, 1984; McDonald & Traktman, 1994a; Traktman et al., 1984) as well as the proteins A20 and D4 which first associate with each other and subsequently with the polymerase to promote processivity. D4 has an additional uracil DNA glycosylase activity, which is not necessary for viral replication (De Silva & Moss, 2003; Klemperer et al., 2001; McDonald & Traktman, 1994b; McDonald et al., 1997; Millns et al., 1994; Stanitsa et al., 2006). Nevertheless, the uracil DNA glycosylase activity is essential for VACV virulence, most probably due to its role in DNA repair by excision of uracil that can result from the deamination of cytosine (De Silva & Moss, 2003; Lindahl, 1993; Upton et al., 1993). In addition to the binding site for D4, which comprises the 25 most N-terminal amino acids, A20 has non-overlapping binding sites for D5 and the late transcription factor H5 (Ishii

& Moss, 2002; McCraith et al., 2000). D5, a nucleoside triphosphatase and primase, is required for VACV replication *in vivo* and might have additional roles in recombination (De Silva et al., 2007; Evans et al., 1995; Evans & Traktman, 1987; Evans & Traktman, 1992). VACV also codes for an early expressed DNA ligase (Kerr & Smith, 1989). The importance of this ligase for replication had long time been underestimated, as a lack of functional viral ligase can be complemented by the cellular DNA ligase I (Colinas et al., 1990; Paran et al., 2009). Other VACV proteins with a possible role in replication are the ssDNA binding protein I3 (Rochester & Traktman, 1998) and the protein kinase B1 (Howard & Smith, 1989; Rempel et al., 1990; Rempel & Traktman, 1992; Traktman et al., 1989). Although VACV replication is performed by viral proteins, it is influenced by several host proteins in a positive or negative way (Beard et al., 2014). For example, the host ubiquitin-proteasome system is necessary for VACV replication (Teale et al., 2009). The origin of VACV replication does not seem to be sequence-dependent, as also plasmids and mini-chromosomes without VACV sequences are replicated by the VACV polymerase in viral factories (DeLange & McFadden, 1986; De Silva & Moss, 2005). In contrast, specific sequences next to the terminal hairpin loops are necessary for the resolution of concatemers by the viral Holliday junction resolvase (Garcia et al., 2000; Garcia & Moss, 2001; Merchlinsky, 1990).

1.2.2.4 Vaccinia Virus Maturation and Release

Two forms of infectious VACV are released from an infected cell: the MV and the EV. MVs form in a complex, not fully understood mechanism involving several viral and some host proteins (see Fig. 2) (Liu et al., 2014). As stated above, the origin of the MV membrane is still under debate. However, recent studies strengthen the theory that the MV membrane or membranes are derived from ruptured ER membranes (Chlanda et al., 2009; Maruri-Avidal et al., 2013b). Trimers of the viral protein D13 interact with the viral ER membrane protein A17 to form a protein scaffold for the formation of the spherical immature virus (IV) membrane. The protein scaffold is released from IVs by proteolytic cleavage of A17 by the virus-encoded protease I7 (Bisht et al., 2009; Szajner et al., 2005). Several virally encoded proteins, for example the protein kinase F10, are required for the formation of crescents and, subsequently, IVs (Lin & Broyles, 1994; Liu et al., 2014; Szajner et al., 2004a, Szajner et al., 2004b; Szajner et al., 2004c; Traktman et al., 1995; Wang & Shuman, 1995;). One of the proteins which are required for the formation of membrane crescents is L2, which localizes to the ER membrane and is therefore another hint for the derivation of MV membranes from the ER (Maruri-Avidal et al., 2011a; Maruri-Avidal et al., 2011b; Maruri-Avidal et al., 2013). In addition to its role in crescent formation, F10 mediates together with six more VACV proteins

the association of the crescents with the viroplasm (Boyd et al., 2010; Liu et al., 2014, Szajner et al., 2003; Szajner et al., 2004a;). In addition to the VACV kinase F10, host PI3Ks play a role in VACV morphogenesis (McNulty et al., 2010).

A subset of MVs is wrapped in a double membrane derived from the trans-golgi network (Schmelz et al., 1994), endosomes (Tooze et al., 1993) or the Golgi complex (Hiller & Weber, 1985) (see Fig. 2). They are transported to the cell surface and fuse with the plasma membrane to be released as cell-associated or extracellular EVs (Payne & Kristenson, 1979) (see Fig. 2). The transport of MVs to the site of envelopement as well as the movement of WVs to the plasma membrane are performed by microtubules and are mediated by viral proteins (Hollinshead et al., 2001; Rietdorf et al., 2001; Sanderson et al., 2000; van Eijl et al., 2002; Ward & Moss, 2001). Viral proteins that are exposed on the host cell membrane after exocytosis of the virion are endocytosed and may be recycled (Husain & Moss, 2005).

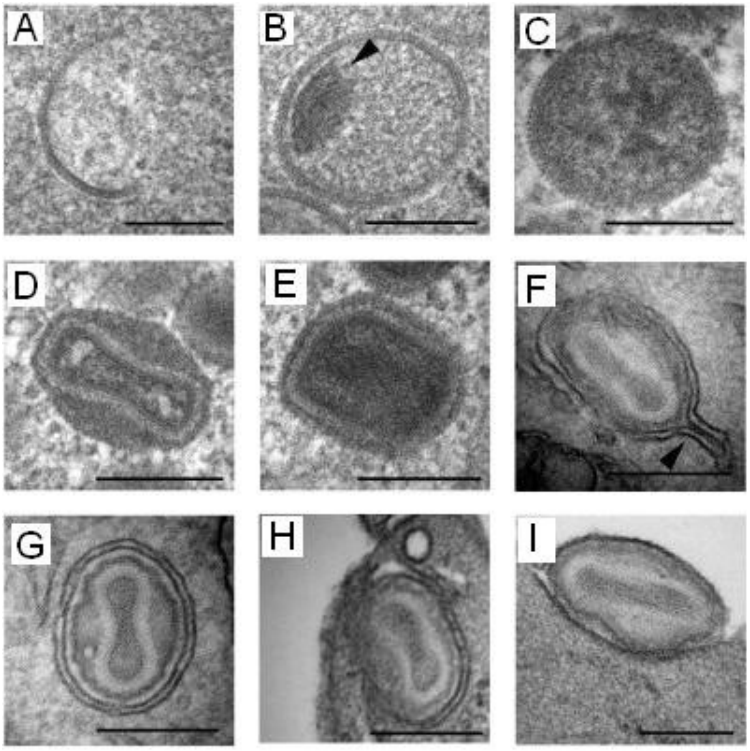

Fig. 2: Vaccinia virus maturation. Transmission electron micrographs of ultrathin sections of HeLa cells infected with VACV (adapted from Capeda & Esteban, 2014). (A) viral crescent; (B) IV with an arrow pointing towards the enclosed DNA; (C) dense transitional form between IV and MV; (D) and (E) MV; (F) wrapping of MV, the arrow points towards the fusion site of two Golgi-derived membranes; (G) WV with additional double membrane; (H) transport of WV to the plasma membrane; (I) EV after exocytosis.

1.3 Vaccinia Virus Immune Evasion

Animals have developed several mechanisms to interfere with the replication and spread of viruses and other pathogens. However, during the course of co-evolution, pathogens have developed ways to evade the host immune system. In this chapter, I will give a short

introduction to some of the most important signaling pathways of the innate immune system and the mechanisms VACV has evolved to subvert them.

1.3.1 Immune Signaling Pathways of the Innate Immune System

1.3.1.1 Toll-like Receptor Signaling

Invading pathogens activate the innate immune system by binding to pattern-recognition receptors (PRRs). In contrast to the antibodies of adaptive immune cells, PRRs detect conserved features that are shared by many pathogens, for example dsRNA or LPS. Those features are called pathogen-associated molecular patterns (PAMPs). Toll-like receptors (TLRs) comprise one family of PRRs (Akira et al., 2006; Kawai & Akira, 2007; Kawai & Akira, 2008). Toll was initially described as a protein that is involved in establishing the dorsal-ventral polarity in Drosophila embryos (Anderson et al., 1985). Ten years later, Toll was found to have an important role in the antifungal immune response in Drosophila. Moreover, homologies between the proteins involved in Toll-mediated signaling and the proteins of the mammalian NF-κB pathway were discovered (Lemaitre et al., 1996). Dorsal, which is activated by Toll signaling, belongs to the same family of proteins as NF-κB, namely the family of rel/NF-κB transcription factors which bind to κB enhancer elements (Ballard et al., 1990; Ghosh et al., 1990; Steward, 1987). The activities of NF-κB as well as dorsal are inhibited by the association with inhibitors, inhibitor of NF-κB (IκB) and cactus, respectively (Beg et al., 1992; Geisler et al., 1992). The inhibitors shield the nuclear localization signals of their targets and therefore retain the transcription factors in the cytoplasm (Beg et al., 1992; Kidd, 1992). Upon signal-induced phosphorylation, ubiquitination and proteosomal degradation of their inhibitors, the transcription factors can translocate to the nucleus and activate their target genes (Chen et al., 1995; Ghosh & Baltimore, 1990). In the case of NF-κB, these target genes are mostly inflammatory cytokines such as interferon (IFN)-γ (Sica et al., 1997), interleukin (IL)-1α (Mori & Prager, 1996), IL-1β (Hiscott et al., 1993), IL-2 (Hoyos et al., 1989), IL-6 (Libermann & Baltimore, 1990; Son et al., 2008) and IL-9 (Zhu et al., 1996), but also growth factors such as early growth response 2 (Nafez et al., 2014) and vascular endothelial growth factor C (Du et al., 2014).

Human TLRs are type I transmembrane proteins. Leucine rich repeats characterize the extracellular domain whereas the intracellular part is a Toll/interleukin-1 receptor (TIR) homology domain which is essential for signaling. TLRs are expressed by immune cells, for

example dendritic cells (DCs), as well as non-immune cells, such as epithelial cells, which are usually the first cells to encounter a pathogen (Akira et al., 2006; Kawai & Akira, 2007).

Different TLRs bind different ligands and recruit different adapter molecules (see Fig. 3). Table 1 lists the ligands that activate different TLRs and the adapter proteins that are recruited.

	Ligands	Adapter proteins
TLR2	lipoproteins, peptidoglycan	MyD88, MAL
TLR3	dsRNA	TRIF
TLR4	LPS	MyD88, MAL, TRAM, TRIF
TLR5	flagellin	MyD88
TLR7	imidazoquinolines, guanosine analogs, ssRNA	MyD88
TLR8	imidazoquinolines, ssRNA	MyD88
TLR9	unmethylated CpG	MyD88

Table 1: TLRs, their ligands and adapter proteins. Ligands that activate different TLRs as well as the adapter proteins that are recruited by each TLR are shown

Although the best characterized ligand for TLR4, namely LPS, is of bacterial origin (Hoshino et al., 1999; Kawai et al., 1999; Poltorak et al., 1998a; Poltorak et al., 1998b), recent findings support a role for TLR4 in antiviral immunity against respiratory syncytial virus, vesicular stomatitis virus and VACV (Haeberle et al., 2002; Hutchens et al., 2008; Georgel et al., 2007). TLR2 forms heterodimers with TLR1 or TLR6 and binds several PAMPs, for example lipoproteins and peptidoglycan (Hirschfeld et al., 1999; Ozinsky et al., 2000; Takeuchi et al., 1999). By associating with either TLR1 or TLR6, TLR2 can discriminate between diacylated and triacylated lipopeptides, respectively (Takeuchi et al., 2001). TLR3 responds to dsRNA (Alexopoulou et al., 2001). TLR5 recognizes flagellin (Hayashi et al., 2001). TLR7 is responsible for the response to the low-molecular weight imidazoquinolines, guanosine analogs and ssRNA. It is specifically produced by plasmacytoid DCs and promotes their increased IFNα production upon viral infection (Diebold et al., 2004; Hemmi et al., 2002; Kawai & Akira, 2007; Kawai & Akira, 2008). TLR8 is also involved in the recognition of imidazoquinolines and ssRNA (Forsbach et al., 2008; Heil et al., 2004). TLR9 responds to unmethylated CpG dinucleotides and is, as TLR7, restricted to plasmacytoid DCs (Hemmi et al., 2000; Kawai & Akira, 2008). The TLRs that are responsible for the detection of nucleic acids, namely TLR3, 7, 8 and 9 reside intracellularly in endosomal or phagosomal membranes (Heil et al., 2005; Kawai & Akira, 2007) This is, in addition to the methylation of

mammalian DNA, a further mechanism to prevent auto-immunity-causing recognition of self DNA (Barton et al., 2005). However, a sole intracellular localization of TLR3 is only observed in conventional DCs. In fibroblasts and epithelial cells, it is present on the plasma membrane as well as on endosomal membranes (Kawai & Akira, 2007). The biological significance of TLR3 in antiviral immunity is still under debate. Although it seems to be important for the defense against herpes simplex virus 1, it does not play a crucial role in the immunity against other RNA viruses (Edelmann et al., 2004; Zhang et al., 2007). In contrast, TLR3 signaling might even have detrimental outcomes. For example, TLR3-mediated inflammation in West Nile virus infection leads to the break-down of the blood-brain-barrier and allows viral entry into the brain, leading to neuropathology (Wang et al., 2004). Similarly, TLR3-deficient mice have an increased survival rate upon infection with influenza virus or VACV, due to a decreased inflammatory response (Hutchens et al., 2008; Le Goffic et al., 2006).

Upon ligand-binding, TLRs recruit TIR-domain containing adapter proteins via homotypic interactions of the TIR domains. The recruitment of adapter proteins is mediated by dimerization or by conformational changes of pre-formed dimers (Akira et al., 2006; Kawai & Akira, 2007; Kawai & Akira, 2008; Latz et al., 2007). The adapter proteins activate several signaling pathways to translate the signal of ligand-binding into the expression of proteins involved in innate immunity (see Fig. 3). Five adapters are involved in TLR signaling (Akira et al., 2006; Kawai & Akira, 2007; Kawai & Akira, 2008). Of those, SARM is the only adapter protein that inhibits instead of activates TLR signaling (Carty et al., 2006).

MyD88 is recruited by all TLRs except TLR3 (see Table 1). TLR2 and TLR4 require in addition MyD88-adapter-like (MAL), also called TIRAP, for the interaction with MyD88 (Akira et al., 2006; Fitzgerald et al., 2001; Horng et al., 2002; Kawai & Akira, 2007; Kawai & Akira, 2008; Yamamoto et al., 2002a). MyD88 recruits IL-1R-associated kinases (IRAKs) (Wesche et al., 1997). IRAK-4, the first to be activated, activates IRAK-1 and IRAK-2. Activated IRAKs associate with the ubiquitin protein ligase TNFR-associated factor 6 (TRAF6). TRAF6 recruits TGF-β-activated kinase 1 (TAK1) and the three TAK1 binding proteins TAB1, TAB2 and TAB3. Alternatively, TRAF6 can recruit the TAK1 complex via the receptor interacting protein (RIP) 1 (Kawai & Akira, 2007; Kawai & Akira, 2008; Maylan et al., 2004; Sato et al., 2003). The TAK1 complex activates the MAPK pathway by the phosphorylation of MAP kinase kinase (MKK) 6 and the NF-κB pathway by the phosphorylation of IKKβ, therefore inducing the transcription of inflammatory cytokines (see Fig. 3) (Akira et al., 2006; Kawai & Akira, 2007; Kawai & Akira, 2008).

In addition to the MyD88-dependent pathways, MyD88-independent pathways exist. TLR3 and TLR4 can activate a MyD88-independent pathway that is mediated by the adapter TIR domain-containing adapter inducing IFN-β (TRIF), also called TICAM-1 (Alexopoulou, 2001; Oshiumi et al., 2003; Yamamoto et al., 2002b; Yamamoto et al., 2003a). Another adapter protein, TRIF-related adapter molecule (TRAM) mediates the interaction between TRIF and TLR4. As MyD88, TRIF can activate TRAF6 and subsequently the NF-κB and MAPK pathways via TAK1 (see Fig. 3) (Kawai & Akira, 2008; Yamamoto et al., 2003b).

In addition, TRIF recruits TANK binding kinase (TBK) 1 and the inducible IKK-i via TRAF3, allowing the phosphorylation and activation of IRF-3 independent of MyD88 and TRAF6 (Fitzgerald et al., 2003; Gohda et al., 2004; Häcker et al., 2005; Hemmi et al., 2004; McGettrick et al., 2006; Oganesyan et al., 2006; Sharma et al., 2003). TAK1 is also involved in IRF-3 activation (Zhang et al., 2009). IKK-i additionally phosphorylates a subunit of the IκB complex, therefore activating not only IRF-3 but also NF-κB (Peters et al., 2000; Shimada et al., 1999). Phosphorylated IRF-3 dimerizes, translocates to the nucleus and activates, in association with CREB binding protein, the expression of type I IFNs (see Fig. 3) (Kawai & Akira, 2007; Lin et al., 1998; Sharma et al., 2003; Yoneyama et al., 1998).

In contrast to TLR3 and TLR4 that induce type I IFN transcription via the MyD88-independent pathway, TLR7 and TLR9 induce type I IFN expression via a MyD88-dependent pathway in plasmacytoid DCs (Kawai & Akira, 2008). The MyD88-dependent expression of type I IFNs in plasmacytoid DCs requires IRF-7 instead of IRF-3, which is activated by the TRIF-mediated pathway, and does not depend on phosphorylation by TBK1 or IKK-i (Honda et al., 2005; Matsui et al., 2006). IRF-7 can directly interact with MyD88 and TRAF6, and its activation depends on the ubiquitin ligase activity of TRAF6 (Kawai et al., 2004) and the kinases IRAK-1 (Uematsu et al., 2005) and IKKα (Hoshino et al., 2006). The complex also involves IRAK-4 (Honda et al., 2004) and osteopontin (Shinohara et al., 2006). The translocation of IRF-7 is further controlled PI3K (Guiducci et al., 2008). In addition to IRF-7, IRF-8 is activated in DCs upon TLR9 signaling. The activation of IRF-8 leads to the activation of IKKα/β and therefore the transcription of NF-κB target genes (Tsujimura et al., 2004).

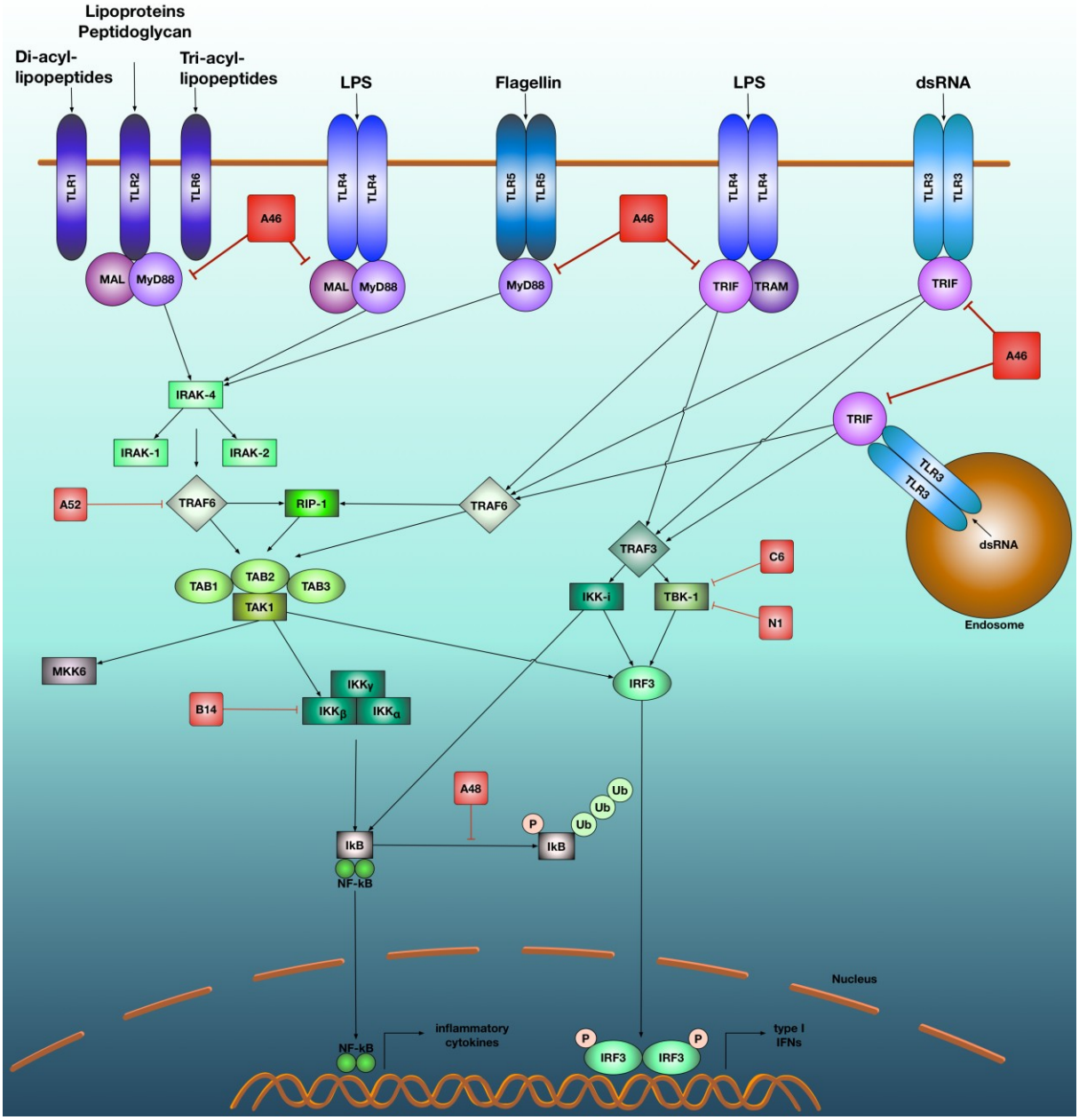

Fig. 3: TLR signaling and VACV-encoded inhibitors. Signaling pathways induced by activation of TLR2, TLR3 or TLR5, for example in epithelial cells and VACV-encoded proteins that inhibit TLR-mediated signaling. TLRs are shown in blue, adapter proteins in violet, proteins involved in the signaling cascades in green and VACV-encoded inhibitors in red. Designed by Patrick Ranz with OmniGraffle.

1.3.1.2 TLR-independent Sensing of Viral Nucleic Acids

In addition to the recognition of viral nucleic acids by TLRs, which is the main route of type I IFN induction in plasmacytoid DCs, other cells, for example fibroblasts, recognize and respond to viral RNA via RIG-I-like receptors (RLRs) (Kato et al., 2005). The importance of RLR signaling upon viral infection was highlighted by Melchjorsen et al. (2005). They showed that non-immune cells depend entirely on this class of receptors for the response to infection with paramyxoviruses, whereas myeloid cells can utilize TLR-dependent and –independent pathways (Melchjorsen et al., 2005). The RLR family comprises three members, RIG-I, MDA5 and LGP2. All three members contain a DExD/H helicase domain and a repressor domain. RIG-I and MDA5 code additionally for two caspase activation and recruitment domains (CARDs) (Kawai & Akira, 2008). The helicase domain with ATPase activity as well as the CARD are necessary for downstream signaling and subsequent activation of NF-κB and IRF-3 and the induction of type I IFNs (Yoneyama et al., 2004). Although RIG-I and MDA5 can both bind and respond to viral RNA, they recognize distinct viruses. For example, type I IFN production in response to influenza virus infection is mediated by RIG-I, whereas MDA5 responds to picornaviruses (Gitlin et al., 2006; Kato et al., 2006). The differential recognition of different viruses depends on the structure of the RNA 5' end. RIG-I selectively recognizes RNA with a 5' triphosphate, as is the case for the genomic ssRNA of influenza virus (Hornung et al., 2006; Pichlmair et al., 2006).

RIG-I and MDA5 associate with IFN-β promoter stimulator (IPS)-1 via homotypic interactions between CARDs. IPS-1 recruits ubiquitinated TRAF3, TBK1, IKKα, IKKβ and IKK-i to induce the expression of type I IFNs via IRF-3 and NF-κB (Kawai et al., 2005; Kumar et al., 2006; Meylan et al., 2005; Saha et al., 2006; Xu et al., 2005). A mitochondrial CARD-like domain containing transmembrane protein called MAVS is involved in the activation of IRF-3 and NF-κB downstream of RIG-I (Seth et al., 2005).

RLR signaling can be controlled by ubiquitination and deubiquitination. The transfer of a polyubiquitin chain to the CARD domain of RIG-I enhances its downstream signaling (Gack et al., 2007). The deubiquitinating enzyme A (DUBA) negatively regulates RLR signaling by cleavage of the polyubiquitin chain off TRAF3, therefore promoting its dissociation from the kinase complex (Kayagaki et al., 2007). A negative feedback loop is activated by the IFN-induced expression of the ubiquitin ligase RNF125, which ligates polyubiquitin chains to RIG-I and MDA5, promoting their proteasomal degradation (Arimoto et al., 2007).

Two more sensors of viral nucleic acids, protein kinase R (PKR) and 2'-5' oligoadenylate synthetase (OAS), were discovered as IFN-induced, dsRNA- and ATP-dependent inhibitors of protein synthesis (Ball & White, 1978; Hovanessian et al., 1977; Kerr et al., 1974; Lebleu et al., 1976; Roberts et al., 1976; Zilberstein et al., 1978). PKR pshophorylates eIF-2α and therefore inhibits initiation of translation (Chong et al., 1992; Farrell et al., 1977; Samuel et al., 1984; Williams, 2001; Zilberstein et al., 1978). In addition, PKR activates the MAPK pathway by phosphorylating MKK6 and promotes NF-κB activation by phosphorylating IKK and IκB (Gil et al., 2000a; Kumar et al., 1994; Silva et al., 2004; Zamanian-Daryoush et al., 2000). An interaction between PKR and TRAFs was observed as well (Gil et al., 2000b).

Different isoforms of OAS exist. Synthetases of 40 kDa and 46 kDa are expressed from one gene by alternative splicing (Benech et al., 1985a; Benech et al., 1985b; Saunders et al., 1985; Wathelet et al., 1986). Two more genes code for a 69 kDa and a 100 kDa isoform (Chebath et al., 1987; Kerr & Brown, 1978; Marié & Hovanessian, 1992). 40/46 kDa, 69 kDa and 100 kDa isoforms contain one, two or three catalytic domains, respectively, and exhibit different catalytic activities (Marié & Hovanessian, 1992; Hovanessian et al., 1988; Rebouillat et al., 1999). They synthesize pppA2'p5'A2'p5'A oligomers (2-5A) of different lengths. The most common molecules synthesized by the 69-kDa isoform consist of three to five adenylates. The 100 kDa isoform of OAS synthesizes dimeric molecules although they have lower, if any, biologic activity (Kerr & Brown, 1978; Marié et al., 1997). 2-5A mediates homodimerization of RNase L, the expression of which is upregulated by IFNs as well. The so activated RNase L degrades mRNAs and therefore acts together with PKR to inhibit protein expression (Baglioni et al., 1978; Clemens & Williams, 1978; Dong & Silverman, 1995; Jacobsen et al., 1983).

1.3.1.3 Interferon Signaling

IFNs were first discovered in 1957 as a soluble factor that is produced when chick chorioallantoic membranes are incubated with heat-inactivated influenza virus for at least 4 hours. This factor interferes with the infection of a subsequently added challenging influenza virus (Isaacs & Lindenmann, 1957). Together with cytokines of the IL-10 family, IFNs belong to the type II cytokines (Gadina et al., 2001). Several paralogous IFN-α genes exist in mammals. Together with IFN-β, IFN-δ, IFN-ε, IFN-κ, IFN-τ and IFN-ω, they comprise the type I IFNs. Type I IFNs can be produced by almost all cells. Several stimuli, for example dsRNA

as a byproduct of viral infection, can induce their transcription, which is regulated by negative and positive regulatory elements. IRF-1 is an example for a transcriptional activator of IFN-α as well as IFN-β, whereas NF-κB activates specifically the transcription of IFN-β. In contrast to the ubiquitously expressed type I IFNs, IFN-γ, the only type II IFN, is specifically expressed by natural killer cells and T cells. The IFN-γ gene is located on chromosome 12 in contrast to the type I IFN genes that are located on chromosome 9. (Gray & Goeddel, 1982; Platanias, 2005; Sen & Lengyel, 1992). IFN-γ binds to a different receptor than type I IFNs and induces a different set of genes (Branca & Baglioni, 1981; Kelly et al., 1985).

The mammalian IFN-α/β receptor (IFN-αR) is composed of two subunits, IFN-αR1 and IFN-αR2 (Branca & Baglioni, 1981; Colamonici et al., 1990; Domanski et al., 1995; Kelly et al., 1985; Kim et al., 1997; Uzé et al., 1990). The binding of a ligand induces association of the two receptor subunits (Cohen et al., 1995). Like the IFN-αR, also the IFN-γ receptor (IFN-γR) is composed of subunits. IFN-γR1 is sufficient for IFN-γ binding, but a second, species-specific subunit, called accessory factor 1 (AF-1) or IFN-γR2, is essential for signal transduction (Aguet et al., 1988; Fountoulakis et al., 1990; Gibbs et al., 1991). During crystallography of the IFN-γR complex, a third subunit was detected (Thiel et al., 2000). Both IFN receptors signal through the phosphorylation and subsequent activation of the receptors themselves, JAKs (Janus kinases) and STATs (signal transducers and activators of transcription). JAK1 is involved in the signaling of type I as well as type II IFNs (Silvennoinen et al., 1993). Tyk2 is only activated by type I IFNs whereas JAK2 mediates the response to type II IFNs (Silvennoinen et al., 1993; Velazquez et al., 1992; Watling et al., 1993). In the case of type I IFNs, the IFN-αR1 subunit is essential for the activation of JAK1 and Tyk2 (Colamonici et al., 1995). In the case of type II IFN signaling, IFN-γR2 recruits JAK2 following the ligand-induced dimerization (Bach et al., 1996; Greenlund et al., 1994; Igarashi et al., 1994; Kotenko et al., 1995).

Stimulation with type I IFNs leads to the activation of IFN-stimulated gene factor 3 (ISGF-3), which is composed of a STAT1-STAT2 heterodimer in association with IRF-9 (Colamonici et al., 1995; David & Larner, 1992; Fu et al., 1990; Platanias, 2005). It binds to the IFN-stimulated response element (ISRE) and therefore activates IFN-stimulated genes (ISGs) (Levy et al., 1988). Type II IFNs lead to the phosphorylation of STAT1 which forms homodimers that translocate into the nucleus to activate IFN-γ-inducible genes by binding to the gamma-IFN activation site (GAS) (Decker et al., 1991; Platanias et al., 2005). IFN-inducible genes are, for example, MHC class I, which is induced by type I as well as type II IFNs, and MHC class II, which is induced by IFN-γ (Sen & Lengyel, 1992).

1.3.1 Vaccinia Virus Immune Evasion Proteins

As summarized in the previous chapter, higher organisms have evolved several mechanisms to interfere with pathogenic replication and spread. However, in the course of co-evolution, pathogens have developed ways to interfere with the host immune system. Therefore, poxviruses code for several immune evasion genes which are, in contrast to the genes required for the viral life cycle, very diverse among the different members of the *Poxviridae.* Whereas IFN- and chemokine-mediated immune pathways are modulated by all poxviruses, only *Orthopoxviruses*, to which VACV belongs, and *Leporipoxviruses* express inhibitors of TLR-mediated pathways (Seet et al., 2003). VACV targets TLR signaling at different points of the pathway (see Fig. 3). A46 interferes with the first step in signal transduction, the association of adapter proteins with activated TLRs (Stack & Bowie, 2012; Stack et al., 2005). A52 acts further downstream. It associates with IRAK-2 and TRAF6 and therefore inhibits NF-κB activation by the disruption of signaling complexes (Harte et al., 2003). In contrast, A52 stimulates the expression of IL-10, which acts in an anti-inflammatory manner, by facilitating TRAF6 oligomerization and subsequent TAK1 recruitment and activation of the MAP kinase pathway (Maloney et al., 2005; Moore et al., 2001; Stack et al., 2013). NF-κB activation is additionally blocked by B14, which inhibits the IKK complex (Chen et al., 2008) and by A48, which inhibits the degradation of IκBα (Mansur et al., 2013). The IRF-3-mediated expression of type I IFNs is inhibited by N1, which binds and inhibits TBK1 (DiPerna et al., 2004), by C6, which acts on the level of TBK1 as well (Unterholzner et al., 2011), and by K7 which targets a DEAD box protein involved in IRF-3 signaling (Schröder et al., 2008). Although all of those proteins act downstream of TLRs, their functions are non-redundant and deletion of only one of them results in decreased virulence of VACV. A52, B14 (Graham et al., 2008), K7 (Kalverad et al., 2009), N1 (Aoyagi et al., 2007; Cooray et al., 2007) and the C-terminal domain of A46 (Fedosyuk et al., 2014; Kim et al., 2014) adopt a Bcl-2-like fold, although they do not share sequence homology with other viral or cellular proteins of the Bcl-2 family (see Fig. 4). In N1, the smallest of these proteins, the structural homology stretches over the whole sequence. However, as seen in Fig. 5, an alignment of the VACV-encoded proteins of the Bcl-2 family shows structural homology only in the C-terminal domains. The N-terminal domains of diverse lengths do not show sequence homology. A46 and A52 have with about 90 and 50 residues, respectively, the longest N-terminal domains not involved in the Bcl-2 fold (see Fig. 5) (Gonzáelz & Esteban, 2010). The structure of these N-terminal domains is unknown, as A46 and A52 could only be crystallized with N-terminal truncations (Fedosyuk et al., 2014; Graham et al., 2008; Kim et al., 2014)

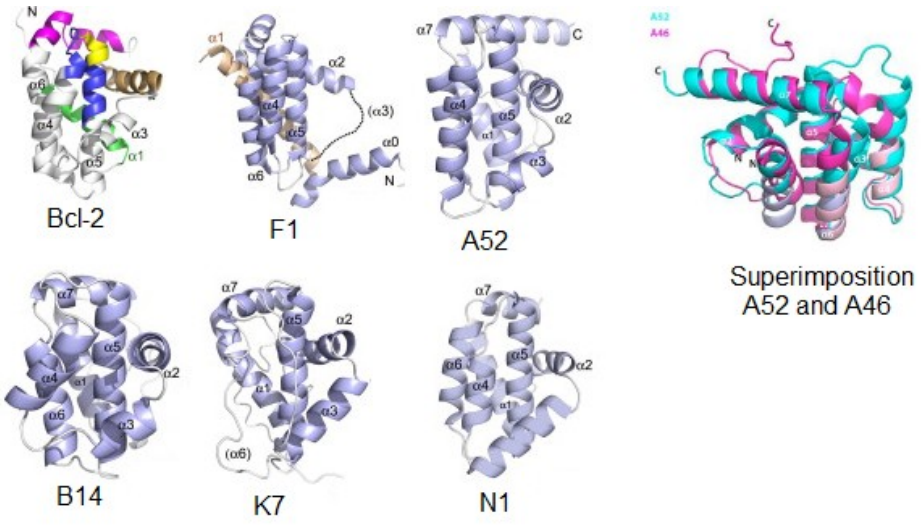

Fig. 4: VACV proteins with Bcl-2-like fold. This figure shows the cellular Bcl-2 and the VACV proteins F1, A52, B14, K7 and N1 that adopt a Bcl-2-like fold (adapted from Franklin & Khan, 2013) as well as a superimposition of the VACV proteins A52 (in cyan) and A46 (in magenta) (adapted from Fedosyuk et al., 2014). In the superimposition, A52 is 180 °C vertically rotated compared to the figure of A52 alone.

```
VACV_WR__N1     ------------------------------------------------------------------------------
VACV_WR__B14    ------------------------------------------------------------MTANFSTHVFSPQ
VACV_WR__K7     ------------------------------------------------------------MATKLDYEDAVFY
VACV_WR__A46    MAFDISVNASKTINALVYFSTQQNKLVIRNEVNDTHYTVEFDRDKVVDTFISYNRHNDTIEIRGVLPEETNIGCAVNTPV
VACV_WR__A52    MDIKIDISISGDKF----------TVTTRRENEER--------------------------KKYLPLQKEKTTDVIKPD

                                -----α1-----> ---α2----> ---------α3------------>   -α4-
VACV_WR__N1     ------------MRTLIIRYILWRND-----NDQTYYNDNFKKLMLLDELVDD-G---DVCTI-IKN-M---RMTLSDGPLL
                           -----α1----->  -------α2------>   ----α3-->         --α4-
VACV_WR__B14    HCGCDRLTSIDDVRQCLTEYIYWSSYAY---RNRQCAGQLYSTLLSFRDDAELVFID--IREI-V-KNM---PW-DDVKDCA
                          -------α1------>  -------α2------>  ------α3---->
VACV_WR__K7     FVDDDKICSRDSIIDLIDEYITWRNHVIVFNKDITSCGRLYKELMKFDDVAIRYYGIDKINEI-V-EAM---SEGD---HYI
                          ----α1--->  -------α2------->    ---α3---->       ------
VACV_WR__A46    --SMTYLYNKYSFKLILAEVIRHRN---------TISGNIYSALMTLDDLAIKQYGD--IDLIFN-EKL-KVDSDSGLFDFV
                         -----α1------>  -------α2------->    ---α3--->        ------
VACV_WR__A52    YLEYDDLLDRDEMFTILEEYFMYRGLLG----LRIKYGRLFNEIKKFDNDAEEQFGT--IEEL-K-QKL-RLNSEEGADNFI

                ---->          ---------α5------>          ------α6----->   ---α7--->
VACV_WR__N1     DRIN-----QPVNNIEDARRMIAISAKVARDIGE---RSEIRWE-ES-FTILFRMIETYFDDLMIDLYGEK------
                -------->     -------α5-------->          ----α6---->    ---α7->
VACV_WR__B14    EIIRCYI-PDEQKTIREISAIIGLCAYAATYWGGEDHPT-SNSL-NALFVMLEMINYVDYNIIFRRMN---------
                          ---------α5------->              -α6->    -----α7---->
VACV_WR__K7     -NF------TKVHDQESLPATIGICAKITEHWGYKKISESRFQS-L--GNITDLMTDDNINILILFLEKKLN-----
                -----α4------->  -------α5-------->  -------α6------>  --------α7------>
VACV_WR__A46    NFVKDM-------ICCDSRIVVALSSLVSKHWELTNKK--YRCMALAEHISDS-IPISELSRIRYNLCKYLRG----
                --α4---->     ----------α5------>   ------α6------->   -------α7---------->
VACV_WR__A52    DYIKVQKQDIVKLTVYDCISMIGLCACVVDVWRNEKLF--SRWK-YCLRAIKLFINDHMLDKIKSILQNRLVYVEMS

VACV_WR__N1     ------------------------------ 117
VACV_WR__B14    ------------------------------ 149
VACV_WR__K7     ------------------------------ 149
VACV_WR__A46    HTESIEDKFDYFEDDDSSTCSAVTDRETDV 240
VACV_WR__A52    ------------------------------ 190
```

Fig. 5: Alignment of VACV N1, B14, K7, A46 and A52. The gene sequences of the VACV (strain Western Reserve) proteins N1, B14, K7, A46 and A52 were aligned with M-Coffee on the T-Coffee web server (Di Tommaso et al., 2011; Moretti et al., 2007; Notredame et al., 2000; Wallace et al., 2006). The alignment was refined according to the alignments published by Franklin & Kahn (2013) and Fedosyuk et al. (2014). Hydrophobic residues important for the alpha-helical fold are underlined with black. The VIPER motif in A46 is shown in green. Residues with a good score in the original alignment are shown in pink. Violet arrows above the sequences mark the resides that form the alpha-helices of the Bcl-2-fold (Cooray et al., 2007; Graham et al., 2007; Fedosyuk et al., 2014; Kalverda et al., 2009).

Only N1 has, in addition to its role in inhibiting type I IFN expression, the anti-apoptotic properties characteristic of Bcl-2 proteins (Aoyagi et al., 2007; Cooray et al., 2007). Apoptosis of virus-infected cells is part of the immune response and often inhibited by viruses (Kvansakul & Hinds, 2013). In addition to the multi-functional N1, VACV codes for F1, another anti-apoptotic protein with Bcl-2-like fold (Kvansakul et al., 2008; Wasilenko et al., 2003).

Two proteins, E3 and K3, inhibit PKR signaling. Both are expressed already 30 minutes after infection. E3 has dsRNA binding activity and K3 prevents the phosphorylation of eIF-2α by PKR (Beattie et al., 1995; Carroll et al., 1993; Chang et al., 1992).

Like TLR signaling, IFN signaling is also blocked by VACV. The virus codes for soluble type I IFN receptors which are secreted and bind to glycosaminoglycans of infected as well as non-infected cells. The binding of viral IFN receptors to as-yet uninfected cells provides the virus with susceptible host cells in which the establishment of an antiviral state is inhibited immediately upon infection without the need of de-novo protein synthesis (Symons et al., 1995; Alcamí et al., 2000; Montanuy et al., 2011). Type II IFN signaling is inhibited by soluble virus-encoded receptors as well (Alcamí & Smith, 1995). In contrast to the species-specific host IFN receptors, the virally encoded receptors can bind IFNs from different species, for example humans and rodents. This might be a hint for an evolution in not only one, but multiple hosts (Symons et al., 1995; Alcamí & Smith, 1995; Alcamí & Smith, 1996)

1.3.1.2 A46 – Current Knowledge

As stated above, A46 is one of the VACV-encoded proteins that inhibit TLR signaling. It was discovered by Bowie et al. (2000) in the course of searching for IL-1R/TLR family members. Despite sequence homology with TIR domains, the C-terminal domain of A46 was predicted to adopt a Bcl-2-like fold (Lysakova-Devine et al., 2010; González & Esteban, 2010). In agreement with this prediction, a mostly α-helical conformation, as is expected for a Bcl-2-like fold, was observed by Oda et al. (2011) using circular dichroism. The Bcl-2-like fold of the C-terminal domain of A46 was confirmed when the structure was solved by X-ray crystallography (see Fig. 6) (Fedosyuk et al., 2014; Kim et al., 2014).

A46 has a strong inhibitory effect on TLR-mediated signaling, due to direct interactions with the adapter proteins MyD88, MAL, TRAM and TRIF as well as the TIR domain of TLR4 (Stack et al., 2005). Although A46 targets all four activating TIR domain-containing adapter

proteins, an A46-derived peptide of eleven amino acids, called viral inhibitory peptide of TLR4 (VIPER), specifically inhibits TLR4 signaling by interacting with TRAM and MAL, but not TRIF or MyD88. Therefore, A46 seems to have distinct binding sites for different adapter proteins. Stack and Bowie (2012) reported that a functional BB loop in the adapter proteins is essential for their interaction with A46. TIR domains are composed of five β strands (βA – βE) that surround five α helices (αA – αE). The BB loop, which connects βB with αB, lies in a highly conserved, surface-exposed area (Xu et al., 2000). An important role for the BB loop in TLR-mediated signaling was found by several groups. For example, a proline to histidine mutation of a conserved proline in the BB loop of human as well as mouse TLR4 inhibits TLR4-dependent LPS-mediated signaling (Poltorak et al., 1998a; Ronni et al., 2003). The corresponding mutation in TLR2 (P186H) inhibits the interaction between TLR2 and MyD88 (Xu et al., 2000). Additionally, Horng et al. (2001) and Fitzgerald et al. (2001) did neither observe binding of MAL P125H to TLR4 nor signaling mediated by this mutant . Moreover, peptides derived from the MyD88 BB loop or peptidomimetics inhibit MyD88 homodimerization and MyD88-dependent signaling (Bartfai et al., 2003; Loiarro et al., 2007). The proline in TLRs seems to be essential for interactions involving MyD88, as TLR3, the only receptor that does not interact with MyD88, codes for an alanine instead of a proline in its BB loop. An alanine to proline mutation enables TLR3 to bind MyD88 (Verstak et al., 2013). Therefore, the conserved BB loop seems to be a likely target for A46 to disrupt at least MyD88-dependent signaling. Accordingly, Stack and Bowie (2012) found that the interaction between A46 and TLR4, MAL, MyD88 and TRIF is abolished *in vitro* as well as *in vivo* upon mutations of the conserved prolines to histidines. Although TRAM codes for cysteine instead of a proline on the respective position in the BB loop, it codes for a proline on the adjacent position. Mutations of either the proline or the cytosine to histidine inhibited interactions with A46 (Stack & Bowie 2012). In contrast, Dunne et al. (2003) observed association of MAL and MyD88 with each other and with TLR4 even if their BB loop prolines were mutated to histidines. Even the proline to histidine mutation in TLR4 that was previously reported to inhibit TLR4-mediated signaling could not abolish the association of the receptor with its adapters. However, as these findings were observed by GST-pull down assays with whole cell lysates and only one of the three binding partners was mutated in each experiment, the authors pointed out the possibility that the endougenous wild-type adapter might facilitate the interaction of the mutant adapter with the receptor (Dunne et al., 2003). A docking model by Fedosyuk et al. (2014) between A46 and TRAM shows possible interactions between the A46 VIPER motif and the TRAM BB loop. Neither the proline nor the histidine in the TRAM BB loop seem to be directly involved in binding, although they were reported to be essential for the interaction (Stack & Bowie; 2012). In contrast, the

phenylalanine on position 112 in TRAM is in close proximity to a leucine and an isoleucine on positions 93 and 94, respectively, in A46 (Fedosyuk et al., 2014). The leucine was shown to be essential for the interaction between VIPER and TRAM. It might, therefore, facilitate binding by hydrophobic interactions (Lysakova-Devine et al., 2010).

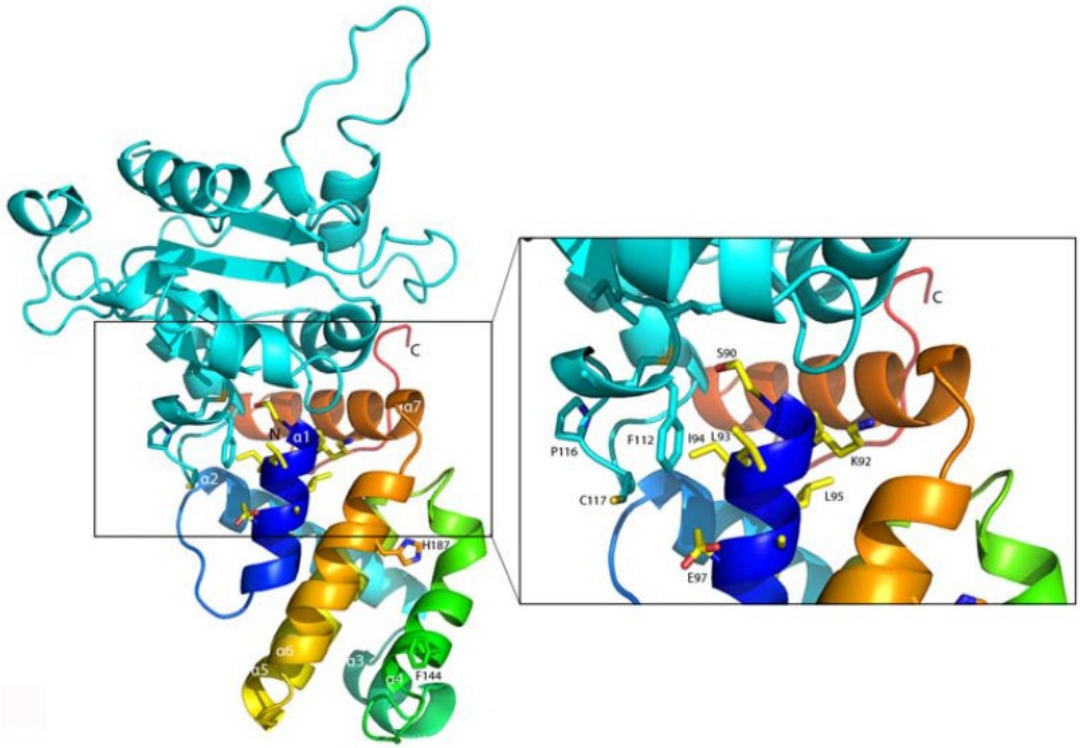

Fig. 6: Docking model of TRAM and A46(N87-T229). Docking model by Fedosyuk et al. (2014) of A46 (colour spectrum von N to C terminus) and TRAM (cyan). Residues of the VIPER motif in A46 and the BB loop in TRAM are shown in sticks. The interaction site between the two molecules is shown enlarged.

1.4 Aim of the Work

As described in the previous chapter, the BB loop in TLR adapter proteins is a likely target for A46. One aim of this study was to investigate if the amino acids F112, P116 and C117 in TRAM as well as I94 in A46 contribute to the binding of these two proteins. For this purpose, we constructed TRAM mutants with histidines on one or all of the positions of interest and an A46(N87-T229) I94A mutant. The affinity of binding between mutant and wild-type proteins was measured by microscale thermophoresis (MST).

The C-terminal domain of A46 is well characterized and its structure has been solved (Fedosyuk et al., 2014; Kim et al., 2014); nevertheless, little is known about the structure and function of the N-terminal 90 amino acids. A46 constructs lacking the first 80 (Oda et al.,

2011) or 86 (Fedosyuk et al., 2014) amino acids bind to MAL and MyD88 with similar affinities as the full-length protein, indicating that the N-terminal domain is not involved in binding to TLR adapter proteins. Moreover, the structural similarity between A46 and other Bcl-2-like proteins encoded by VACV does not include the N-terminal 90 amino acids (see Fig. 5). Given the lack of knowledge on the N-terminus, we wanted to investigate the function and structural features of this domain of A46. We therefore set out to express and purify the A46 N-terminus. During the course of this thesis, we determined the oligomeric state of A46 N-terminal variants by SEC-MALLS and investigated its role in the interaction with TLR adapter proteins by MST.

Additionally, we wanted to further characterize MyD88, one of the TLR adapter proteins that is targeted by A46. The structure of the human TIR domain of MyD88 has been published (Ohnishi et al., 2009) and the structure of the murine counterpart has recently been solved (Fedosyuk et al., unpublished data). As can be seen in Fig. 7, the protein sequences of the human and murine orthologs are very similar, especially in the C-terminal TIR domain that is formed by residues 160 to 296. We wanted to test whether the altered residues in human MyD88 are important for the interaction with human MAL by comparing the affinities of human and murine MyD88 TIR domains to the TIR domain of human MAL. We therefore tried to express and purify amino acids 157 to 296 of human and murine MyD88. These residues are covered by the structure published by Oshini et al. (2009) and a protocol for the expression and purification of human MyD88(157-296) has been published (Synders et al., 2013). The corresponding amino acids are underlined in yellow in Fig. 7.

```
MyD88_mouse       MSAGDPRVGSGSLDSFMFSIPLVALNVGVRRRLSLFLNPRTPVAADWTLLPEEMGFEYLE 60
MyD88_human       MAAGGPGAGSAAPVSSTSSLPLAALNMRVRRRLSLFLNVRTQVAADWTALAEEMDFEYLE 60
                  *:**.* .**.:  *   *:**.***: ********** ** ****** *.***.*****

MyD88_mouse       IRELETRPDPTRSLLDAWQGRSGASVGRLLELLALLDREDILKELKSRIEEDCQKYLGKQ 120
MyD88_human       IRQLETQADPTGRLLDAWQGRPGASVGRLLELLTKLGRDDVLLELGPSIEEDCQKYILKQ 120
                  **:***:.***  ********.***********: *.*:*:* ** . ********: **

MyD88_mouse       QNQESEKPLQVARVESSVPQTKELGGITTLDDPLGQTPELFDAFICYCPNDIEFVQEMIR 180
MyD88_human       QQEEAEKPLQVAAVDSSVPRTAELAGITTLDDPLGHMPERFDAFICYCPSDIQFVQEMIR 180
                  *::*:******* *:****:* **.**********: ** *********.**:*******

MyD88_mouse       QLEQTDYRLKLCVSDRDVLPGTCVWSIASELIEKRCRRMVVVVSDDYLQSKECDFQTKFA 240
MyD88_human       QLEQTNYRLKLCVSDRDVLPGTCVWSIASELIEKRCRRMVVVVSDDYLQSKECDFQTKFA 240
                  *****:************************************************************

MyD88_mouse       LSLSPGVQQKRLIPIKYKAMKKDFPSILRFITICDYTNPCTKSWFWTRLAKALSLP 296
MyD88_human       LSLSPGAHQKRLIPIKYKAMKKEFPSILRFITVCDYTNPCTKSWFWTRLAKALSLP 296
                  ******.:**************:*********:************************
```

Fig. 7: Alignment of murine and human MyD88. The protein sequences of murine and human MyD88 were aligned using the ClustalW2 online alignment tool. Residues 157 to 296 that were expressed are underlined with yellow.

2 Methods and Materials

2.1 Standard Techniques

2.1.1 Centrifugation

Centrifugations were performed with Sorvall RC-5C, Sorvall RC 6 Plus or Eppendorf 5810 R centrifuges at 4 °C. For plasmid midi preparations (see chapter 2.1.3.2) and centrifugations in the course of protein purifications (see chapter 2.2.2), Sorvall centrifuges with a Fiberlite™ F21S-8x50y rotor were used. For the harvesting of protein expressing cells, Sorvall centrifuges with a F9S-4x1000 rotor were used. Harvesting of cells in the course of making them competent, as well as the concentration of protein solutions were performed with an Eppendorf 5810 R centrifuge. Centrifugations of 1.5 or 2 ml tubes, for example for plasmid mini preparations, were performed in Eppendorf 5415 D table-top centrifuges at room temperature or in Eppendorf 5415 C centrifuges at 4 °C.

2.1.2 Electrophoresis

2.1.2.1 Agarose Gel Electrophoresis

Agarose gels were prepared by dissolving the desired amount of agarose (for x % gels: x g agarose/100ml) in 1 x TAE buffer in a microwave. The DNA samples were mixed 1:6 with 6 x Orange DNA Loading Dye (Thermo Scientific) and loaded into the pockets. As marker, 5 µl GeneRuler™ 1kb Plus DNA Ladder (Thermo Scientific) was used. Agarose gel electrophoresis was performed at 120 V for 15 – 20 min. The gel was stained in an ethidium bromide bath for 15 – 30 min. Ethidium bromide intercalates DNA. Only DNA-bound ethidium bromide fluoresces upon excitation with UV light. Therefore, DNA bands are visible under UV light.

100 x TAE buffer:	20 mM Tris base, 5 mM sodiumacetate, 1 mM EDTA, pH to 8.2 with acetic acid
Ethidium bromide bath:	10^{-4} % ethidium bromide in 1 x TAE buffer

2.1.2.2 SDS Polyacrylamide Gel Electrophoresis

SDS polyacrylamide gel electrophoresis (SDS-PAGE) separates proteins by means of mass. The gel consists of a separating and a stacking gel, differing in the acrylamide concentration

and the pH. Proteins are concentrated at the interface between the two gels before entering the separating gel. SDS shields charged residues. Therefore, the proteins are separated only by means of mass but not by charge. For the separation of small proteins, higher concentrations of acrylamide and bis-acrylamide are used than for the separation of larger proteins. We used separating gels with 17.5 % acrylamide. The compositions of separating and stacking gels are listed in Table 2. Protein samples were mixed with 2 x Laemmli sample buffer prior to loading. Electrophoresis was performed at 300 V for 25 – 30 min. in 1 x Laemmli running buffer. The gels were stained in Coomassie staining solution for 5 – 20 min. and destained in H_2O. Coomassie is a blue dye that binds proteins unspecifically, therefore making them visible as blue bands. The strength of the colour correlates with the amount of protein.

	Separating gel	Stacking gel
MQ H_2O	1 ml	853 µl
Upper Gel Buffer	---	375 µl
Lower Gel Buffer	1 ml	---
Acrylamide:Bis-Acrylamide (1:29)	2 ml	255 µl
APS	50 µl	15 µl
TEMED	5 µl	1.5 µl

Table 2: Composition of 17.5 % SDS polyacrylamide gels for electrophoresis. Recipe for the preparation of separating and stacking gel. APS and Temed induce radical polymerization of acrylamide to polyacrylamide.

2 x Laemmli sample buffer:	20 % v/v glycerol, 10 % β-mercaptoethanol, 6 % SDS, 125 mM Tris/HCl pH = 6.8, 0.01 % bromphenol blue
10 x Laemmli running buffer:	30 g/L Tris, 144 g/L glycine, 10 g/L SDS
Coomassie staining solution:	45 % methanol, 10 % acetic acid, 0.4 % Coomassie brilliant blue R250
Upper Gel Buffer:	0.5 M Tris/HCl pH 6.8
Lower Gel Buffer:	1.5 M Tris/HCl pH 8.8

2.1.2.3 Western Blot

Western Blots are used to identify a protein of interest on an SDS-PAGE gel by specific antibodies. After performing an SDS-PAGE, the proteins were transferred from the gel onto a Protran® nitrocellulose membrane (Sigma Aldrich) by wet blotting in a Mini Trans-Blot® cell (Bio-Rad) in transfer buffer. Blotting was performed at 300 V for 50 min. To prevent

unspecific binding of the primary antibodies to the membrane, the membrane was blocked with 20 mg caseine dissolved in 10 ml of PBS-T for one hour. 3.3 µl of mouse anti-His antibody (GE Healthcare Life Sciences) were directly added into the blocking solution (resulting in a 1:3 000 dilution). After incubation for at least one hour, the primary antibody was removed and the membrane was washed 3 times 10 min. in PBS-T. 10 ml of goat anti-mouse antibody (IgG H+L), conjugated to horseradish peroxidase (Jackson Laboratories, diluted 1:10 000 in PBS-T) were incubated with the membrane for 1.5 – 2 hours. After washing 3 times for 10 min. with PBS-T, the reporter reaction was induced using the SuperSignal Western Blot Enhancer kit (Thermo Scientific) as described by the manufacturer. A CL-XPosure Film (Thermo Scientific) was exposed to the membrane for 10 sec. to 1 min., depending on the strength of the signal, and was developed in the dark (AGFA Entwickler G 153, AGFA Fixer G354). Horseradish peroxidase catalyzes the conversion of a substrate to a luminescent product. The photons emitted by the product stain the film. As the peroxidase is coupled to the secondary antibody which in turn is bound to the anti-His-antibodies, a stain on the film indicates the position of His-tagged proteins on the membrane.

Transfer buffer:	25 mM Tris base, 192 mM glycine, 20 % methanol
PBS:	137 mM NaCl, 2.7 mM KCl, 10 mM Na_2HPO_4, 1.8 mM KH_2PO_4, pH to 7.4 with HCl
PBS-T:	PBS + 0.1 % Tween-20

2.1.3 Purification, Mutation and Transformation of Plasmids

2.1.3.1 Plasmid Mini-Prep

For small amounts of cell culture, plasmid mini preparations were performed using Wizard® *Plus* SV Minipreps DNA Purification Systems from Promega as described by the manufacturer.

2.1.3.2 Plasmid Midi-Prep

Plasmid preparations for larger quantities of plasmid were performed with NucleoBond® PC 100 from Macherey-Nagel with only minor deviations from the manual provided by the manufacturer. The cells of 100 ml over-night culture were harvested at 6 000 rpm at 4 °C for 15 min. The cell pellet was resuspended in 4 ml buffer S1 with added RNase A. 4 ml buffer S2 were added and the tubes were inverted several times to mix the solutions. 4 ml buffer S3

(pre-cooled to 4 °C) were added. The samples were mixed by inverting the tubes and centrifuged at 15 000 rpm at 4 °C for 10 min. A filter was inserted into each NucleoBond® column. 5 ml buffer N2 were added to each column to pre-wet the filters and to equilibrate the columns. The cleared supernatant was loaded onto the columns and bound to the resin by gravity flow. Bound DNA was washed with 10 ml buffer N3 and eluted with 5 ml buffer N5 into a 50 ml centrifugation tube. After precipitating the plasmids with 3.5 ml isopropanol, the solutions were centrifuged at 18 000 rpm at 4 °C for 20 min. The pellets were washed by adding 2 ml of 70 % ethanol and subsequent centrifugation at 17 000 rpm for 10 min. The ethanol was removed and the pellets were air-dried. DNA pellets were dissolved in 200 µl of MQ H_2O and the concentration was determined by Nanodrop ND-1000.

2.1.3.3 Polymerase Chain Reactions

Polymerase Chain Reactions (PCRs) are performed to amplify a desired DNA region. The region is defined by specific primers complementary to the ends of the desired fragment. The samples are heated to 95 °C to break base-pairing interactions of the DNA template. After cooling down to the annealing temperature, the primers can bind to the now single-stranded DNA strands. The samples are heated to 72 °C to allow elongation of the primers by a heat-resistant DNA polymerase. Two polymerases are widely used: Taq, which was isolated from *Thermus aquaticus* (Chien et al. 1976) or Pfu, which was isolated from *Pyrococcus furiosus* (Lundberg et al. 1991). In contrast du Taq, Pfu has 3'-5' exonuclease activity and therefore a higher fidelity (Cline et al. 1996; Lundberg et al. 1991). The elongation time depends on the length of DNA to be amplified. The cycle of heating and cooling the samples is repeated several times. The DNA is duplicated in every cycle. Therefore, the amount of DNA increases exponentially. Table 3 shows the composition of PCR samples for different purposes.

After transformation of plasmids resulting from the cloning of A46 or MyD88 variants (see chapter 2.1.3.6), colony PCR was used to identify E. coli clones bearing the desired plasmid resulting from successful ligation of vector and insert. For each construct, 10 single colonies were picked and inoculated into 10 µl sterile MQ H_2O. These cell suspensions served as template. The composition of the PCR samples is listed in Table 3. A positive control was set up by using the plasmid that was used as template for cloning as template for the colony PCR.

	Site-directed mutagenesis	A46 and MyD88 variants	Colony PCR
MQ H_2O	37.5 µl	32.5 µl	15.75 µl
10 x Pfu Buffer (Promega)	5 µl	-	-
5 x GoTaq Buffer (Promega)	-	10 µl	5 µl
dNTPs (2 mM, Invitrogen)	5 µl	5 µl	2.5 µl
forward primer	0.5 µl	0.5 µl	0.25
reverse primer	0.5 µl	0.5 µl	0.25
template	1 µl	1 µl	1 µl
Pfu	0.5 µl	-	-
GoTaq polymerase (Promega)	-	0.5 µl	0.25
annealing temperature	50 °C	50 °C	50 °C (A46) 55 °C (MyD88)
elongation time	12 min.	30 sec. (A46) 80 sec. (MyD88)	30 sec. (A46) 1 min. (MyD88)
number of cycles	25	30	25

Table 3: PCR set-ups. Composition of PCR samples, annealing temperature, elongation time and number of cycles for PCRs in the course of site-directed mutagenesis, amplification of A46 and MyD88 gene fragments and colony PCR

2.1.3.4 Isolation of DNA from PCR Samples

PCR products were isolated using the Wizard® SV Gel and PCR Clean-Up System (Promega). The PCR samples were mixed with an equal volume of Membrane Binding Solution and loaded onto the SV minicolumn inserted into a collection tube. To isolate DNA out of an agarose gel, the band containing the DNA of interest was cut out and mixed with 1 µl Membrane Binding Solution per mg gel. The gel was dissolved by heating at 65 °C and vortexing. The DNA was bound to the membrane by centrifuging at 13 000 rpm at room temperature for one minute. The flow-through was discarded and the DNA was washed twice with 650 µl Wash Solution. After discarding the flow-through, the column was centrifuged again at 13 000 rpm for 3 min. to remove any residual ethanol. The DNA was eluted with MQ H_2O.

2.1.3.5 Site-Directed Mutagenesis of A46(N87-T22) and TRAM(66-235)

Point mutations were introduced into the TIR domain of the TLR adapter protein TRAM as well as into A46(N87-T229) by site-directed mutagenesis. In this approach, a mutation is introduced during a PCR by primers coding for the desired mutation. The primers are overlapping and complementary. Therefore, the PCR product consists of single-stranded DNA with sticky ends. When the complementary strands base-pair, they form plasmids with one nick on each strand. This PCR product can be directly used for transformation (see chapter 2.1.3.8). The nicks are sealed by E. coli. The PCR set-up is listed in table 3 (chapter 2.1.3.3).

The efficiency of the PCR was checked by agarose gel electrophoresis with a 0.8 % agarose gel (see chapter 2.1.2.1). If a product with the size of the desired plasmid but no side products were observed, the DNA was isolated from the PCR samples using the Wizard® SV Gel and PCR Clean-Up System (see chapter 2.1.3.4). The DNA was eluted in 50 µl MQ H_2O.

5 µl MQ H_2O, 6 µl 10 x CutSmart Buffer (New England BioLabs) and 1 µl DpnI (New England BioLabs) were added and the sample was incubated at 37 °C for 3 hours. DpnI degrades methylated, but not unmethylated DNA. Therefore, it specifically degrades the template plasmid but not the PCR products. After DpnI treatment, the PCR product was isolated using the Wizard® SV Gel and PCR Clean-Up System. The product was eluted in 30 µl MQ H_2O. 4 µl of purified PCR product were transformed into E. coli Top 10 (see chapter 2.1.3.8). The cells were plated on LB agar plates with ampicillin (Amp.) in the case of TRAM-encoding E. coli and kanamycin (Kan.) in the case of E. coli transformed with plasmids coding for A46(N87-T229). The cells were incubated at 37 °C over-night. A plasmid midi preparation (see chapter 2.1.3.2) was performed to isolate the amplified plasmids. The presence of the desired mutation was confirmed by sequencing (by Microsynth). The primers gex3-rev and T7term from the standard primer list were used for sequencing of TRAM mutants and the A46(N87-T229) mutant, respectively.

Table 4 shows the primers and templates that were used for the production of different mutants. For the triple mutant TIR/TRAM F112A P116H C117H, the mutation P116H was introduced first. The resulting plasmid was used as template for the PCR introducing the mutation F112A with the primer pair TIM2107/TIM2108. The primer pair TIM2117/TIM2118 (coding for the mutations P116H as well as C117H) was used to introduce the mutation C117H, using the plasmid with the double mutation as template. The template plasmids

coding for wild-type TRAM(66-235) or A46(N87-T229) were kindly provided by Sofiya Fedosyuk.

Mutation to be introduced	Forward primer	Reverse primer	Template
P116H in TIR/TRAM	TIM2103	TIM2104	pGEX6-TIR/TRAM
C117H in TIR/TRAM	TIM2105	TIM2106	pGEX6-TIR/TRAM
F112A in TIR/TRAM	TIM2107	TIM2108	pGEX6-TIR/TRAM
C117H in TIR/TRAM F112A/P116H	TIM2117	TIM2118	pGEX6-TIR/TRAM F112A/P116H
I94A in A46(N87T229)	TIM2113	TIM2114	pHISTEV-A46N87T229)

Table 4: Mutations introduced into TRAM(66-235) and A46(N87-T229). Point mutations were introduced into a TRAM(66-235)-encoding pGEX-6 plasmid and an A46(N87-T229)-encoding pHISTEV plasmid by site-directed mutagenesis. This table shows the point mutations as well as the primers and templates for the mutagenesis PCR.

TIM2103:	CTTTGCTGAGATGCACTGTGGCAGACAGC
TIM2104:	GCTGTCTGCCACAGTGCATCTCAGCAAAG
TIM2105:	CTTTGCTGAGATGCCACATGGCAGACAGC
TIM2106:	GCTGTCTGCCATGTGGCATCTCAGCAAAG
TIM2107:	CCCGGAATAATCGCTGCTGAGATG
TIM2108:	CATCTCAGCAGCGATTATTCCGGG
TIM2113:	GTTTTAAACTGGCTTTAGCAG
TIM2114:	CTGCTAAAGCCAGTTTAAAAC
TIM2117:	GTTCCATGGGTGATGGGGTTACATTTCCATTTAAACCAG
TIM2118:	CCACCAGTCATGCTAGCCATGGTCACTAGTGGTG

2.1.3.6 Production of Plasmids Coding for A46 and MyD88 Variants

Different A46 N-terminal domain variants as well as murine and human TIR domains of MyD88 and full-length hMyD88 were amplified by PCR and cloned into expression vectors. The composition of the PCR samples is listed in table 3 (chapter 2.1.3.3). Template plasmids and expression vectors were kindly provided by Sofiya Fedosyuk.

For the amplification of the A46 N-terminus, a plasmid coding for amino acids 1 to 229 of A46 was used. The annealing temperature was 50 °C and the elongation time was 30 sec. TIM2119 was used as forward primer. This primer contains an NcoI restriction site and codes for a TEV cleavage site. TEV cleaves between the glycine and glutamine of the sequence

ENLYFQ/G. In addition to the glycine that remains from the TEV cleavage site, the primer codes for five additional amino acids, AMAQQ, in between the cleavage site and the first methionine of A46. The reverse primers TIM2120, TIM2121 and TIM2122 contain a cleavage site for BamHI and a stop codon after S90, T83 or G73, respectively. The resulting PCR products were inserted into the plasmids pTRX or pMBP. They are derived from the pET vector series (Novagen) and code for a kanamycine resistance gene. Moreover, they code for six histidines and maltose-binding protein (MBP) in the case of pMBP or thioredoxin (TRX) in the case of pTRX in line with the inserted gene. MBP and TRX serve as solubility and affinity tags. Resulting proteins were named MBP-/TRX-A46(6M1-G73/T83/S90). The digit “6” is written in front of the “M1” to refer to the additional six amino acids GAMAQQ on the N-terminus.

A plasmid coding for mMyD88(146-296), derived from pGEX-4T-1 (GE Healthcare), served as template for the amplification of amino acids T157 to P296 of murine MyD88. Primers TIM2138 (forward) and TIM2137 (reverse) were used. A pcDNA3.0 plasmid (Invitrogen) with inserted Flag-tagged full-length human MyD88 was used as template to amplify the full-length human MyD88 gene, using the primers TIM2134 (forward) and TIM2133 (reverse). The human MyD88 TIR domain covering amino acids M157 to P296 was cloned from the same template with the primers TIM2135 (forward) and TIM2133 (reverse). The PCR to amplify the genes was performed with an annealing temperature of 55 °C and an elongation time of 1:20 min (see Table 3, chapter 2.1.3.3). The forward and reverse primers coded for NcoI or BamHI restriction site, respectively. The isolated inserts were cloned into pTRX.

A test PCR with 25 cycles was performed. 5 µl of the PCR samples were analysed by gel electrophoresis using a 1 % agarose gel. After confirming the correct size of the product bands, the PCR was repeated with four samples per gene and 30 cycles. All five PCR samples were pooled and the DNA was isolated using the Wizard® SV Gel and PCR Clean-Up System as described (see chapter 2.1.3.4). The DNA was eluted in 80 µl of MQ H_2O.

The PCR products as well as the vectors were cleaved with NcoI and BamHI. The use of two different restriction enzymes ensures that the PCR product is inserted into the plasmid in the correct orientation. Moreover, the frequency of religation events of the plasmids is reduced. To cleave the inserts, 10 µl MQ H_2O, 10 µl 10 x CutSmart Buffer (New England BioLabs) and 1 µl of BamHI and NcoI (New England BioLabs) were added to the purified PCR products. About 30 ng of plasmid were mixed with 10 µl 10 x CutSmart Buffer and 1 µl of BamHI and NcoI. The volume was adjusted to 100 µl by MQ H_2O. The samples were incubated for 2.5

hours at 37 °C. After one hour, 1 µl Calf Intestine Protease (New England BioLabs) was added to the vector samples. Dephosphorylation of the cleaved vectors is an additional pre-caution to prevent re-ligation without insert. Plasmids and inserts were isolated with the Wizard® SV Gel and PCR Clean-Up System as described (see chapter 2.1.3.4). The restricted PCR products were eluted in 30 µl of MQ H_2O and stored at -20 °C. The plasmids were eluted in 50 µl MQ H_2O and mixed with 20 µl of 6 x DNA Loading buffer (Thermo Scientific). Cleaved plasmids were separated from uncleaved plasmids by agraose gel electrophoresis with a 0.8 % agarose gel (see chapter 2.1.2.1). The restricted plasmids were cut out of the gel and isolated using the Wizard® SV Gel and PCR Clean-Up System (see chapter 2.1.3.4). The plasmids were eluted in 30 µl MQ H_2O. Vector and insert were ligated by Quick Ligase. 1 µl of restricted insert was mixed with approximately 100 ng of restricted, dephosphorylated vector. 10 µl 2 x Quick Ligase Buffer and 1 µl Quick Ligase (New England BioLabs) were added. The volume was adjusted to 20 µl with MQ H_2O. After 5 minutes of incubation at room temperature, the ligation reaction was transformed into competent E. coli Top 10 (see chapter 2.1.3.8).

Colony PCR was used to test the colonies for the plasmids of interest (see chapter 2.1.3.3). To identify clones bearing the plasmids for A46 N-terminal variants, the forward primer TIM2119 and the reverse primer TIM2121 were used. The annealing temperature was 50 °C and the elongation time was 30 sec. To identify colonies coding for the MyD88 variants, the primer pairs TIM2134/TIM2135 or TIM2137/TIM2138 were used to test for human or murine MyD88-coding plasmids, respectively. The annealing temperature was 55 °C and the elongation time was 1 min. The PCR samples were analysed by gel electrophoresis using a 1 % agarose gel. As the primers bind to the insert but not the plasmid, a PCR product is only observed if the resistance-conferring plasmid contains the insert. The cell suspensions of positive clones were inoculated into 100 ml LB with 0.5 µg/ml Kan. and were grown at 37 °C, 220 rpm over-night for subsequent plasmid midi preparation (see chapter 2.1.3.2). The plasmids were sequenced by Microsynth AG. As primer for sequencing, T7term from the standard primer list was used.

TIM2120:	GCCCGGATCCACTATACTTATTATACAAGTAAGTC
TIM2121:	GCCC GGATCC AGTCATACTAACCGGCGTATTAAC
TIM2122:	GCCC GGATCC ACCAATATTAGTTTCCTCTG
TIM2133:	CGCAAGCCATGGCTGCAGGAGGTCCCGGTG
TIM2134:	CCAC GGATCC TCAGGGCAGGGACAAGGCC
TIM2135:	CGCAAGCCATGGGAATGCCTGAGCGTTTCGATGC
TIM2137:	CCACGGATCCTCAGGGCAGGGACAAAGC
TIM21:38:	CGCAAGCCATGGGAACGCCGGAACTTTTCGATG

2.1.3.7 Making E. Coli Competent

E. coli do not inherently have the ability to take up foreign DNA. Therefore, it is necessary to make them competent to do so prior to transformation. Cells of the desired strain from a glycerol stock stored at -80 °C were inoculated into 3 ml of 2 x TY medium and grown at 37 °C, 220 rpm over-night. The over-night culture was inoculated into 100 ml of 2 x TY and incubated at 37 °C, 220 rpm until the OD600 reached 0.5 – 0.6. The cell culture was split into two 50 ml Falcon tubes and incubated on ice for 15 min. The cells were harvested at 2 500 rpm at 4 °C for 15 min. The supernatant was discarded and the pellets were resuspended in a total of 30 ml RF1. After incubation on ice for 15 min., the cells were pelleted again at 2 500 rpm. The supernatant was discarded and the pellets were resuspended in a total of 8 ml RF2. The competent cells were aliquotted (200 µl in the case of Top 10, 50 µl in the case of strains for expression), snap-freezed in liquid nitrogen and stored at -80 °C.

2 x TY medium:	16 g/L tryptone, 10 g/L yeast extract, 5 g/L NaCl, pH to 7.0 with NaOH
RF1:	100 mM KCl, 50 mM $MnCl_2$, 30 mM KAc, 10 mM $CaCl_2$, 15 % (w/v) glycerol, pH to 5.8 with HCl
RF2:	10 mM MOPS, 10 mM KCl, 75 mM $CaCl_2$, 15 % (w/v) glycerol, pH to 6.8 with KOH

2.1.3.8 Transformation

Competent E. coli of the desired strain were thawed on ice for five to ten min. E. coli Top 10 were used for the amplification of plasmids. For protein expression, E. coli B834, B834 LysS, T7 Express, BL21(DE3), BL21(DE3) LysS or BL21(DE3) Codon Plus were used. 1 µl of the desired plasmid (50 – 200 ng/µl) or a ligation reaction were added to the competent cells. After incubation on ice for 10 min., the cells were heat-shocked at 42 °C for 45 seconds. 400 µl LB medium were added and the cells were incubated at 37 °C for at least 30 min. For primary transformation with ligation reactions or after site-directed mutagenesis, all cells were plated on selective LB agar plates. For protein expression, one fourth to one third of transformed cells was plated on selective LB agar plates or directly inoculated into 100 ml LB medium with respective antibiotics.

LB medium:	10 g/L tryptone, 5 g/L yeast extract, 10 g/L NaCl, pH 7

2.2 Protein Expression and Purification

2.2.1 Protein Expression

Recombinant proteins were expressed in E. coli. A single colony of transformed cells plated on LB agar plates or one third to one fourth of a transformation sample were inoculated into 100 ml LB with respective antibiotics and incubated at 37 °C, 220 rpm over-night. 20 – 25 ml of the over-night culture were inoculated into 2 L LB with respective antibiotics and grown at 37 °C, 180 rpm until the OD600 reached ~ 0.6. As the expression of the recombinant proteins was under the control of a lac operon, expression could be induced by IPTG. IPTG is an analogon of galactose which cannot be metabolized and therefore continuously activates expression. Different proteins were expressed at different temperatures for either four hours or over-night. Table 5 shows the strain of E. coli, the concentration of IPTG, the antibiotics for selection as well as the temperature and duration of expression for different proteins. Any mutant forms of those proteins were expressed under the same conditions as the wild-type form.

Protein	E. coli strain	[IPTG]	Antibiotic	Temperature	Duration
A46(N87-T229)	B834 LysS	0.25 mM	Amp. (1 µg/ml), CAM. (0.34 µg/ml)	16 °C after cold-shock	o/n
TRAM(66-235)	T7 Express	1 mM	Amp. (1 µg/ml)	25 °C	o/n
mMyD88 (146-296)	BL21	1 mM	Amp. (1 µg/ml)	37 °C	o/n
MAL(79-221)	B834	0.25 mM	Amp. (1 µg/ml)	25 °C	o/n
A46(6M1-G73) A46(6M1-T83) A46(6M1-S90)	BL21(DE3)	0.25 mM	Kan. (0.5 µg/ml)	23 °C	4 hours
His-TEV	BL21(DE3)	0.5 mM	Amp. (1 µg/ml)	37 °C	4 hours
PreScission protease	BL21(DE3) pLysS Rosetta	0.2 mM	Amp. (1 µg/ml)	16 °C	o/n

Table 5: Expression conditions for different proteins. This table shows the strain of E. coli, the IPTG concentration for induction, the antibiotics used for selection as well as the temperature and duration of expression for different proteins.

2.2.2 Protein Purification

The cells expressing the protein of interest were harvested at 6 000 rpm and resuspended in a buffer specific for the expressed protein (see chapters 2.2.2.2 - 2.2.2.6). The resuspended cells were stored at -80 °C. After thawing, cells were lysed by three to four passages through a French pressure cell press (EmulsiFlex-C3 from Avestin) or four to five times 1 min sonication with Sonopuls HD200 (Bandelin) with a MS 73/D microtip and 40 cycles. 0.5 – 2 mg DNase I were added and the cell lysates were centrifuged at 18 000 rpm for 20 to 30 min. to separate soluble proteins from insoluble material. The soluble phase was filtered through a 0.45 µm polyvinyl difluoride Rotilabo® syringe filter (Carl Roth). Proteins of interest were purified by affinity chromatography and, in most cases, subsequent size exclusion chromatography (SEC). The peak fractions of SEC were analysed by SDS-PAGE. Samples containing the highest concentration of protein of interest without impurities were concentrated to 100 – 500 µl using Amicon® Ultra 4 ml or Amicon® Ultra 15 ml centrifugal filter devices (Merck Millipore) with a cut-off of 10 kDa. Protein concentrations were determined by measuring the UV absorption at 230 nm using a Nanodrop ND-1000. Absorption coefficients and molecular weights of the proteins of interest were calculated with the ExPASy ProtParam tool. The samples were flash-freezed in liquid N_2 and stored at -80 °C.

2.2.2.1 Chromatographies

The first protein purification step was an affinity chromatography. His-tagged proteins were purified by Ni-NTA chromatography. Ni-NTA agarose (Qiagen) was charged with 300 mM $NiCl_2$. Ni^{2+} is immobilized by nitrilotriacetic acid (NTA) in the resin and can chelate histidines. Bound proteins were eluted with high concentrations of imidazole which competes with histidines for binding to Ni^{2+}. Low concentrations of imidazole in the resuspension buffers prevent unspecific binding of proteins to the resin. The Ni^{2+} ions can be stripped off the column with 50 mM EDTA. GST-tagged proteins were purified with a 5 ml GSTrap FF column (GE Healthcare) used in an ÄKTA FPLC system (GE Healthcare). Bound proteins were eluted with reduced glutathione which is a competitive inhibitor of the interaction between GST and the resin. The columns were pre-equilibrated with the respective resuspension buffer, which had been filtered through a 0.22 µm nitrocellulose filter membrane (Sigma-Aldrich).

SECs were performed with HiLoad 16/600 or 26/600 Superdex 75 or Superdex 200 prep grade gel filtration columns (GE Healthcare) in an ÄKTA FPLC system. The columns were pre-equilibrated in the respective, filtered storage buffer.

2.2.2.2 Purification of His-TEV Protease

TEV protease was used to cleave His-TRX and His-MBP tags off recombinant proteins. The soluble phase of the TEV protease-containing cell lysate from 2 L expression culture was passed through 5 ml of Ni-NTA agarose by gravity flow. Bound proteins were washed with 15 ml resuspension buffer and eluted with 15 ml TEV elution buffer into 5 ml of TEV storage buffer. The resulting 20 ml were aliquotted á 1 ml, flash-freezed in liquid N_2 and stored at -80 °C.

TEV resuspension buffer:	20 mM Tris/HCl pH 8.0, 300 mM NaCl, 5 % glycerol, 20 mM imidazole, 15 mM β-mercaptoethanol
TEV elution buffer:	20 mM Tris/HCl pH 8.0, 300 mM NaCl, 5 % glycerol, 200 mM imidazole, 15 mM β-mercaptoethanol
TEV storage buffer:	20 mM Tris/HCl pH 8.0, 300 mM NaCl, 5 % glycerol, 20 mM imidazole, 15 mM β-mercaptoethanol, 20 % glycerol

2.2.2.3 Purification of PreScission Protease

PreScision protease was expressed as GST-fusion protein. The filtered soluble phase of the cell lysate was passed through a 5 ml GSTrap FF column with a flow rate of 1 ml/min and was washed with five column volumes of resuspension buffer. The protease was eluted with 3 – 5 column volumes of elution buffer. The soluble phase, flow-through and peak fractions were analysed by SDS-PAGE. Protease-containing elution fractions were pooled and dialysed against 2 L of storage buffer at 4 °C over-night. The dialysed sample was centrifuged at 18 000 rpm at 4 °C for 30 min. to remove precipitated protein. The supernatant was analysed by SDS-PAGE and flash-freezed as 300 µl aliquots. The protease was stored at -80 °C.

PreScission Protease resuspension buffer:	50 mM Tris/HCl pH 8.0, 1 M NaCl, 1 mM EDTA, 1 mM DTT
PreScission Protease elution buffer:	50 mM Tris/HCl pH 8.0, 1 M NaCl, 1 mM EDTA, 1 mM DTT, 10 mM GSH
PreScission Protease storage buffer:	50 mM Tris/HCl pH 8.0, 150 mM NaCl, 10 mM EDTA, 1 mM DTT, 20 % glycerol

2.2.2.4 Purification of A46 Variants

A46(6M1-S90), A46(6M1-T83) and A46(6M1-G73) were expressed as His-MBP- or His-TRX fusion proteins. His-tagged A46(N87-T229) wt or I94A were purified in the same way. The first purification step was an affinity chromatography performed with Ni-NTA resin as described (chapter 2.2.2.1). Bound proteins were washed with 15 – 20 ml A46 resuspension buffer and eluted in 15 – 20 ml A46 elution buffer. 0.25 – 1 ml of previously purified TEV protease was added to the elution and the sample was dialysed against 2 L of A46 dialysing buffer I at 4 °C over-night. The protease as well as uncleaved fusion protein and the cleaved-off tags were removed by four passages through 5 ml Ni-NTA resin pre-equilibrated with the filtered dialysing buffer I. The cleaved protein of interest is present in the flow-through whereas the protease, tags and uncleaved fusion proteins bind to the column. In between each load, bound proteins were eluted with 15 ml of elution buffer, the column was washed with 15 ml of ddH_2O and equilibrated with 10 ml of dialysing buffer I. After four passages, the flow-through was dialysed against 2 L of A46 dialysing buffer II at 4 °C for at least two hours or over-night. The last purification step was SEC. The dialysed sample was concentrated to 1 – 5 ml using Centriprep YM-10 filter units (Merck Millipore) with a 10 kDa cut-off. The chromatography was performed in A46 storage buffer with HiLoad 16/600 or 26/600 Superdex 75 prep grade columns, depending on the amount of protein. The chromatography was performed at a speed of 1 ml/min in case of the column with a diameter of the 16/600 column and 1.5 to 2 ml/min in the case of the 26/600 column. The samples containing the highest concentration of pure protein of interest were pooled and concentrated to a volume of 250 µl to 1 ml to achieve protein concentrations higher than 5 mg/ml. The protein concentration was determined by NanoDrop ND-1000. To determine the accuracy of NanoDrop measurements, the concentration of two samples was additionally determined with the “BCA Protein Assay – Reducing Agent Compatible” kit (Thermo Scientific) as described by the manufacturer.

A46 resuspension buffer:	20 mM Tris/HCl pH 8.5, 100 mM NaCl, 25 mM imidazole, 5 % glycerol, 10 mM β-mercaptoethanol
A46 elution buffer:	20 mM Tris/HCl pH 8.5, 300 mM NaCl, 200 mM imidazole, 15 mM β-mercaptoethanol
A46 dialysing buffer I:	20 mM Tris/HCl pH 8.5, 150 mM NaCl, 10 mM imidazole, 15 mM β–mercaptoethanol
A46 dialysing buffer II:	20 mM Tris/HCl pH 8.5, 2 mM DTT
A46 storage buffer:	20 mM Tris/HCl pH 8.5, 5 mM DTT

2.2.2.5 Purification of hMAL(79-225)

A plasmid derived from the pET vector series (Novagen) coding for the TIR domain of MAL, covering amino acids 79 to 221 with a His-tag on the N-terminus, was kindly provided by Sofiya Fedosyuk. The recombinant protein was purified as described for A46 variants. The protein of 4 L expression culture was eluted from a 5 ml Ni-NTA column in 30 ml MAL elution buffer. Cleavage by TEV was performed simultaneous to dialysation against 4 L of MAL dialysing buffer I at 4 °C over-night. After serial Ni-NTA chromatography (as described in chapter 2.2.2.4), the cleaved protein was dialysed against 4 L of MAL dialysing buffer II at 4 °C for 2 hours. SEC was performed with a HiLoad 26/600 Superdex 75 prep grade column pre-equilibrated with MAL storage buffer.

MAL resuspension buffer:	20 mM Tris/HCl pH 8.5, 100 mM NaCl, 25 mM imidazole, 10 mM β–mercaptoethanol
MAL dialysing buffer I:	20 mM Tris/HCl pH 8.5, 300 mM NaCl, 25 mM imidazole, 1 mM EDTA, 15 mM β–mercaptoethanol
MAL dialysing buffer II:	20 mM HEPES pH 7.0, 150 mM NaCl, 2 mM DTT
MAL storage buffer:	20 mM HEPES pH 7.0, 150 mM NaCl, 10 mM DTT

2.2.2.6 Purification of hTRAM(66-235) Variants

TIR/TRAM wt and mutants were expressed as GST-fusion proteins. The first purification step was affinity chromatography using a 5 ml GSTrap column equilibrated with TRAM resuspension buffer. The filtered, soluble phase of the cell lysate of 2 L expression culture was loaded onto the column with a speed of 1 ml/min. The bound proteins were washed with resuspension buffer. The protein of interest was eluted with elution buffer. The peak fractions were analysed by SDS-PAGE and four to five fractions with the highest protein concentration were pooled. 0.5 to 1 ml of previously isolated PreScission protease was added and the sample was incubated at 4 °C over-night. The efficiency of proteolytic cleavage was checked by SDS-PAGE. If the cleavage was incomplete, the sample was incubated for one to two more hours at room temperature. The last purification step was SEC in TRAM storage buffer. For the first purifications of TRAM single mutants, a HiLoad 16/600 Superdex 75 column was used. As the protein of interest was not separated very well from the protease and GST tag, a HiLoad 26/600 Superdex 75 column was used for subsequent purifications. The protein of interest was concentrated as described above.

TRAM resuspension buffer:	20 mM Tris/HCl pH 8.0, 150 mM NaCl, 5 % glycerol, 2 mM DTT, 1 mM EDTA
TRAM elution buffer:	20 mM Tris/HCl pH 8.5, 10 mM GSH, 2 mM DTT
TRAM storage buffer:	20 mM Tris/HCl pH 8.5, 150 mM NaCl, 5 mM DTT.

2.2.2.7 Purification of mMyD88(146-296) wt and R196A R288A

The TIR domain of murine MyD88 was expressed from a pGEX-4T1-based plasmid coding for amino acids 146 to 296 of murine MyD88 (kindly provided by Sofiya Fedosyuk). MyD88 variants were purified as described for TIR/TRAM (see chapter 2.2.2.6). Instead of PreScission protease, a pinch of thrombin was added to the four pooled GST elution factions with the highest protein concentrations to cleave off the GST tag. Cleavage was performed at 4 °C over-night. SEC was performed with a HiLoad 16/600 Superdex 75 prep grade gel filtration column.

MyD88 resuspension buffer:	20 mM Tris/HCl pH 8.0, 400 mM KCl, 1 mM EDTA, 10 mM β-mercapthoethanol
MyD88 elution buffer:	20 mM Tris/HCl pH 8.5, 10 mM GSH, 10 mM β-mercapthoethanol
MyD88 storage buffer:	20 mM K_2HPO_4/KH_2PO_4 pH 6.5, 100 mM NaCl, 10 mM DTT

2.2.3 Establishing a Protocol for the Expression and Purification of Human and Murine MyD88 TIR Domains

The TIR domains of human and murine MyD88, covering amino acids 157 to 296, were expressed as His-TRX-fusion proteins. The first expression was performed in E. coli BL21. Expression was induced with 0.25 mM IPTG and the proteins were expressed at 25 °C for 4 hours. The resuspension buffer consisted of 20 mM Tris/HCl pH 8.5, 100 mM NaCl, 25 mM imidazole, 5 % glycerol and 10 mM β-mercaptoethanol. One third of the cell suspension was frozen separately to analyze the efficiency of expression and solubility of the proteins of interest. The thawed cell suspensions were filled up to 30 ml with resuspension buffer and the cells were lysed using a French pressure cell press. 1 ml of the total cell lysate was centrifuged separately at 13 000 rpm at 4 °C for 10 min. The supernatant was discarded, the pellet was washed with H_2O and resuspended in 1 ml of H_2O, representing the insoluble phase of the cell lysate. The rest of the lysate was treated as described above (see chapter 2.2.2). The soluble phase was passed through 1.5 ml of Ni-NTA resin. Bound proteins were washed with 5 ml of resuspension buffer and eluted in 10 ml elution buffer (20 mM Tris/HCl pH 8.5, 300 mM NaCl, 200 mM imidazole, 15 mM β-mercaptoethanol). The total, soluble and insoluble fractions of the cell lysate as well as the flow-through and elution of the affinity chromatography were analysed by SDS-PAGE. The fusion proteins were highly expressed, but approximately 90 % were insoluble (see chapter 3.3). Therefore, different expression conditions were tested. The strain of E. coli (BL21(DE3) or BL21(DE3) Codon Plus), the growth medium (LB or TB medium), the length of expression (4 hours at 25 °C or over-night

at 16 °C after cold-shock on ice) and the pH (KH_2PO_4/K_2HPO_4 pH 6.5, HEPES pH 7 or Tris/HCl pH 8.5) and composition (0, 100 or 300 mM NaCl) of the resuspension buffer were varied and the solubilities of the fusion proteins were tested by Ni-NTA chromatography as described above or by Western Blotting of the total, soluble and insoluble phases.

The solubility did not change notably under different conditions (see chapter 3.3). Therefore, further expressions were performed in E. coli BL21(DE3) in LB medium. Expression was induced with 0.25 mM IPTG. After induction, the cells were incubated at 25 °C, 150 rpm for four hours or over-night to increase the yield. The cells were lysed and treated as described in chapter 2.2.2. The proteins of interest were purified as described for the N-terminal variants of A46 with the buffers listed below. SEC was performed with a HiLoad 16/600 or 26/600 Superdex 75 prep grade column.

MyD88(157-296) resuspension buffer:	20 mM Tris/HCl pH 8.5, 100 mM NaCl, 25 mM imidazole, 5 % glycerol, 10 mM β-mercaptoethanol
MyD88(157-296) Ni-NTA elution buffer:	20 mM Tris/HCl pH 8.5, 200 mM imidazole, 100 mM NaCl, 5 % glycerol, 15 mM β-mercaptoethanol
MyD88(157-296) dialysing buffer I:	20 mM KH_2PO_4/K_2HPO_4 pH 6.5, 150 mM NaCl, 25 mM imidazole, 15 mM β-mercaptoethanol
MyD88(157-296) dialysing buffer II:	20 mM KH_2PO_4/K_2HPO_4 pH 6.5, 150 mM NaCl, 2 mM DTT
MyD88(157-296) storage buffer:	20 mM KH_2PO_4/K_2HPO_4 pH 6.5, 150 mM NaCl, 5 mM DTT
TB medium:	12 g/L tryptone, 24 g/L yeast extract, 0.4 % (v/v) glycerol, 17 mM KH_2PO_4, 72 mM K_2HPO_4

2.2.4 Establishing a Protocol for the Expression and Purification of Full-length Human MyD88

Like the TIR domains of MyD88, also the full-length protein was expressed as fusion protein with a His-TRX tag. The first expression yielded only insoluble protein. Therefore, the solubility was tested under the same conditions as described for the TIR domains (chapter 2.2.3).

In addition, we tried to refold the precipitated protein in the pellet of the first centrifugation step after cell lysis. The pellet of 2 L expression was resuspended in 20 ml refolding buffer 1. The resuspension was centrifuged at 18 000 rpm at 4 °C for 30 min. The supernatant was discarded. The pellet was again resuspended in refolding buffer I and centrifuged at 18 000 rpm at 4 °C for 30 min. The pellet was resuspended in 5 ml of refolding buffer II. It was not possible to fully resuspend the pellet. The resuspension was dialysed against 300 ml

refolding buffer III two times for 30 min. and subsequently over-night. The dialysed sample was centrifuged at 18 000 rpm at 4 °C for 30 min. Refolded proteins should be in the supernatant.

Further expressions were performed in E. coli BL21 at 25 °C over night. The purification was performed as described for His-TRX-tagged N-terminal A46 variants with the buffers listed below. The last dialysation step before SEC was tested with 5 ml aliquots against either 20 mM Tris/HCl pH 8.0 and 5 mM DTT or 20 mM Tris/HCl pH 8.0, 400 mM Urea and 5 % glycerol, as a His-tagged version of the full-length human MyD88 is commercially available in this buffer. SEC was performed with a HiLoad 16/600 Superdex 75 prep grade column.

hMyD88(1-296) resuspension buffer:	20 mM Tris/HCl pH 8.5, 25 mM imidazole, 5 % glycerol, 10 mM β-mercaptoethanol
hMyD88(1-296) Ni-NTA elution buffer:	20 mM Tris/HCl pH 8.5, 200 mM imidazole, 5 % glycerol, 15 mM β-mercaptoethanol
hMyD88(1-296) dialysing buffer I:	20 mM Tris/HCl pH 8.5, 25 mM imidazole, 15 mM β-mercaptoethanol
hMyD88(1-296) dialysing buffer II:	20 mM Tris/HCl pH 8.0 , 400 mM Urea, 5 % glycerol
hMyD88(1-296) storage buffer:	20 mM Tris/HCl pH 8.0, 400 mM Urea, 10 % glycerol
Refolding buffer I:	50 mM Tris/HCl pH 8.0, 2 mM EDTA, 100 mM NaCl, 0.5 % Triton X-100
Refolding buffer II:	50 mM HEPES/KOH pH 7.6, 6 M guanidine hydrochloride, 5 mM DTT
Refolding buffer III:	50 mM HEPES/KOH, 100 mM KCl and 1 mM DTT

2.3 Protein-Protein Interaction Studies

2.3.1 Size Exclusion Chromatography and Multi Angle Laser Light Scattering

SEC and SEC in combination with static multi angle laser light scattering (SEC-MALLS) were used to determine the oligomeric state of the A46 N-terminal variants as well as to test for interactions between different proteins. For interaction studies by SEC, the two purified and concentrated proteins of interest were mixed in a molar ratio according to their putative binding ratio.

To test for an interaction of the N-terminal and C-terminal domains of A46, 0.45 mg of A46(N87-T229) were incubated with 0.45 mg of A46(6M1-T83) at 4 °C over-night. The

sample was filled up to 1 ml with A46 storage buffer (see chapter 2.2.2.4). The chromatography was performed in A46 storage buffer with a HiLoad 16/600 Superdex 200 column. As comparison, SECs with 0.45 mg of either A46(N87-T229) or A46(6M1-T83) alone were performed under the same conditions. The peak fractions of the chromatography containing both protein domains were re-concentrated to approximately 100 µl and further analysed by SEC-MALLS. Therefore, 95 µl of the re-concentrated sample were used for another SEC with a Superdex 10/300 200 GL column in A46 storage buffer. In addition to the UV adsorption, light scattering was detected by miniDAWN^{TM} TREOS. The way a particle scatters light is dependent on its shape and volume. Therefore, the average molecular weight of the particles in the solution can be calculated. As the UV adsorption is detected simultaneously, the average molecular mass can be set in correlation with the protein concentration.

The same set-up was used to determine the oligomeric conformation of the three A46 N-terminal variants. 120 to 450 µg of protein (in a volume of 10 to 80 µl) were used. SEC-MALLS was performed in the A46 storage buffer or the A46 storage buffer with additional 150 mM NaCl.

2.3.2 Microscale Thermophoresis

Microscale thermophoresis (MST) was used to determine the interaction of A46 variants with TIR/TRAM mutants as well as the interaction of A46(6M1-T83) with the TIR domains of MyD88, TRAM and MAL. MST makes use of thermophoresis, the movement of dissolved particles in a temperature gradient. Thermophoresis depends on the hydration shell, size and charge of a protein and is therefore altered by protein-protein interactions. This change in thermophoresis is determined. One of the putative binding partners is fluorescently labeled. Serial two-fold dilutions of the unlabeled protein are mixed 1:1 with labeled protein of constant concentration. Saturation of binding should be achieved with the highest concentration of unlabeled binding partner. This mix is transferred into capillaries that are locally heated by an infrared laser. The fluorescence intensity over time before, during and after heating is monitored in real time and the relative change in fluorescence is calculated. If the labeled protein interacts with the unlabeled protein, the movement in the temperature gradient of the labeled protein changes with increasing concentration of the binding partner (Jerabek-Willemsen et al., 2011).

TIR/TRAM wt, F112A, P116H, C117H and the triple mutant F112A P116H C117H, as well as TIR/MAL and TIR/mMyD88(146-296) were fluorescently labeled using the Monolith™ Protein Labeling Kit RED-NHS (from Nanotemper) as described by the manufacturer. Cysteine-labelled Mal(79-235) was kindly provided by Sofiya Fedosyuk. The binding partners 4N-A46, A46(N87-T229), A46(N87-T229) I94A and A46(6M1-T83) were dialysed against 500 ml MST buffer at 4 °C over-night. A Monolith NT.115 instrument was used for the measurements. Cap measurements of the labeled proteins were performed to determine a proper dilution to ensure a sufficient but not too high fluorescence signal. 10 µl of 16 serial two-fold dilutions with MST buffer of the unlabelled binding partner were mixed with 10 µl of labeled binding partner in the previously determined dilution. The mixtures were transferred into Monolith™ NT.115 Standard Treated Capillaries (Nanotemper) by capillary force. The change of fluorescence intensity after heating of the capillaries was measured. The measurements were performed with 60 % or 80 % MST power and 50 % laser power.

MST buffer:	20 mM Tris/HCl pH 8.5, 100 mM NaCl, 5 % glycerol, 1 mM TCEP, 1 mM EDTA, 0.025 % Tween-20

3 Results

3.1 Effect of BB Loop Mutations on the Interaction of A46 and TRAM

Stack and Bowie (2012) reported the necessity of an intact BB loop in the TLR adapter proteins for their interaction with A46. We wanted to test this hypothesis by MST (see chapter 2.3.2). We constructed mutants of TRAM(66-235) by site-directed mutagenesis (see chapter 2.1.3.5). We introduced the mutations F112A and P116H and in addition constructed the triple mutant TIR/TRAM F112A P116H C117H. Moreover, the point mutation I94A was introduced into A46(N87-T229). The mutations P116H and C117H were previously shown to abolish interactions between A46 and TRAM (Stack & Bowie, 2012). F112A of TRAM and I94A of A46 are in close proximity in a docking model constructed by Fedosyuk et al. (2014) (see Fig. 6). The TRAM variants were fluorescently labeled and the change of their thermophoresis upon addition of A46(N87-T229) wt or I94A was determined. In addition, the interaction between TRAM(66-235) wt or the triple mutant with the full-length A46 with four additional amino acids on the N-terminus (therefore named "4N-A46") was determined. Against our expectations, we observed binding between A46(N87-T229) and TRAM(66-235), independent of any mutations in either molecule (representative pictures see Fig. 8 – 11). To test for the specificity of TRAM interactions, we performed an MST measurement with TRAM(66-235) variants and Leader protease (Lb^{pro}) from FMDV. Binding was neither observed with TRAM(66-235) wt (Fig. 12) nor with the single mutants (not shown). When A46(N87-T229) was denatured by heating at 65 °C, TRAM(66-235) still seemed to bind, but the calculated K_D was about 10-fold higher (43.7 µM). Table 6 shows the calculated K_D of individual measurements assuming dimerization of A46(N87-T229).

	A46(N87-T229) wt K_D [µM]	A46(N87-T229) I94A K_D [µM]	4N-A46 K_D [µM]
TRAM(66-235) wt	8.4; 5.1; 1.9; 3.3	2.5; 3.6	2.7; 2.3; 1.9
TRAM(66-235) F112A	2.5; 1.7; 1.6	2.9; 4.6	not determined
TRAM(66-235) P116H	1.3; 2.7	2.2; 2.4	not determined
TRAM(66-235) F112A P116H C117H	4.6; 4.4	3.5; 4.1	2.3; 2.9

Table 6: Affinity of TRAM variants to A46 variants. The K_D of the interactions between TRAM(66-235) wt and mutants with A46 variants was determined by MST. Individual values represent individual measurements.

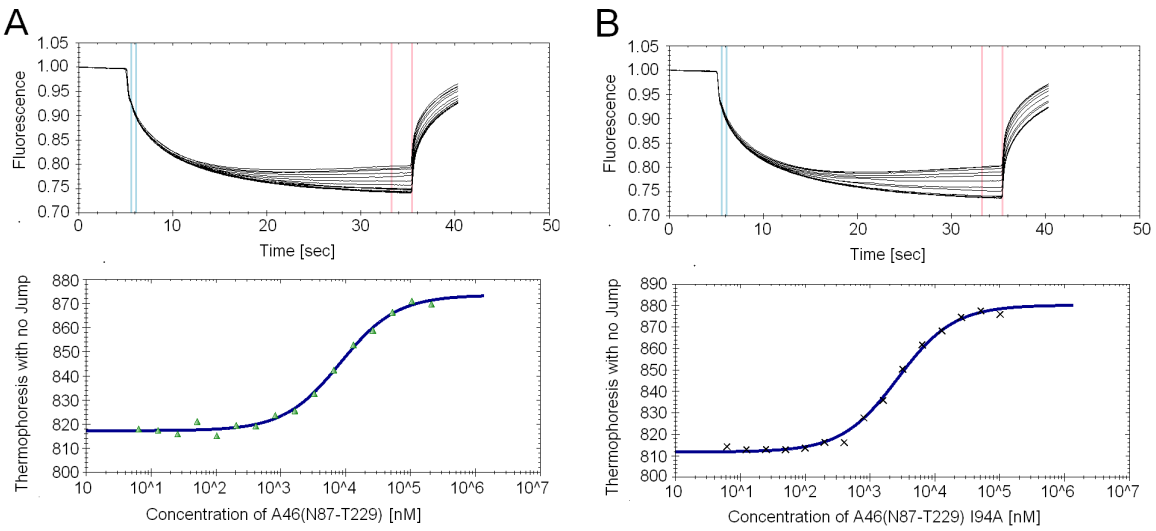

Fig. 8 MST of TRAM(66-235) wt with A46(N87-T229) wt and I94A. Fluorescently labeled TRAM(66-235) wt was mixed with A46(N87-T229) wt (A) or A46(N87-T229) I94A (B) with end-concentrations between 6.4 nM and 210.5 µM or between 6.2 nM and 203.25 µM, respectively. The LED power for fluorophor excitation was 50 %, the laser power for localized heating of the capillary was 60 %. The upper panels show the change of fluorescence over time from individual measurements with different concentrations of A46(N87-T229). The bottom panels show the thermophoresis of the different measurements plotted against the concentrations of A46(N87-T229) wt or I94A in nM.

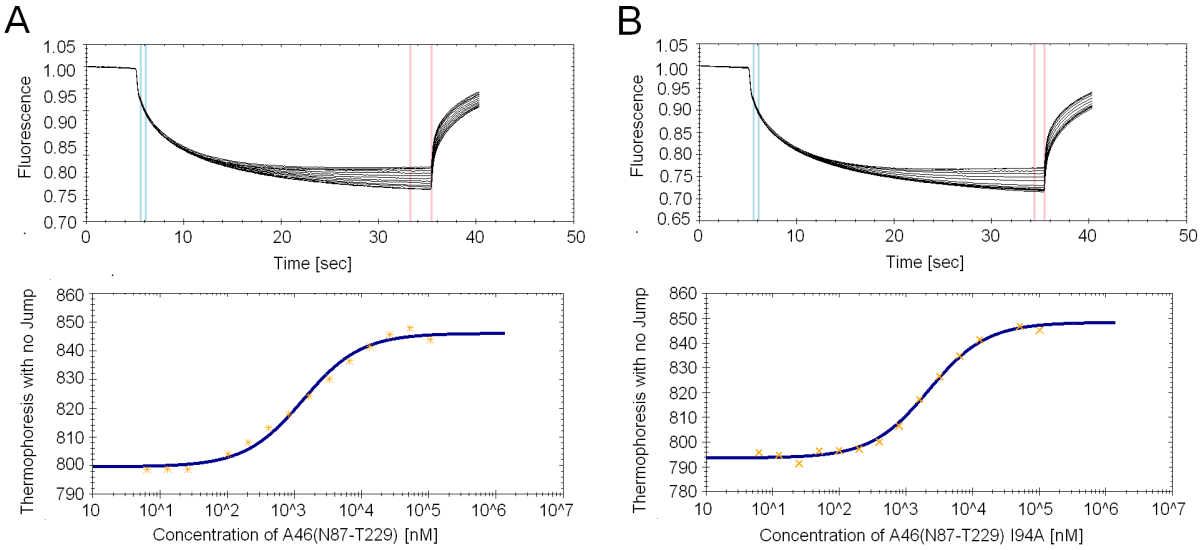

Fig. 9: MST of TRAM(66-235) P116H with A46(N87-T229) wt and I94A. Fluorescently labeled TRAM(66-235) P116H was mixed with A46(N87-T229) wt (A) or A46(N87-T229) I94A (B) with end-concentrations between 6.4 nM and 210.5 µM or between 6.2 nM and 203.25 µM, respectively. The LED power for fluorophor excitation was 50 %, the laser power for localized heating of the capillary was 60 %. The upper panels show the change of fluorescence over time from individual measurements with different A46(N87-T229) concentrations. The bottom panels show the thermophoresis of the different measurements plotted against the concentrations of A46(N87-T229) wt or I94A in nM.

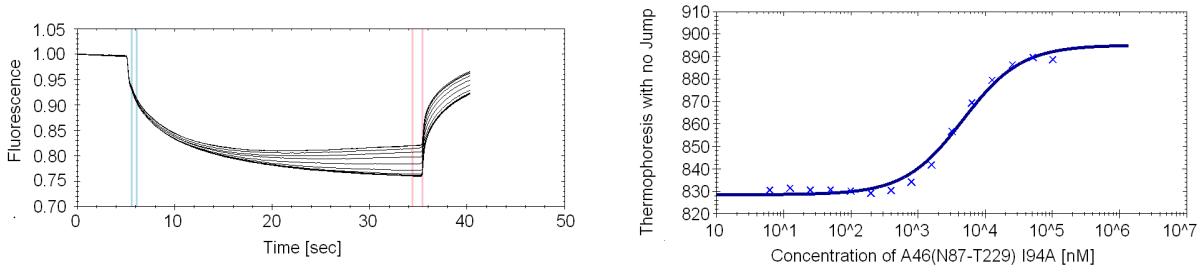

Fig. 10: MST of TRAM(66-235) F112A with A46(N87-T229) I94A. Fluorescently labeled TRAM(66-235) F112A was mixed with A46(N87-T229) I94A with end-concentrations between 6.2 nM and 203.25 µM. The LED power for fluorophor excitation was 50 %, the laser power for localized heating of the capillary was 60 %. The left panel shows the change of fluorescence over time from individual measurements with different concentrations A46(N87-T229). The right panel shows the thermophoresis of the different measurements plotted against the concentration of A46(N87-T229) I94A in nM.

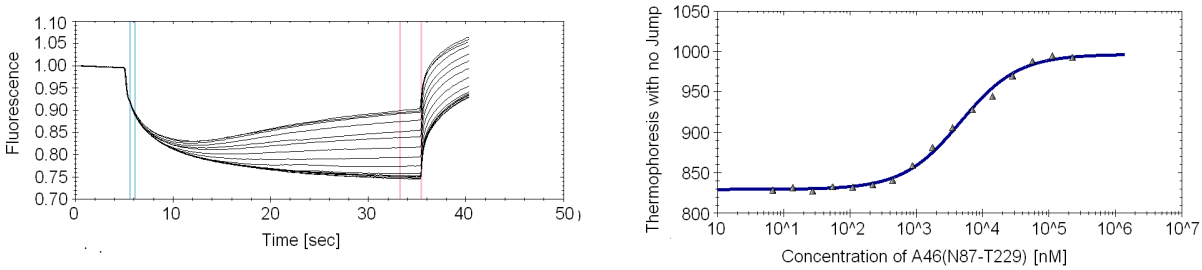

Fig. 11: MST of TRAM(66-235) F112A P116H C117H with A46(N87-T229) wt. Fluorescently labeled TRAM(66-235) F112A P116H C117H was mixed with A46(N87-T229) wt with end-concentrations between 6.4 nM and 210.5 µM. The LED power for fluorophor excitation was 50 %, the laser power for localized heating of the capillary was 60 %. The left panel shows the change of fluorescence over time from individual measurements with different concentrations of A46(N87-T229). The right panel shows the thermophoresis of the different measurements plotted against the concentration of A46(N87-T229) wt in nM.

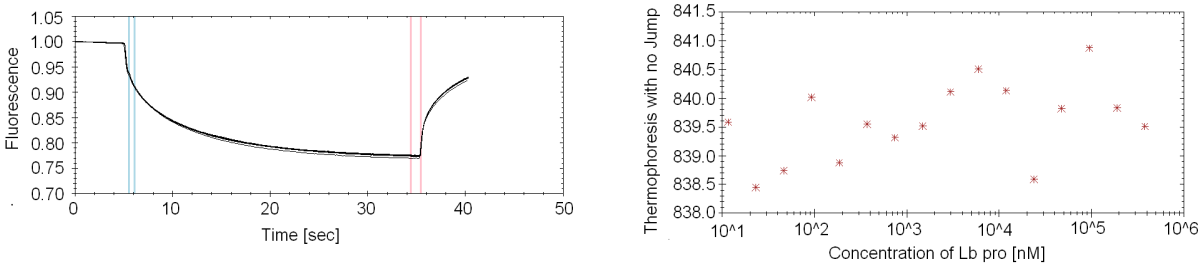

Fig. 12: MST of TRAM(66-235) wt with Lb^{pro}. Fluorescently labeled TRAM(66-235) wt was mixed with Lb^{pro} with end-concentrations between 11.6 nM and 379 µM. The LED power for fluorophor excitation was 50 %, the laser power for localized heating of the capillary was 60 %. The left panel shows the change of fluorescence over time from individual measurements with different Lb^{pro} concentrations. The right panel shows the thermophoresis of the different measurements plotted against the concentration of Lb pro in nM.

3.2 Investigation of the N-terminal Part of the Vaccinia Virus Protein A46

3.2.1 Expression and Purification of N-terminal A46 Variants

Three variants of different lengths of the A46 N-terminal domain were expressed in E. coli BL21(DE3). The proteins were expressed with a His-MBP- or His-TRX-tag and were purified via Ni-NTA chromatography and SEC (see chapter 2.2.2.4).

3.2.1.1 Purification of A46(6M1-S90)

The longest fragment covered amino acids M1 to S90. This fragment overlaps with the C-terminal part for which the structure has been determined (Fedosyuk et al., 2014) and was therefore considered as the most informative construct.

The expression efficiency and solubility of MBP-A46(6M1-S90) and TRX-A46(6M1-S90) were tested by SDS-PAGE of samples taken from the total cell lysate, as well as from the soluble and insoluble phases after centrifugation (Fig. 13). The MBP-fusion protein has a weight of about 54 kDa. As seen in Fig. 13, the protein was highly expressed and more than 50 % soluble. The TRX-labelled A46(6M1-S90) has a molecular weight of about 25 kDa. The corresponding band is not as prominent in the total fraction as the band of the MBP-fusion protein. This indicates a lower abundance relative to the other proteins present in the cell lysate. Still, a light band of correct size is visible in the soluble fraction. The lighter band in the total fraction might be a result of lower expression. However, the TRX-tag is about 10 kDa smaller than the MBP-tag. Therefore, even in equimolar concentrations, an MBP-tagged protein has a higher concentration in terms of weight per volume than a TRX-tagged protein.

The recombinant proteins were isolated by affinity chromatography using Ni-NTA resin. The tags were cleaved off by over-night incubation with TEV protease at 4 °C. Fig.14 shows SDS-PAGE gels representing the purification by Ni-NTA chromatography, as well as the over-night cleavage by TEV. In Fig. 14A, MBP-A46(6M1-S90) was present in the wash fraction. This indicates either over-loading of the column due to very high expression, or the formation of aggregates. Aggregates might bind weakly to the column during loading but are subsequently removed during washing before elution. In contrast, almost all of TRX-A46(6M1-S90) bound to the Ni-NTA resin and can be observed in the sample taken from the

elution (Fig. 14B). Both constructs were cleaved efficiently, although a light band of uncleaved fusion protein is visible in the case of MBP-tagged A46(6M1-S90).

Serial Ni-NTA chromatography was performed to separate the cleaved protein of interest from the cleaved-off tags and TEV protease. TEV protease as well as MBP and TRX are His-tagged. Therefore, they bind to the Ni-NTA resin whereas the cleaved protein of interest is present in the flow-through. To ensure removal of all impurities, the flow-through was passed through the column three to four times. In between each load, bound proteins were eluted. After each passage, aliquots were taken from the flow-through and elution for later analysis by SDS-PAGE. Representative SDS-PAGE gels are shown in Fig. 15. TEV protease and uncleaved proteins can be seen mostly in the first elutions. The sample resulting from TRX-tagged protein was very pure after the fourth passage (Fig. 15B). On the contrary, it was not possible to completely remove MBP impurities (Fig. 15A). The highest band, corresponding to uncleaved MBP-A46(6M1-S90), is no longer visible in the third elution. However, although most of MBP, represented by the second highest band, is present in the first elution, MBP is still detectable in the flow-through after the fourth passage. The amount of MBP impurity hardly decreases during the fourth passage, as the corresponding band looks similar in flow-through 3 (FT3) and flow-through 4 (FT4). Also, hardly any MBP is visible in the fourth elution (E4). Therefore, the remaining MBP does not seem to bind to the resin and further passages would not increase the purity of the sample.

Following serial Ni-NTA chromatography, SEC with a HiLoad 16/600 Superdex 75 prep grade column was performed as a last purification step. Fig.16A shows the chromatogram of the SEC of A46(6M1-S90) resulting from the MBP-tagged fusion construct. The peak merges with the void volume peak and has an irregular shape. A46(6M1-S90) has a molecular weight of around 11 kDa as a monomer. A protein of that size would be expected to have an elution volume of about 90 ml (calculated with the calibration curve provided by EMBL http://www.embl.de/pepcore/pepcore_services/protein_purification/chromatography/hiload16-60_superdex75/GF75_16.pdf). Therefore, A46(6M1-S90) seems to form oligomers. This was confirmed by SEC-MALLS (see chapter 3.2.2). Fig. 16B shows the SDS-PAGE gel of the fractions A3 to B14. The fractions A3 and B14 are marked with arrows in the chromatogram. The gel does not show one single band corresponding to A46(6M1-S90) as would be expected. Instead, three protein bands are observed. The highest band between 37 and 50 kDa probably corresponds to the MBP impurities that could not be removed by serial Ni-NTA chromatography. The second lowest band shows the protein of interest, A46(6M1-S90). The slightly lower band probably results from a processed form of A46(6M1-S90).

Fig. 17A shows the SEC of A46(6M1-S90) resulting from the TRX-fusion construct. The corresponding SDS-PAGE gel is shown in Fig. 17B. A void volume peak of high amplitude is observed. The void volume fraction A2 was analysed by SDS-PAGE. As can be seen in Fig. 17B, the protein of interest is not observed in the void volume peak. Instead, protein bands at the height of 25 kDa and slightly higher are observed. These bands most probably correspond to uncleaved TRX-A46(6M1-S90) and TEV protease, respectively. In contrast to the sample resulting from the MBP-tagged construct, no impurities can be observed in the peak fractions. However, again two bands are observed, indicating specific proteolysis of A46(6M1-S90). The presence of two proteins with similar size could also explain the left shoulder that is visible on the peak in the chromatogram (indicated by a red arrow). The yield was very low, as is indicated by the small amplitude of protein peaks.

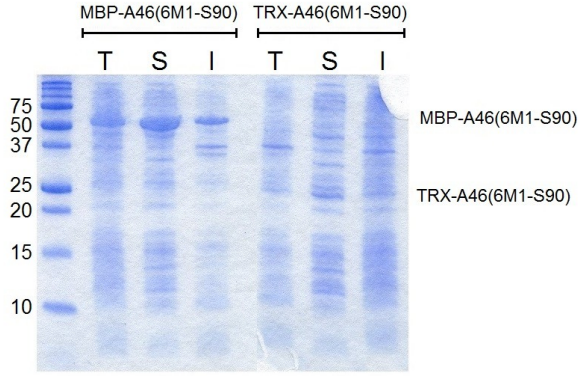

Fig. 13: Expression of A46(6M1-S90) fusion proteins. E. coli BL21(DE3) expressing A46(6M1-S90) with either an MBP- or TRX-tag were lysed using a French pressure cell press. The resulting cell lysate was centrifuged at 18 000 rpm for 30 min. at 4 °C to separate soluble from insoluble material. This figure shows the SDS-PAGE gel of 1 µl samples taken from the total cell lysates (T), as well as the soluble (S) and insoluble (I) phases. A band for MBP-A46(6M1-S90) is visible in all three fractions, indicating a high expression. About 75 % of the over-expressed protein is soluble. TRX-A46(6M1-S90) is hardly visible in the total and insoluble fractions. However, it is visible in the soluble fraction.

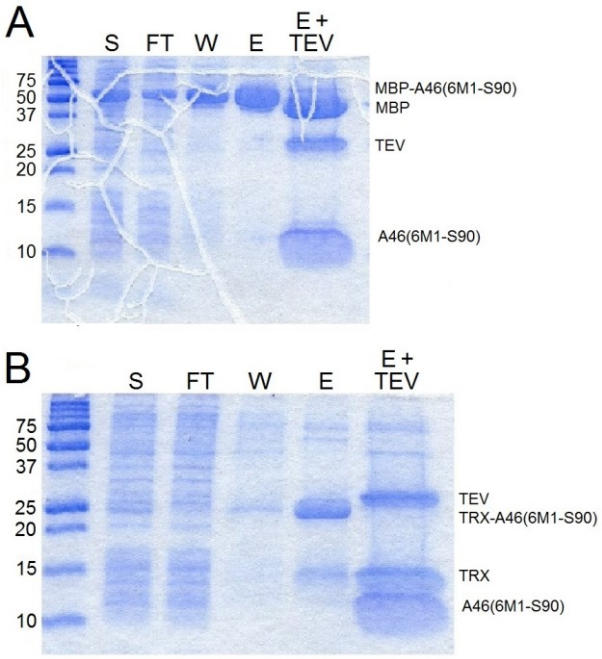

Fig. 14: Ni-NTA chromatography and cleavage of TRX- and MBP-A46(6M1-S90). SDS-PAGE gels of samples representing the Ni-NTA chromatography and the cleavage of MBP-A46(6M1-S90) (A) as well as TRX-A46(6M1-S90) (B) by TEV protease. For each construct, the soluble phase of 2 L expression was used for affinity chromatography. 1 µl of the soluble phase (S) of the cell lysate and the flow-through (FT), 5 µl of the wash (W) and the elution (E) and 10 µl of the elution after over-night incubation with TEV-protease (E + TEV) were used for SDS-PAGE.

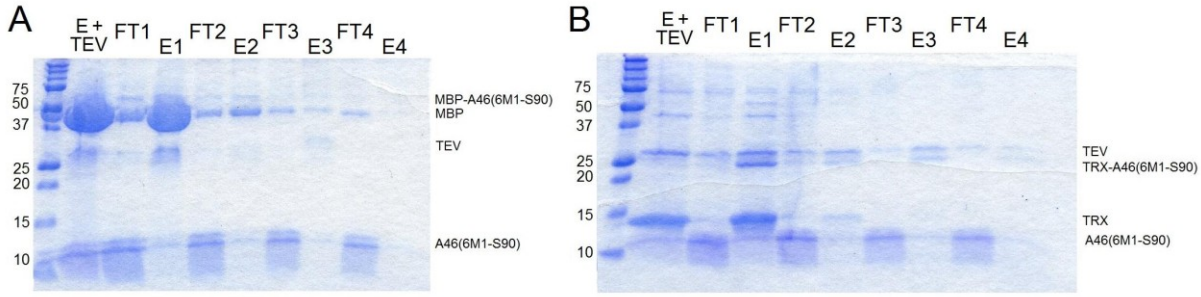

Fig. 15: Serial Ni-NTA chromatography of A46(6M1-S90). SDS-PAGE gels of 6 µl (A) or 7 µl (B) of samples taken from each flow-through (FT) and elution (E) during the course of serial Ni-NTA chromatography of A46(6M1-S90) after cleavage of MBP (A) or TRX (B). Tags were cleaved off by over-night incubation with TEV protease.

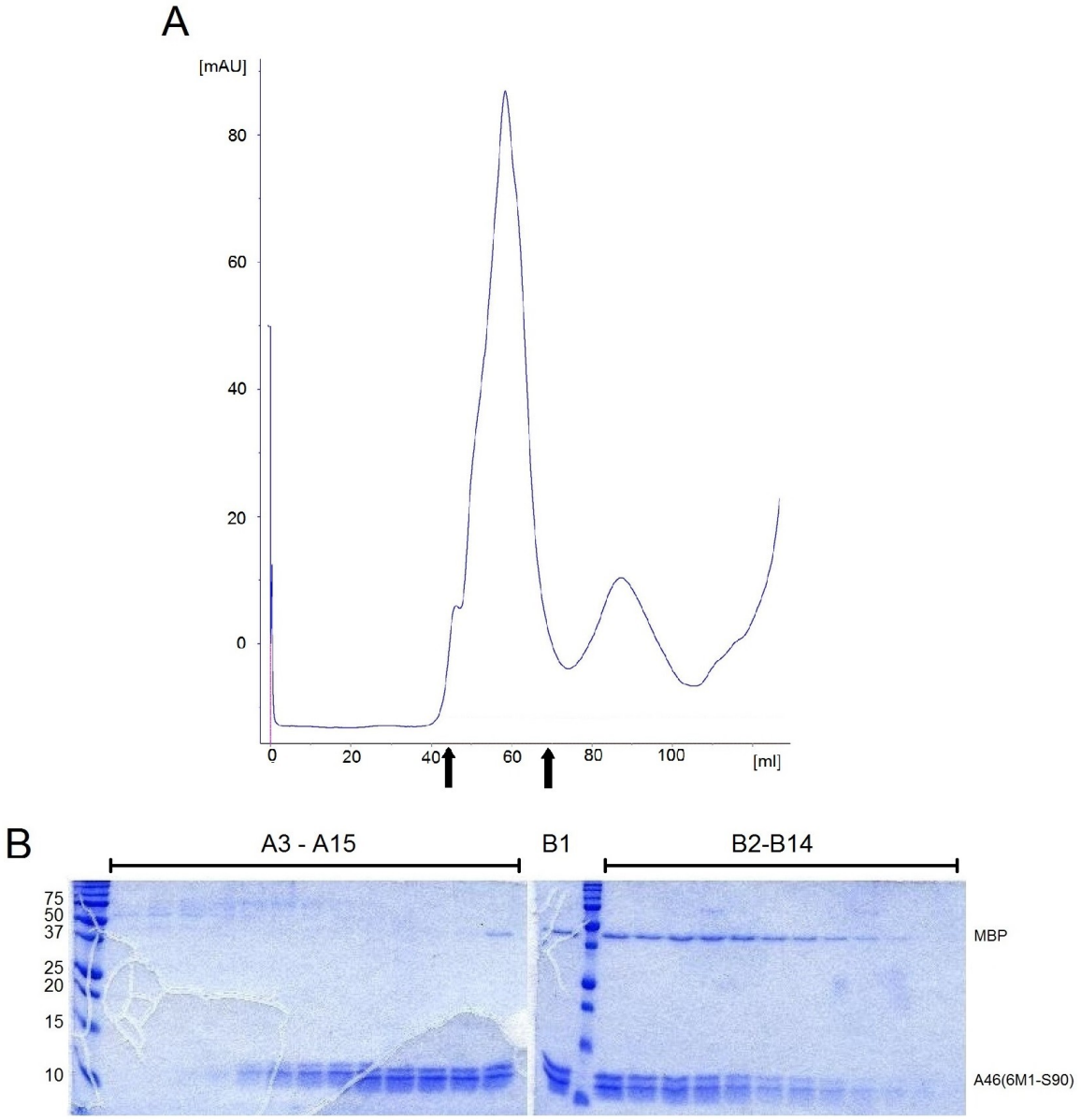

Fig. 16: SEC of A46(6M1-S90) expressed as MBP fusion protein. Chromatogram (A) and SDS-PAGE gel of 5 µl of the fractions A3 to B14 (B). SEC was performed as the last step in the purification of A46(6M1-S90) from 2 L expression culture. A HiLoad 16/600 Superdex 75 prep grade column was used in an ÄKTA FPLC system. Fractions A3 and B14 are marked in the chromatogram by black arrows.

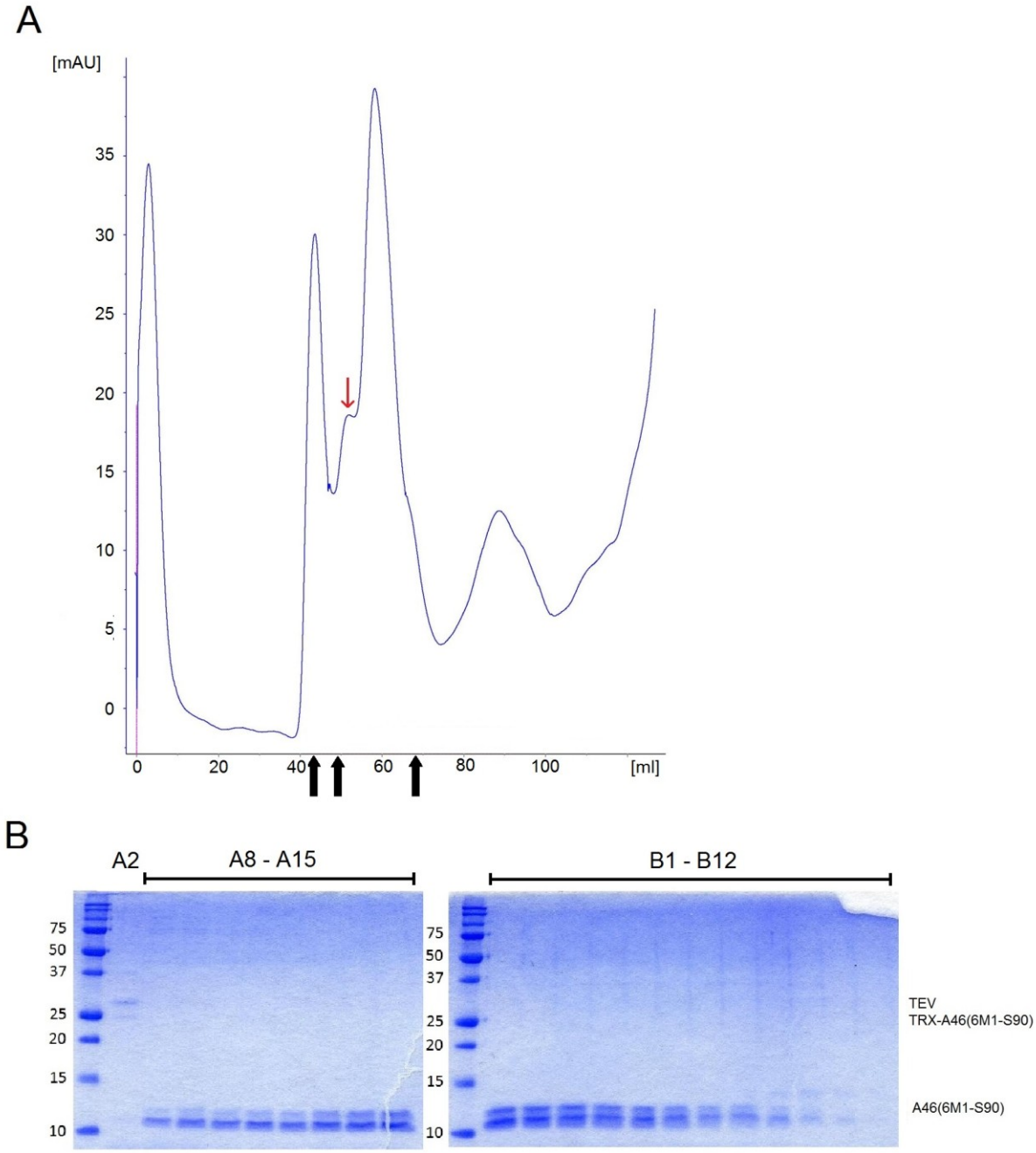

Fig. 17: SEC of A46(6M1-S90) expressed as TRX- fusion protein. Chromatogram (A) and SDS-PAGE gels of 10 µl of the fractions A2 and A8 to B12 (B). SEC was performed as last step in the purification of A46(6M1-S90). The protein of interest was expressed with an MBP-tag in E. coli BL21(DE3) in 2 L LB medium. A HiLoad 16/600 Superdex 75 prep grade column was used in an ÄKTA FPLC system. Fractions A2, A8 and B12 are marked in the chromatogram by black arrows.

3.2.1.2 Purification of A46(6M1-T83) and A46(6M1-G73)

The MBP-tagged version of A46(6M1-S90) resulted in MBP impurities. Therefore, the two shorter fragments, comprising amino acids M1 to T83 and M1 to G73, were expressed only as TRX-fusion proteins. The two constructs were purified in the same way as A46(6M1-S90). Only the purification of the middle construct A46(6M1-T83) is documented with figures, as it is representative also for A46(6M1-G73). Fig. 18 shows the SDS-PAGE gel representing the purification process of TRX-A46(6M1-T83) by Ni-NTA chromatography. Although the fusion protein was not highly enough expressed to be seen clearly in the total cell lysate, the corresponding band is prominent in the soluble phase. TRX-A46(6M1-T83) was observed in the flow-through, indicating an overload of the resin. No fusion protein is observed in the sample taken after over-night incubation with TEV protease (E + TEV), indicating complete cleavage. The expression, purification and cleavage of the shorter TRX-A46(6M1-G73) was similarly successful (not shown). Fig. 19 shows the SDS-PAGE gel of samples representing the course of serial Ni-NTA chromatography of A46(6M1-T83). TEV protease and TRX are gradually removed from the protein of interest because their His-tags bind to the Ni-NTA resin. Therefore, they are visible in the elutions (E1 – E4). The protein of interest does not bind to the resin and is therefore present in the flow-through (FT1 – FT4). The purity of A46(6M1-T83) increases with each passage through the Ni-NTA resin.

Fig. 20 shows the chromatogram and corresponding SDS-PAGE gel of the SEC of A46(6M1-T83). In contrast to A46(6M1-S90), the peak has the expected shape of a Gauss distribution curve, except for a small shoulder on the right side which might result from different oligomeric states. Three bands can be observed in the sample taken from the void volume (fraction A5). They correspond to A46(6M1-T83), TEV and uncleaved TRX-A46(6M1-T83). No impurities were observed in the peak fractions A12 to B9. Moreover, in contrast to the slightly longer A46(6M1-S90), A46(6M1-T83) does not seem to be processed, as only one band can be observed on the gel.

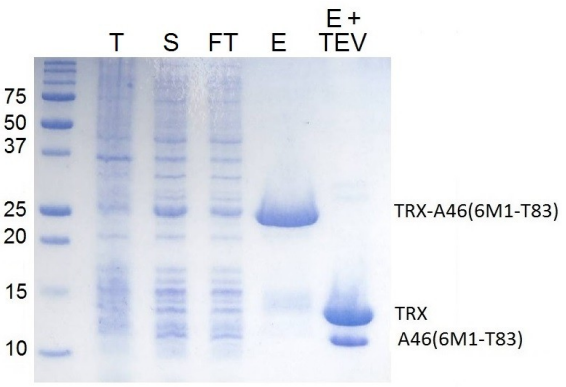

Fig. 18: Purification of A46(6M1-T83). A46(6M1-T83) was expressed as fusion protein with TRX in E. coli BL21(DE3) in 3 L LB medium. 1 µl of the total cell lysate (T), the soluble phase (S) and the flow-through (FT) as well as 5 µl of the elution (E) of Ni-NTA chromatography before and after (E + TEV) over-night incubation with TEV protease were used for SDS-PAGE.

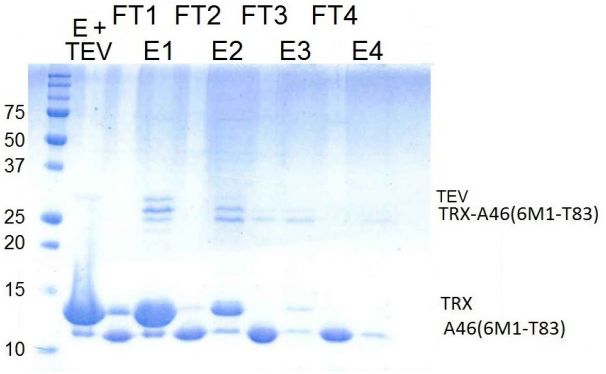

Fig. 19: Serial Ni-NTA chromatography of A46(6M1-T83) after TEV cleavage. After over-night incubation with TEV protease, the sample (E + TEV) from 3 L expression culture was passed four times through 5 ml of Ni-NTA resin that binds to His-TRX and His-TEV but not A46(6M1-T83). After each passage, a sample of the flow-through (FT) and elution (E) (5 µl each) was taken for analysis by SDS-PAGE.

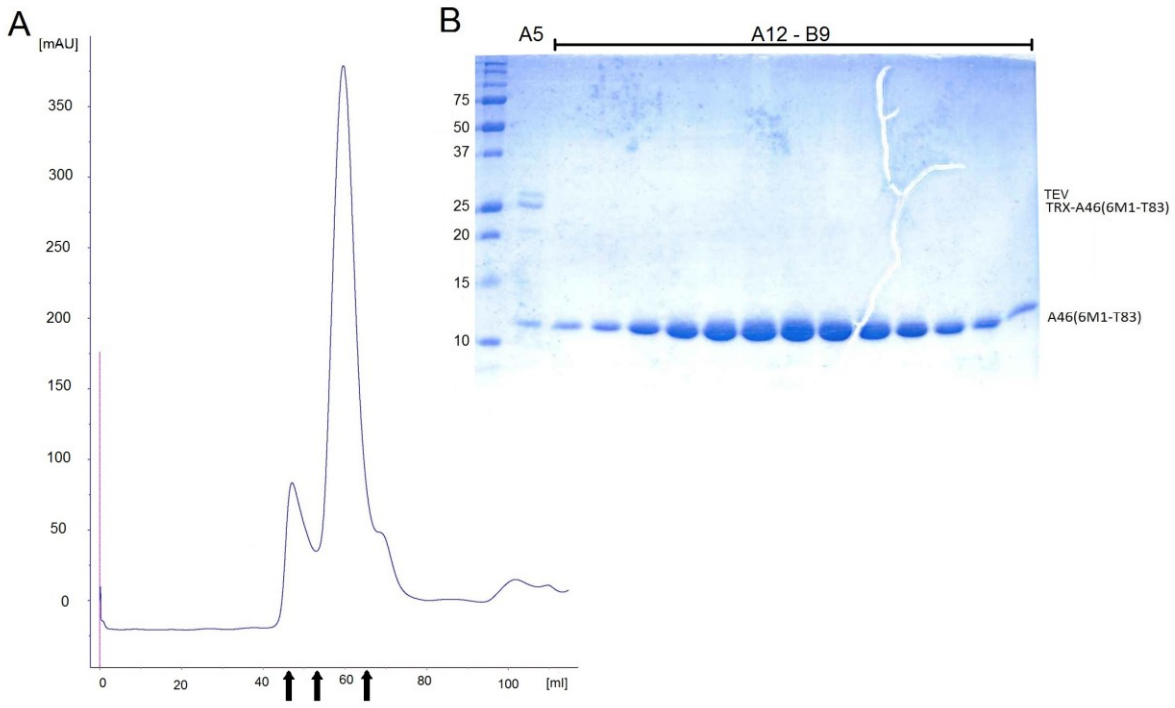

Fig. 20: SEC of A46(6M1-T83). Chromatogram (A) and the SDS-PAGE gel (B) of 5 µl of the fractions A5 and A12 – B9 (B). SEC was performed as last step in the purification of A46(6M1-T83). Protein resulting from 3 L expression culture was purified via a HiLoad 16/600 Superdex 75 prep grade column in an ÄKTA FPLC system. The fractions A5, A12 and B9 are marked with arrows in the chromatogram. A5 represents the void volume whereas A12 to B9 are the peak fractions and contain only the protein of interest.

3.2.2 Determining the Oligomeric State of the A46 N-terminus

SEC-MALLS was used to determine the oligomeric states of A46(6M1-T83) and A46(6M1-G73) under two conditions. The storage buffer that was used for the first measurement consists of only Tris/HCl and DTT. A buffer of such low ionic strength does not represent the physiological conditions of the cytoplasm. Therefore, the experiment was also performed in the storage buffer with additional 150 mM NaCl which better resembles the physiological conditions. An analytical SEC with a Superdex 200 10/300 GL column was performed with 230 – 450 µg of purified A46(6M1-G73) or A46(6M1-T83). In addition to the UV detector to determine protein concentrations, the MALLS detector miniDAWN^{TM} TREOS was used to calculate the average molecular mass. As the proteins were already purified, only one UV absorbance peak was observed. Fig. 21 shows the UV absorbances and calculated average molecular masses at each point of the chromatogram for A46(6M1-T83) in red and A46(6M1-G73) in blue. When the measurement was performed in a buffer containing 20 mM Tris/HCl pH 8.5 and 10 mM DTT (Fig. 21A), the calculated masses are about 30 kDa for A46(6M1-T83) and about 27 kDa for A46(6M1-G73) at the UV absorbance peaks indicating the highest protein concentrations. This indicates a trimeric state, as the monomers have a weight of 10 kDa and 9 kDa, respectively. According to the higher mass, the A46(6M1-T83) trimer elutes earlier than the A46(6M1-G73) trimer. The average molecular masses are relatively constant over the range of the UV absorbance peaks, indicating a stable trimeric state. The higher masses on the very left side of the peaks might result from aggregation. The average masses drop towards the right side of the peak. Due to the lower concentration of protein, the trimers probably disassemble to dimers and monomers.

Interestingly, the calculated average molecular masses were different when the experiment was repeated in the same buffer with additional 150 mM NaCl (Fig. 21B). Again, A46(6M1-T83) elutes earlier. The average molecular masses at the UV absorbance peaks are about 40 kDa for A46(6M1-T83) and about 36 kDa for A46(6M1-G73), indicating a tetrameric state. However, the average molecular masses are not as constant as in the buffer consisting of only Tris/HCl and DTT. Instead, they drop continuously to the masses referring to a trimeric state at the right sides of the peaks. This indicates that the tetrameric state is predominant only at the highest protein concentration. The lower the concentration, the more the tetramers disassemble into trimers until mostly trimers are present.

It can be seen in Fig. 21 that the trimers elute at smaller volume than the tetramers. This is the opposite of what would be expected, because larger proteins elute earlier in SEC than

smaller proteins. However, the two measurements are not completely comparable. The SECs in the buffer containing 150 mM NaCl (Fig. 21B) were performed at a flow rate of 0.85 ml/min, as the pressure was too high at the default flow rate of 1.00 ml/min that was used in the SECs in A46 storage buffer without NaCl (Fig. 21A). Moreover, the chromatography stopped several times at the beginning because of pressure alarms. Therefore, the proteins had more time to dissolve inside the column. This might explain the unexpected difference in elution volumes. However, the calculation of the average molecular weight should not be affected.

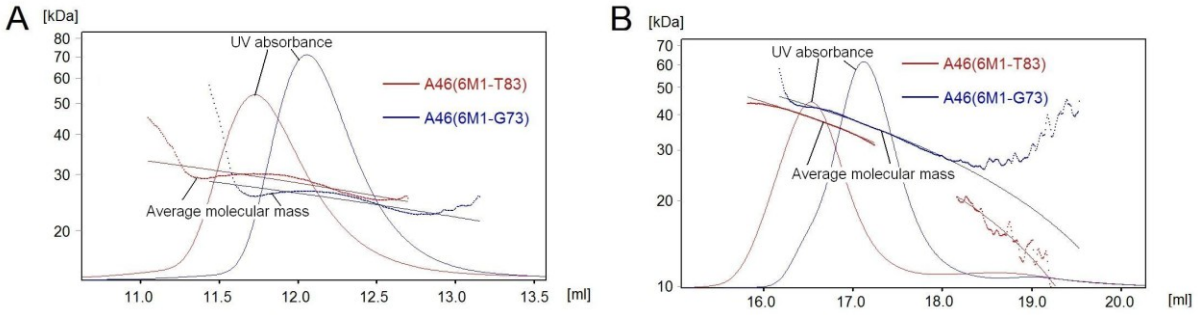

Fig. 21: Determining the oligomeric states of A46(6M1-T83) and A46(6M1-G73). SEC-MALLS was performed with purified and concentrated A46(6M1-T83) (red) and A46(6M1-G73) (blue) in 20 mM Tris/HCl pH 8.5 and 10 mM DTT (A) or 20 mM Tris/HCl pH 8.5, 10 mM DTT and 150 mM NaCl (B). In addition to the UV absorbance, the calculated average molecular masses, determined by the MALLS detector minDAWN^{TM} TREOS, are shown.

3.2.3 Protein-Protein Interaction Studies with A46(6M1-T83)

Binding studies were performed with A46(6M1-T83). This variant covered a larger part of the uncharacterized N-terminal A46 domain than A46(6M1-G73) but was, in contrast to A46(6M1-S90), not processed.

3.2.3.1 Testing for an Interaction Between A46(6M1-T83) and A46(N87-T229)

We wanted to test whether the N-terminal and C-terminal domains of A46 interact to reconstitute the full-length protein. To do so, 0.45 mg of A46(6M1-T83) and A46(N87-T229) were incubated together at 4 °C over-night. With this mix, SEC with a HiLoad 16/600 Superdex 200 prep grade column was performed. Fig. 22 shows the chromatogram (A) and corresponding SDS-PAGE gel (B). Only one peak can be observed in the chromatogram. Both proteins eluted in this peak, indicated by two bands of about 10 kDa (A46(6M1-T83))

and 15 kDa (A46(N87-T229)) on the SDS-PAGE gel. However, as it is unlikely that all of the protein molecules form complexes, three peaks are expected if the N-terminal and C-terminal domains interacted: one peak for each monomer and one peak for the complex. In contrast, only one peak indicates co-elution of the proteins, but probably not due to complex formation. Also, if SEC is performed with both proteins individually, they have the same elution volume as the peak in Fig. 22A (not shown). This seems at first unexpected, as the mass of A46(N87-T229) is 150 % the mass of A46(6M1-T83). However, as described above (see chapter 3.1.2), we showed that the N-terminal domain of A46 forms trimers in the conditions we used for SEC whereas the C-terminal domain was shown to form dimers (Fedosyuk et al., 2014). To confirm these findings, the peak fractions were re-concentrated and analysed by SEC-MALLS. Again, only one UV absorbance peak was observed (Fig. 22C). The average molecular mass was 30 kDa, corresponding to dimeric A46(N87-T229) and trimeric A46(6M1-T83).

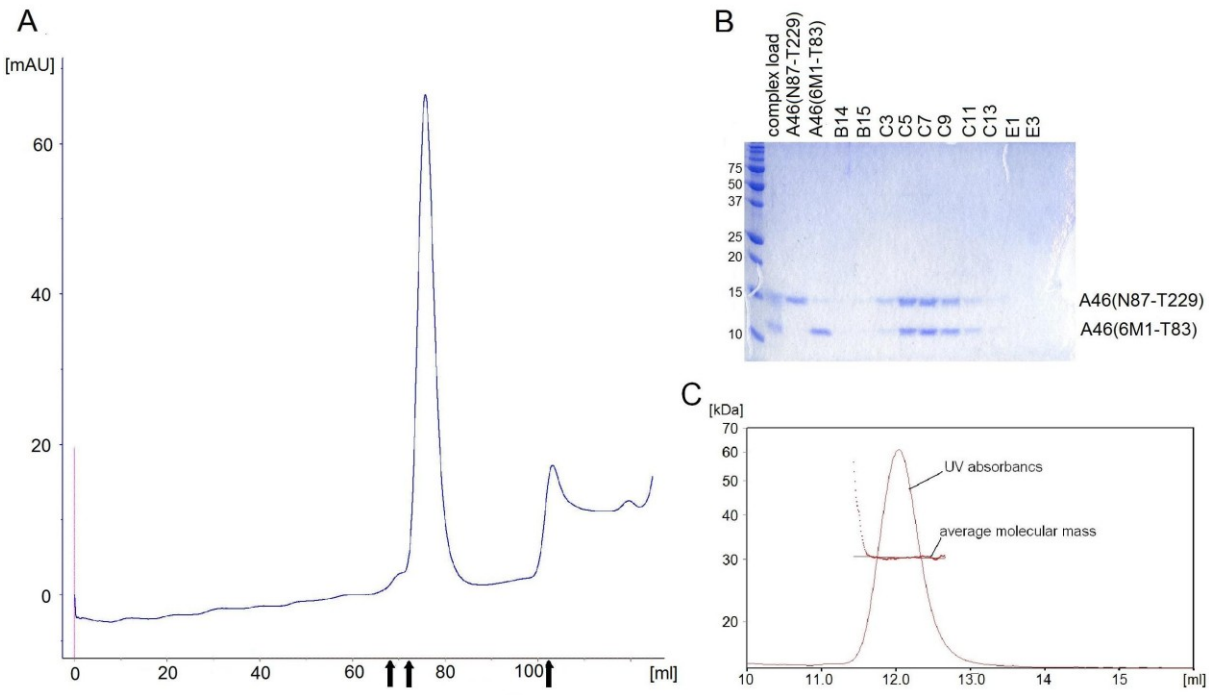

Fig. 22: Testing for an interaction between A46(6M1-T83) and A46(N87-T229). 0.45 mg of A46(6M1-T83) were incubated with 0.45 mg of A46(N87-T229) at 4 °C over-night and subsequently analysed by SEC with a HiLoad 16/600 Superdex 200 prep grade column. Chromatogram (A) and SDS-PAGE (B) of the load (complex load), both domains separately (0.45 mg/ml) and selected peak fractions (7 µl each). The fractions B14, C3 and E3 are marked by black arrows in the chromatogram. The peak fractions were re-concentrated and analysed by SEC-MALLS with a Superdex 10/300 200 GL column (C). Only one peak is observed, with a constant molecular weight of about 30 kDa.

3.2.3.2 MST of A46(6M1-T83) and TIR/TRAM, TIR/MyD88 or TIR/MAL

A46 binds and therefore inhibits the TLR adapter proteins MyD88, TRAM, TRIF and MAL (Stack et al., 2005). However, the C-terminal domain of A46 covering amino acids N87 to T229 is sufficient for binding to the TIR domains of MAL and MyD88 (Fedosyuk et al, 2014). We wanted to test whether the N-terminal domain of A46 is also capable of binding to the TIR domains of TRAM, MAL or MyD88. Accordingly, interaction studies were performed by MST (see chapter 2.3.2). The amino groups of TRAM(66-235) and MyD88(146-296) were labelled using the Monolith™ Protein Labeling Kit RED-NHS. Cys-labelled MAL(75-235) was kindly provided by Sofiya Fedosyuk. As can be seen in Fig. 23, no interaction between A46(6M1-T83) and the NHS-labelled TRAM(66-235) was observed. The change in thermophoresis is only marginal and not dependent on the concentration of A46(6M1-T83). The same applied for the MST measurement performed with the Cys-labelled MAL(75-235) and A46(6M1-T83) (Fig. 24). To test, whether NHS-TRAM and NHS-MAL were functional, the measurement was performed with A46(N87-T229) instead of A46(6M1-T83) and binding was observed (not shown). In contrast, when NHS-labelled MyD88(146-296) was used as binding partner, the thermophoresis of MyD88(146-296) increased with increasing A46(6M1-T83) concentrations (Fig. 25). The upper panel shows the fluorescence over time of the individual measurements with 15 different concentrations of A46(6M1-T83). In the measurements with Cys-MAL and NHS-TRAM, those curves mostly overlapped. However, in the case of NHS-MyD88, the curves changed with increasing A46(6M1-T83) concentrations. The higher the concentration of A46(6M1-T83), the faster the fluorescence intensity increased and the higher was the fluorescence intensity at the end of the measurement. If a trimeric state of A46(6M1-T83) is assumed, the K_D of the interaction was calculated to be approximately 12 µM with a laser power of 80 %. However, when only 60 % laser power was used to heat the capillary, a K_D of about 4 µM was calculated.

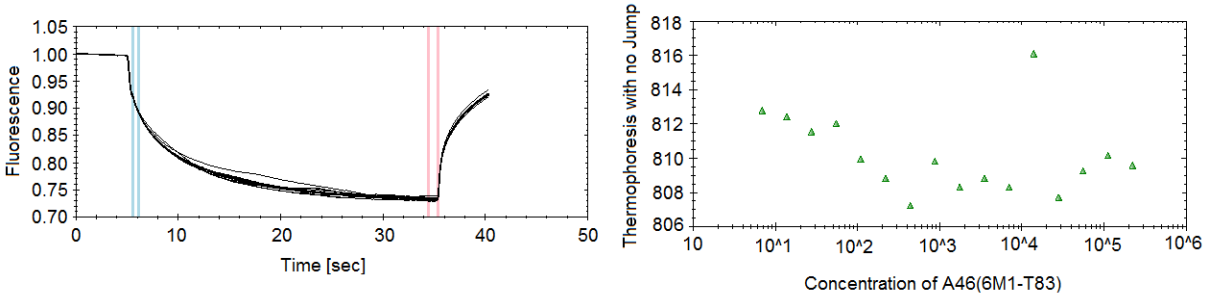

Fig. 23: MST of A46(6M1-T83) and NHS-TRAM(66-235)). The MST measurement was performed with NHS-labelled TRAM(66-235) and serial dilutions of A46(6M1-T83) with end concentrations between 223.25 µM and 6.81 nM, assuming a trimeric state. The LED power was 50 %, the laser power was 80 %. The left panel shows the relative fluorescence over time of 15 individual measurements with different concentrations of A46(6M1-T83). The right panel shows the thermophoresis of the individual measurements against the concentration of A46(6M1-T83) in nM.

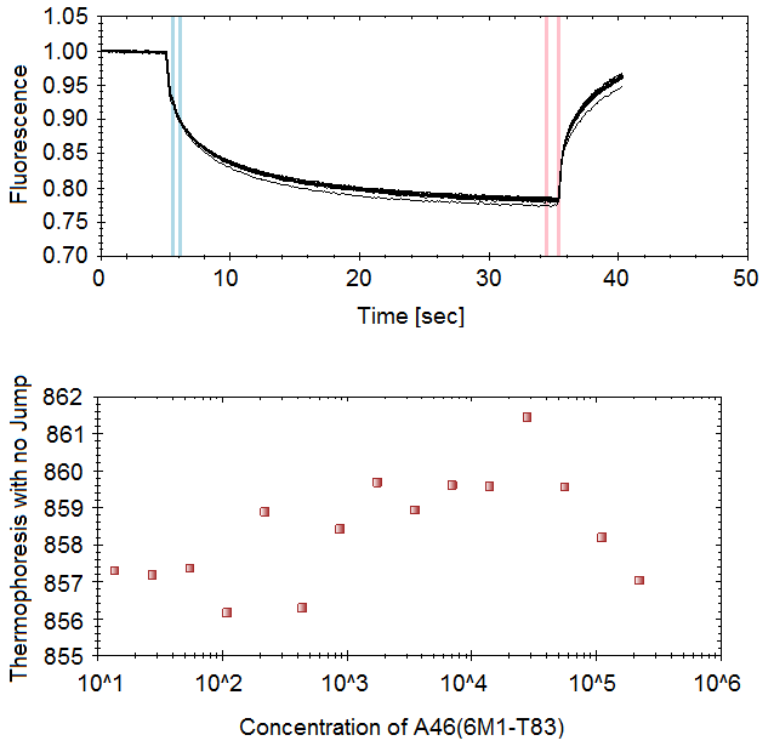

Fig. 24: MST of A46(6M1-T83) and Cys-labelled MAL(75-253). The MST measurement was performed with Cys-labelled MALl(75-235) and serial dilutions of A46(6M1-T83) with end concentrations between 223.25 µM and 13.63 nM. The LED power was 50 %, the laser power was 60 %. The upper panel shows the relative fluorescence over time. The curves of 14 individual measurements with different concentrations of A46(6M1-T83) are over-laid. The lower panel shows the thermophoresis of the individual measurements plotted against the concentration of A46(6M1-T83) in nM.

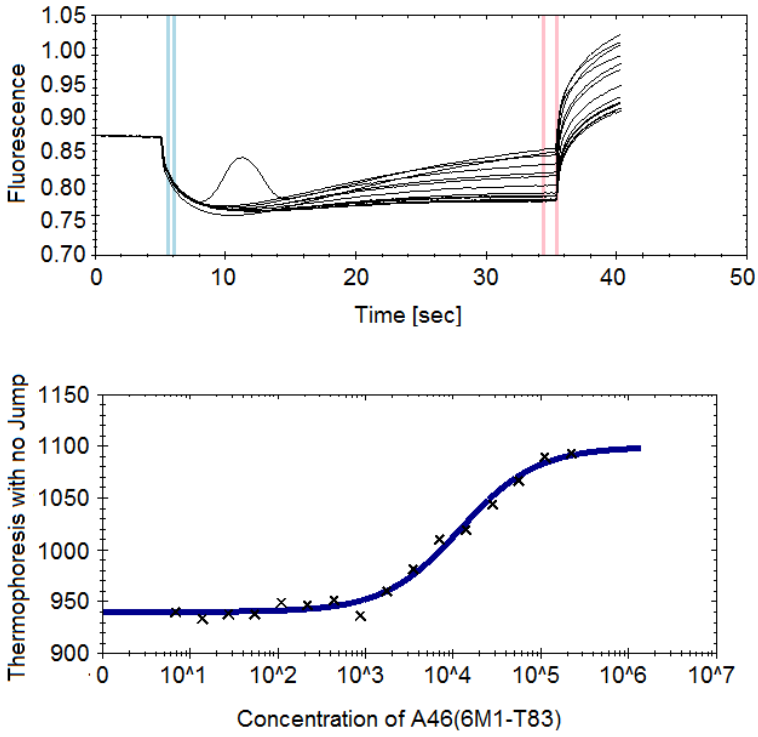

Fig. 25: MST of A46(6M1-T83) and NHS-MyD88(146-296). The MST measurement was performed with NHS-labelled MyD88(146-296) and serial dilutions of A46(6M1-T83) with end concentrations between 223.25 µM and 6.81 nM, assuming a trimeric state. The LED power was 50 %, the laser power was 80 %. The upper panel shows the relative fluorescence over time of 15 individual measurements with different concentrations of A46(6M1-T83). The lower panel shows the thermophoresis of the individual measurements plotted against the concentration of A46(6M1-T83) in nM.

3.3 Expression and Purification of MyD88 variants

To test whether the sequence variation between human and murine MyD88 TIR domains affects their binding to MAL, we wanted to compare the affinities of murine and human TIR/MyD88 to the TIR domain of human MAL. The murine MyD88 construct used for MST, covering amino acids 146 to 296, was hard to purify. Therefore, we aimed to purify the human and murine orthologs covering amino acids 157 to 296, as a protocol for the purification of hMyD88(157-296) has been published (Synder et al., 2013). Moreover, we wanted to establish a protocol for the purification of full-length human MyD88 to test for a difference in binding between the full-length proteins and the TIR domains alone.

3.3.1 Optimizing the Expression and Purification of Human and Murine MyD88(157-296)

The first expression trials were based on the purification protocol published by Synder et al. (2013). Instead of G protein β1, His-TRX was used as solubility tag, as we have successfully used the pTRX expression vector for previous protein purifications. Moreover, the first expression was performed in E. coli BL21(DE3) instead of E. coli BL21(DE3) Codon Plus RIPL. The temperature and duration of expression were not described by Synder et al. (2013). Therefore, we expressed at 25 °C for four hours after induction with 0.25 mM IPTG. After harvesting, the cells were resuspended in a buffer consisting of 20 mM Tris/HCl pH 8.5, 100 mM NaCl, 25 mM imidazole and 10 mM β-mercaptoethanol, as we had successfully used this resuspension buffer for other TRX-tagged proteins.

To test for the expression and solubility of the recombinant proteins in this first expression trial, an affinity chromatography was performed with the soluble phases of the cell lysates. Only 1.5 ml Ni-NTA resin, compared to 5 ml in former purifications, was used, because the sample resulted from only 1 L expression culture. Bound proteins were eluted in approximately 10 ml elution buffer. The total, soluble and insoluble phases as well as the flow-through and elution of the chromatographies were analysed by SDS-PAGE (Fig. 26). The recombinant proteins of about 31 kDa were highly expressed, as indicated by prominent bands between 25 and 37 kDa in the samples taken from the total cell lysates (T). However, the majorities of both human and murine MyD88(157-296) were insoluble. This is indicated by similar intensities of the bands in the samples taken from the insoluble phases (I) and in the samples taken from the total cell lysates. Accordingly, only very light bands can be

observed in the samples taken from the soluble phases (S). Nevertheless, protein bands of correct sizes are visible in the elution fractions (E).

As Synder et al. (2013) used a codon-optimized strain of E. coli, the next expression test was performed with E. coli BL21(DE3) Codon Plus. For each recombinant protein, the cells of 2 L expression culture were cold-shocked prior to induction of expression with 0.25 mM IPTG and incubated at 16 °C over-night. Two more litres of expression culture for each protein were incubated at 25 °C for 4 hours without cold-shock prior to induction. Of each condition, 1 L was resuspended in 20 mM Tris/HCl pH 8.5, 300 mM NaCl, 10 mM imidazole and 10 mM β-mercaptoethanol. The remaining 1 L for each condition was resuspended in the same buffer except for the use of 20 mM KH_2PO_4/K_2HPO_4 pH 6.5 for cells expressing TRX-hMyD88(M157-P296) or 20 mM HEPES pH = 7.5 for cells expressing TRX-mMyD88(T157-P296) instead of Tris/HCl pH 8.5. Buffers of different pH were used for the two recombinant proteins because of their different isoelectric points (pI). The theoretical pI of TRX-hMyD88(157-296), calculated with the protparam tool of ExPASy, is 7.55 whereas the theoretical pI for TRX-mMyD88(157-296) is 6.38. Again, the solubility of the recombinant proteins was tested by Ni-NTA chromatographies and subsequent SDS-PAGE of the total (T), soluble (S) and insoluble (I) fractions of the cell lysates (Fig. 27A) as well as the flow-through (FT) and elution (E) of the chromatographies (Fig. 27B). Again, most of the proteins of interest are visible in the insoluble phases of the cell lysates and the protein concentrations in the elutions did not increase notably. Therefore, neither the expression in BL21(DE3) Codon Plus instead of BL21(DE3) nor the resuspension in a buffer of pH 6.5 or 7.5 instead of pH 8.5 seem to increase the solubility. Interestingly, when the proteins were expressed at 16 °C over-night, three prominent bands were visible in the total cell lysates and the insoluble phases. In addition, the proteins of interest were not observed in the elution of Ni-NTA chromatography. Instead, a low band with a molecular weight between 10 kDa and 15 kDa was observed. This band might result from the TRX-tag alone. A representative SDS-PAGE gel with samples of TRX-mMyD88(157-296) expression is shown in Fig. 28. The samples of TRX-hMyD88(157-296) expression looked similar (not shown). The pH of the resuspension buffer did not have an influence on this unexpected observation. However, this phenomenon was not observed when the proteins were expressed in BL21 at 25 °C over-night. Neither the use of TB medium instead of LB medium, nor the resuspension in buffers containing 0 or 300 mM NaCl instead of 100 mM NaCl increased the solubility of the recombinant proteins (not shown).

As the solubility could not be enhanced by any of the tested methods, the final expression was performed in E. coli BL21(DE3) at 25 °C over-night. After harvesting, cells were resuspended in 20 mM Tris/HCl pH 8.5, 0, 100 or 300 mM NaCl, 25 mM imidazole, 5 % glycerol and 10 mM β-mercaptoethanol. In contrast to the over-night expression at 16 °C in BL21(DE3) Codon Plus, the recombinant proteins were expressed and could be purified by Ni-NTA chromatography. Representative SDS-PAGE gels of TRX-mMyD88(157-296) purification by Ni-NTA chromatography and serial Ni-NTA chromatography after over-night incubation with TEV protease are shown in Fig. 29 and Fig. 30. The purification of the human ortholog was similarly successful. SEC was used as last step in the purification process. Fig. 31A shows a representative chromatogram of mMyD88(157-296) The void volume peak has a small amplitude, indicating only small amounts of aggregates. The purities of the concentrated samples were analysed by SDS-PAGE (Fig. 31B). No impurities could be observed. The yields of the murine and human orthologs were about 4.5 and 5.5 mg, respectively. This is a nevertheless low yield considering the use of 12 L expression culture for each protein.

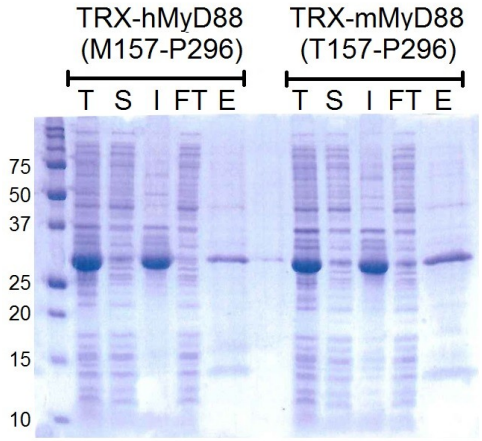

Fig. 26: Expression of human and murine MyD88(157-296). SDS-PAGE of the total (T), soluble (S) and insoluble (I) phases and the flow-through (FT) and elution (E) of Ni-NTA chromatography (2 µl each). Human or murine TRX-MyD88(157-296) were expressed in E. coli BL21(DE3) in 1 L of LB medium. The soluble proteins of interest were purified using 1.5 ml of Ni-NTA resin. Bound proteins were eluted in 10 ml elution buffer. The prominent bands between 25 and 37 kDa correspond to the TRX-tagged proteins of interest.

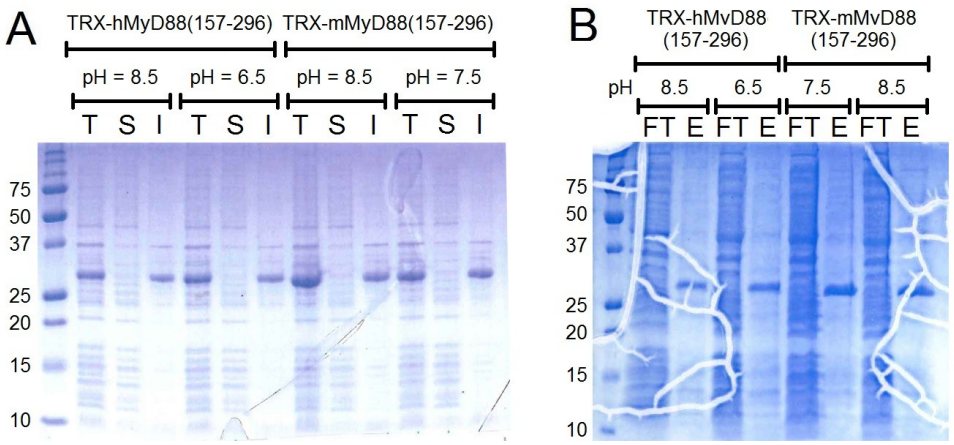

Fig. 27: Influence of pH on the solubility of TRX-MyD88(157-296). TRX-hMyD88(157-296) and TRX-mMyD88(157-296) were expressed in E. coli BL21(DE3) Codon Plus in 1 L LB medium per condition. After harvesting, cells were resuspended in a buffer with a pH of 8.5, 7.5 or 6.5. 1 µl of the total cell lysates (T) as well as the soluble (S) and insoluble (I) phases were used for SDS-PAGE (A). In addition, the soluble phases were analysed by Ni-NTA chromatography. Bound proteins were eluted in 5 ml. 1 µl of the flow-throughs (FT) and elutions (E) were used for SDS-PAGE (B). The proteins of interest of about 31 kDa are visible in the samples taken from the total cell lysates, the insoluble phases, as well as the elutions.

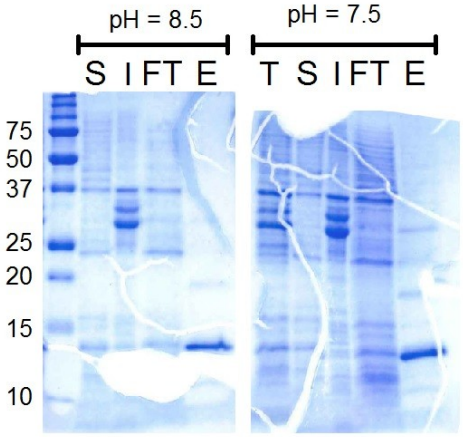

Fig. 28: Expression of TRX-mMyD88(T157-P296) in E. coli BL21(DE3) Codon Plus at 16 °C over-night. TRX-mMyD88(T157-P296) was expressed in E. coli BL21(DE3) Codon Plus in 1 L LB medium at 16 °C over-night. Harvested cells were resuspended in a buffer with a pH of either 8.5 or 7.5. His-tagged proteins in the soluble phases were purified via 1.5 ml of Ni-NTA resin. Bound proteins were eluted in 5 ml. 1 µl of the total cell lysate (T) of the cells resuspended in the buffer with pH = 7.5, of the soluble (S) and insoluble (I) phases of both cell lysates as well as the flow-throughs (FT) of the affinity chromatographies and 5 µl of the elutions (E) were used for SDS-PAGE.

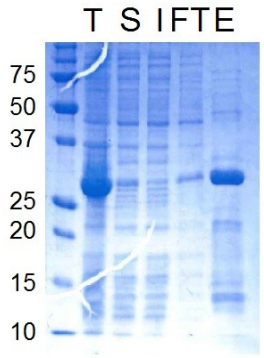

Fig. 29: Ni-NTA chromatography of TRX-mMyD88(T157-P296). TRX-mMyD88(T157-P296) was expressed in E. coli BL21(DE3) in 2 L of LB medium at 25 °C over-night. After harvesting, cells were resuspended in 20 mM Tris/HCl pH 8.5, 25 mM imidazole, 5 % glycerol and 10 mM β-mercaptoethanol. The soluble phase was used for Ni-NTA chromatography. The protein of interest was eluted in 15 ml elution buffer. 0.5 µl of the total cell lysate (T), the soluble (S) and insoluble (I) phases and the flow-through (FT) of the chromatography, as well as 5 µl of the elution were used for SDS-PAGE. The recombinant protein of interest with a molecular mass of about 31 kDa is visible as prominent band between 25 and 37 kDa in the samples taken from the total cell lysate and the elution.

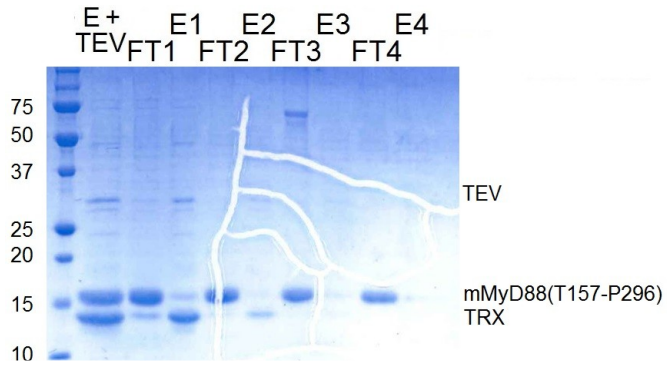

Fig. 30: Serial Ni-NTA chromatography of mMyD88(T157-P296). TRX-mMyD88(T157-P296) was cleaved by over-night incubation with TEV protease. The protease as well as the TRX-tag, have a His-tag and can therefore be removed from the protein of interest by serial Ni-NTA chromatography. 5 µl of the cleaved sample (E + TEV) as well as the flow-throughs (FT) containing the protein of interest and elutions (E) containing TEV protease and TRX-tag were used for SDS-PAGE.

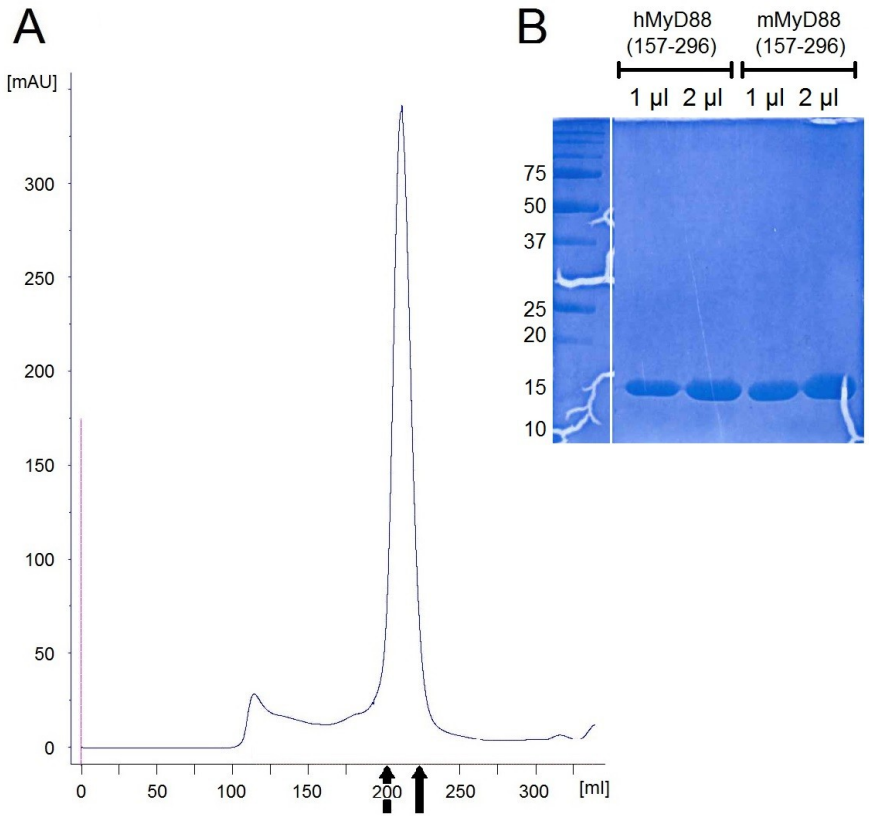

Fig. 31: SEC and concentrated MyD88(157-296). SEC was the last step in the purification o-mMyD88(157-296) (A). The protein of 12 L expression cultures was separated from any residual impurities with a HiLoad 26/60 Superdex 75 prep grade column. Black arrows show the start and end of the fractions that were used for concentration. In (B), 1 and 2 µl of the concentrated mMyD88(T157-P296) as well as concentrated hMyD88(157-296) were loaded. Both proteins were purified from 12 L expression culture. The murine and human orthologs were concentrated to ~ 750 µl with concentrations of ~ 7.5 mg/ml and ~ 5.7 mg/ml, respectively.

3.3.1 Establishing a Protocol to Purify Human Full-length MyD88

In contrast to the TIR domains of murine and human MyD88, which were are at least partly soluble, the full-length hMyD88 was almost completely insoluble in the first expression tests with E. coli BL21(DE3) or BL21(DE3) Codon Plus. Neither the expression in TB medium instead of LB medium, nor a change in the pH of the resuspension buffer enhanced the solubility (not shown). Also, the trial to refold the precipitated protein of interest remained unsuccessful. After the last centrifugation step, the protein was again present in the pellet instead of the supernatant (not shown).

However, as can be seen in Fig. 32, when a resuspension buffer without NaCl was used, the protein of interest was soluble enough to be visible in the elution of Ni-NTA chromatography. The expression was performed in E. coli BL21 in LB medium at 25 °C for either 4 hours or over-night. The concentration of protein of interest in the elution of Ni-NTA chromatography was slightly higher in the sample from over-night expression. A Western Blot was performed with the samples taken from the total cell lysates as well as the soluble and insoluble phases (Fig. 33). On the corresponding SDS PAGE gel, a band of correct size was visible for both 4 h and over-night expression, as is also the case on the SDS-PAGE gel shown in Fig. 21. However, on the Western Blot, a signal is only observed in the sample from over-night expression. Due to the large amounts of protein in the total and insoluble fractions, the film was exposed to the membrane for only 10 seconds. When the film was exposed for a longer time, the signals from the total and insoluble fractions overlapped with the lane of the soluble fraction. Probably, the signal of the sample from the over-night expression is already visible after a 10 second exposure due to a higher over-all yield, while the signal of the four-hour expression is not yet visible.

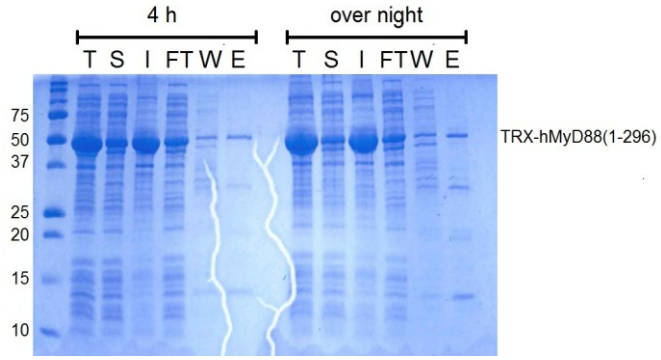

Fig. 32: Ni-NTA chromatography of TRX-hMyD88(M1-P296). TRX-hMyD88(M1-P296) was expressed in E. coli BL21 for either four hours or over-night in 1 L of LB medium. Harvested cells were resuspended in 20 mM Tris/HCl pH 8.5, 10 mM imidazole, 5 % glycerol and 10 mM β-mercaptoethanol. The total cell lysate (T), the soluble (S) and insoluble (I) phases as well as the flow through (FT) (0.5 µl each), the wash (W) and the elution (E) (10 µl each) of the chromatography were used for SDS-PAGE. The recombinant protein of interest has a molecular weight of about 47.6 kDa and is therefore represented by the bands slightly below the 50 kDa marker.

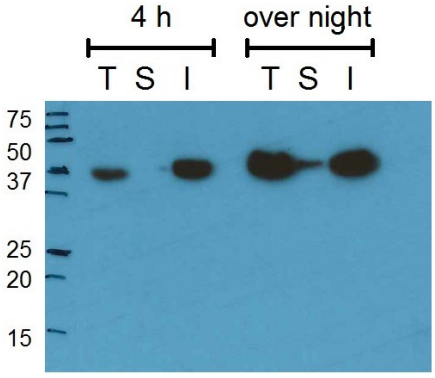

Fig. 33: Western Blot of TRX-hMyD88(M1-P296). A Western Blot with samples taken from the total cell lysate (T) as well as the soluble (S) and insoluble (I) phases (0.5 µl each) of E. coli BL21 expressing TRX-hMyD88(M1-P296) for either four hours or over-night. Mouse anti-His antibody was used as primary antibody. Goat anit-mouse antibody coupled to horseradish peroxidase was used as secondary antibody After starting the luminescent reaction, the film was exposed to the membrane for about 10 seconds before development.

For further purifications, the protein of interest was expressed in E. coli BL21(DE3) in 6 to 12 L of LB medium at 25 °C over-night. As can be seen in Fig. 32 and Fig. 34A, instead of one prominent band at around 50 kDa as is expected due to the molecular weight of TRX-hMyD88(M1-P296) of about 47.6 kDa, three bands are visible in the elution, especially in the samples from over-night expression. Therefore, a Western Blot was performed with samples taken from the total cell lysate, the soluble phase, the flow-through and elution of the Ni-NTA chromatography as well as the elution after over-night incubation with TEV protease to cleave off the TRX-tag (Fig. 34B). The smear in the total fraction above 50 kDa might result from protein that did not enter the separating gel properly due to the stickiness of the total fraction. However, also below 50 kDa a strong signal is observed. This might result from naturally occurring histidine patches in endogenous E. coli protein or degradation of the protein of interest. In the soluble fraction, only one prominent band of the correct size is observed. However, below this prominent band, three very light but distinctive bands are visible. Some of the protein of interest was also present in the flow-through. As the

concentration of the protein of interest in the soluble fraction is not high enough to account for over-loading of the column, protein of interest in the flow-through most probably indicates precipitated or aggregated proteins. All of the three bands in the sample taken from the elution visible on the SDS-PAGE gel gave a signal on the Western Blot. In addition, one more band that is hardly visible on the SDS-PAGE gel can be observed. These additional proteins might be impurities resulting from naturally occurring E. coli proteins with histidine patches. However, after addition of TEV protease, all of the bands, except the lowest one, became lighter or even disappeared. This indicates a His-tag that is cleaved by TEV protease. The uppermost band represents the protein of interest. It is efficiently cleaved by TEV. The His-tagged TEV protease is not visible on the Western Blot, probably due to its low concentration in the sample. The lowest band represents the His-TRX-tag. A band of the same size is already present in the elution, indicating cleavage before the addition of TEV protease or a premature stop in translation. The middle bands probably result from degradation of the protein of interest. This degradation already starts in the soluble fraction, giving raise to the three bands below the protein of interest. During Ni-NTA chromatography, the degradation proceeds. The distinctive character of the bands indicates specific degradation of the protein of interest as opposed to unspecific degradation resulting in a smear. The purity of the protein of interest was enhanced by serial Ni-NTA chromatography. After serial Ni-NTA chromatography, 5 – 10 ml samples were dialysed against either 20 mM Tris/HCl pH 8.5 and 5 mM DTT or 20 mM Tris/HCl pH 8.5, 400 mM Urea and 5 % glycerol. No precipitation was observed in any of them and no degradation products were observed by SDS-PAGE (not shown). The urea-containing buffer was used, as a His-tagged version of the protein is commercially available in this buffer (for example from Acris Antibodies GmbH, product number AR50718PU-S). However, protein precipitation was observed during concentration for SEC. The remaining protein was present only in the void volume, indiciating further aggregation.

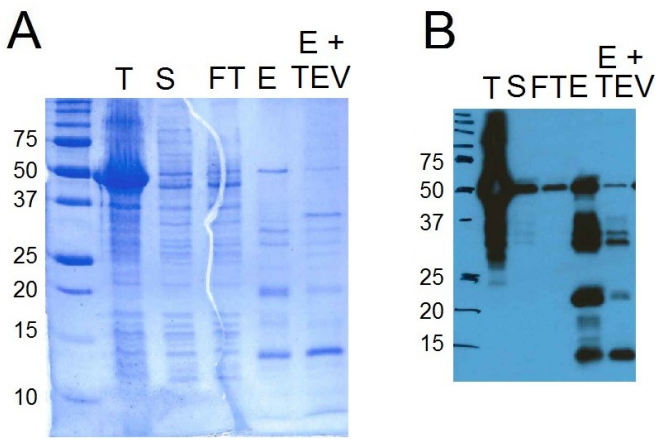

Fig. 34: Ni-NTA chromatography and Western Blot of TRX-hMyD88(M1-P296). The soluble phase of the cell lysate of 3 L expression culture was used for Ni-NTA chromatography. Bound proteins were eluted in 20 ml elution buffer. The total cell lysate (T), the soluble phase (S) and the flow-through (FT) (1 µl each) and elution before (E) and after (E + TEV) over-night incubation with TEV protease (10 µl each) were used for SDS-PAGE and Western Blot. The film was exposed for about 10 seconds.

4 Discussion

4.1 Effect of BB Loop Mutations on the Interaction Between A46 and TRAM

A46 interferes with the activation of NF-κB by binding to the TLR adapter molecules TRAM, TRIF, MyD88 and MAL (Stack & Bowie, 2012; Stack et al., 2005). Structural models of TLR4, TRAM and MAL suggest a role of the BB loop in TLR4 for receptor dimerization as well as involvement of the BB loop in TRAM and MAL in binding to the receptor (Fig. 35) (Miguel et al., 2007). The BB loop might therefore be a likely target for A46 to disrupt the binding of TLRs to their adapter proteins.

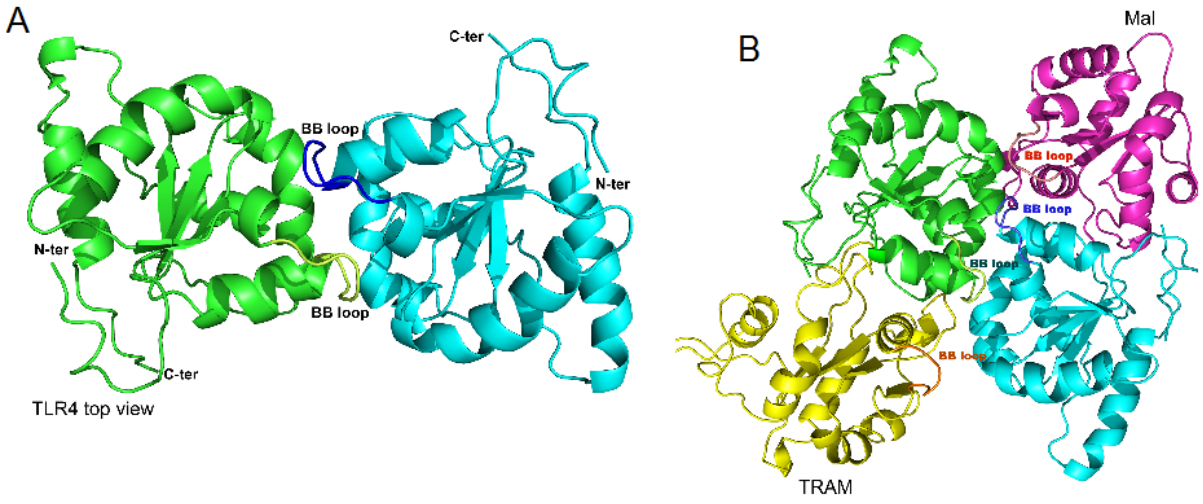

Fig. 35: Structural model of TLR4 dimer alone and interacting with MAL and TRAM. A structural model of the TLR4 dimer shows the BB loop on the interacting site (A). The dimer interface forms an interaction site for the adapter proteins MAL and TRAM. The BB loops of the adapter proteins are involved in the binding to TLR4 (B). Adapted from Miguel et al. (2007).

Indeed, several findings point towards an intact BB loop of these proteins as a pre-requisite for the interaction with A46. For example, A46 interacts with TLR2 and TLR4, but not TLR3 (Stack & Bowie, 2012). In contrast to the former, which code for a conserved proline in their BB loop, TLR3 codes for an alanine instead of the proline. The conserved proline also seems to play a role in the recruitment of MyD88 to TLRs, as TLR3 is the only TLR that cannot recruit MyD88. However, if the alanine is mutated to proline, TLR3 can activate the MyD88-dependent pathway (Verstak et al., 2013). In agreement with the hypothesis that a conserved BB loop proline mediates not only the interaction between TLR2 and TLR4 with MyD88, but

also with A46, the interaction between TLR2 and TLR4 with A46 is abolished upon a proline to histidine mutation. Similarly, MyD88 P200H, MAL P125H and TRIF P434H did not interact with A46 in co-immunoprecipitation or GST pulldown assays. TRAM codes for a cysteine instead of the proline on position 116, but for a proline on position 117. Both amino acids seem to be important for the interaction with A46, as a mutation to histidine of either P116 or C117 abolished binding (Stack et al., 2005; Stack & Bowie, 2012). Accordingly, a docking model of the A46 C-terminus and the TIR domain of TRAM, published by Fedosyuk et al. (2014) shows the BB loop of TRAM in close proximity to the VIPER motif in A46 that has been shown to mediate binding of A46 to TRAM and MyD88 (Fig. 36) (Lysakova-Devine et al., 2010).

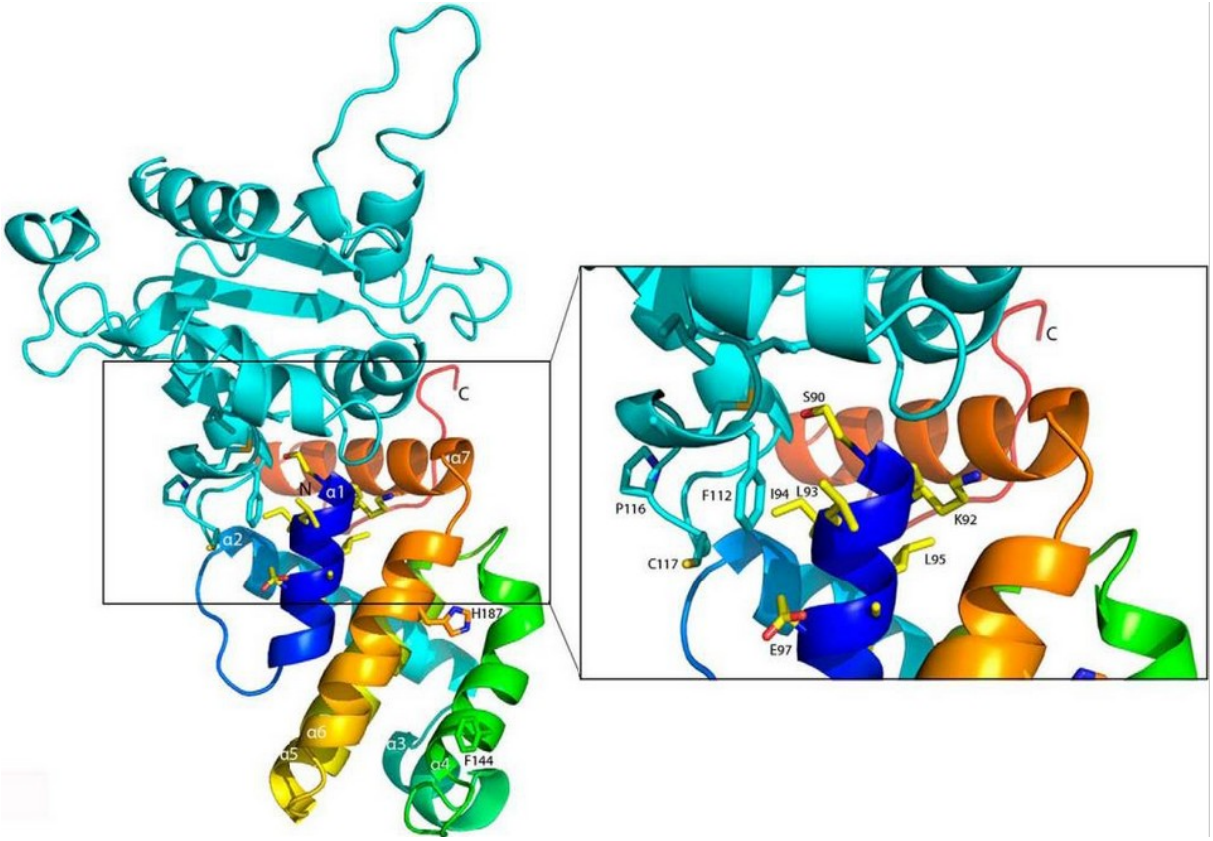

Fig. 36: Docking model of TRAM and A46(N87-T229). Docking model by Fedosyuk et al. (2014) of A46 (colour spectrum von N to C terminus) and TRAM (cyan). Residues of the VIPER motif in A46 and the BB loop in TRAM are shown in sticks. The interaction site between the two molecules is shown enlarged.

We wanted to assess the importance of P116 and C117 in TRAM for binding to A46. Another amino acid in the BB loop of TRAM, F112, might facilitate binding by hydrophobic interactions with I94 in A46 (Fedosyuk et al., 2014). Therefore, we expressed mutants of TRAM(66-235) and the A46 C-terminus, namely A46(N87-T229) I94A, TRAM F112A or P116H and the triple mutant TRAM F112A P116H C117H. Against our expectations and in

contrast to the results obtained by Stack and Bowie (2012), we observed binding between TRAM(66-235) F112A or P116H and A46(N87-T229) wt or I94A. Even the triple mutant form of TRAM(66-235) interacted with A46(N87-T229) wt or I94A. The binding affinities were in the range of 1 to 5 µM for all tested combinations. Moreover, the wt and triple mutant form of TRAM(66-235) bound to A46(N87-T229) wt or I94A with similar affinities as to the full-length A46 with four additional amino acids on the N-terminus. This is in line with the observation that the C-terminal part of A46 is sufficient for the binding of MAL and MyD88 (Fedosyuk et al., 2014). One difference to the experiments performed by Stack and Bowie (2012) was the expression of the recombinant proteins. We expressed all proteins in E. coli, whereas Stack and Bowie (2005) expressed the proteins in mammalian HEK293T cells. The same mutations might affect protein folding differently in bacterial and mammalian cells. However, mammalian cells are the natural host of VACV and would therefore be expected to facilitate correct folding of VACV proteins better than bacterial cells. In addition to the different expression conditions, the experimental set-up was different. We removed any tags from both putative binding partners prior to MST experiments whereas at least one of the binding partners was fused to a tag in the experiments performed by Stack and Bowie (2005). A tag might further hamper already weakened binding by steric hindrance. Moreover, we measured direct protein-protein interactions between purified binding partners, whereas Stack and Bowie (2005) performed GST-pulldown assays with whole cell lysates of HEK293 cells. This cell line, derived from human embryonic kidney cells, codes for MyD88 (Li et al., 1999). It is therefore likely that the other TLR adapter proteins are endogenously expressed as well. If a mutation in the BB loop of TRAM lowers the affinity for A46, endogenous wild-type TRAM would act as comparative inhibitor of the interaction and might, due to higher affinity, prevent binding of the tagged, mutated TRAM to A46.

4.2 Investigating the N-terminal Domain of the Vaccinia Virus Protein A46

One aim of this thesis was to investigate the N-terminal domain of the vaccinia virus protein A46. Fedosyuk et al. (2014) showed that the C-terminal domain of A46, lacking the first 86 amino acids, is sufficient for binding of MAL and MyD88, although with a slightly lower affinity. As viruses tend to keep their genomes small to ensure more rapid replication, it is likely that the N-terminal part of A46 does have at least one biologically significant role. Moreover, as described in the introduction, although the structure of the C-terminal domain of A46 has been solved and shown to share structural homology with other VACV-encoded inhibitors of TLR signaling, the structure of the N-terminal 90 amino acids of A46 is unknown

(Fedosyuk et al., 2014; Kim et al., 2014). A protein BLAST (http://blast.ncbi.nlm.nih.gov/Blast.cgi) excluding poxviral proteins yields ankyrin domain-containing proteins. The best hit of human origin is chain D of a complex of human varp-ankrd1 with rab32-gppcp (E-value 3.49e-04, bis-score 33.88, identity 31 %). The according alignment is shown in Fig. 37.

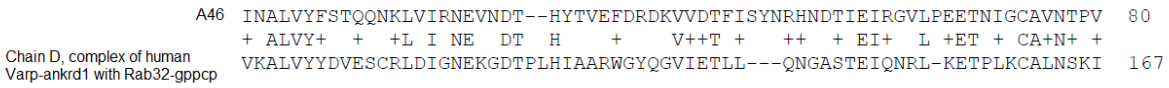

Fig. 37: Alignment of A46 N-terminal domain with chain D of a complex of human varp-ankrd1 with rab32-gppcp. A BLAST search was performed with the N-terminal 80 amino acids of A46. The alignment with the best hit of human origin is shown. A plus denotes amino acids with similar properties (for example hydrophobic or charged)

Due to the lack of knowledge about the structure and function of the A46 N-terminus, we aimed to characterize this domain. We expressed three recombinant proteins, comprising the first 73, 83 or 90 amino acids of A46 coupled to TRX or MBP as solubility and affinity tag. The recombinant proteins were highly expressed and at least 50 to 75 % soluble in E. coli BL21(DE3). However, A46(6M1-S90) was proteolytically processed during the course of purification, resulting in two proteins with slightly different weights after the last purification step. Due to their similar sizes, the processed form could not be separated from the unprocessed form by SEC. The processing seems to be specific, as two distinctive protein bands were observed on SDS-PAGE gels instead of smearing bands typical for unspecific degradation. This phenomenon was not observed for the smaller constructs A46(6M1-T83) and A46(6M1-G73). A possible explanation for this behaviour could be a cleavage site between amino acid 83, the last amino acid of the middle construct, and amino acid 90. However, A46(6M1-S90) was continuously processed during the whole purification procedure, although any endogenous E. coli proteases were removed from the sample in the first purification step. TEV protease is added to cleave the solubility tag off the protein of interest, but A46 does not code for a TEV cleavage site. In addition, the full-length A46 can be purified. However, it cannot be ruled out that full-length A46 is cleaved as well. The cleavage products, which would be significantly shorter than the full-length protein, would be separated from the unprocessed A46 by SEC.

Nevertheless, the two shorter variants A46(6M1-T83) and A46(6M1-G73) could be purified. The oligomeric states of these proteins were determined by SEC-MALLS. In buffer consisting of only Tris/HCl pH 8.5 and 10 mM DTT, the calculated molecular masses for those peptides are about 27 kDa and 30 kDa, respectively. This indicates trimerization. However, when the

experiment was repeated in a buffer containing additional 150 mM NaCl, the formation of tetramers with masses of about 36 kDa for A46(6M1-G73) and 40 kDa for A46(6M1-T83) was observed. As the conditions of the latter experiment resemble the physiological environment of VACV, namely the cytoplasm, more closely, the tetrameric state is probably biologically significant. The tetrameric state of the full-length A46 observed by Fedosyuk et al. (2014) strengthens our observations. Interestingly, the C-terminal part of A46 does not form tetramers but dimers (Fedosyuk et al., 2014). Hence, the N-terminal domain of A46 might have a role in the oligomerisation of A46.

To test whether the N-terminal domain of A46 is involved in the binding of TLR adapter proteins, we performed MST measurements with A46(6M1-T83) and the TIR domains of MAL, TRAM and MyD88. No interaction was observed between A46(6M1-T83) and TRAM or MAL. However, A46(6M1-T83) interacted with MyD88(146-296) with an K_D of approximately four or five µM, assuming a trimeric or tetrameric state, respectively. These affinities are in the same range as was observed for the C-terminal part or the full-length protein (Fedosyuk et al., 2014). However, several factors complicate the calculation of the affinity. First, the molarity of A46(6M1-T83) has to be calculated from the concentration (w/v) that was measured by UV absorbance. To do so, the oligomeric state has to be considered. As we could show that A46(6M1-T83) can form trimers as well as tetramers, the calculated molarity might not reflect the real molarity. The MST buffer contains 150 mM NaCl. Using SEC-MALLS, we observed the formation of tetramers in a buffer containing 150 mM NaCl. However, the tetrameric state was not stable over the whole range of protein concentration but shifted to a trimeric state at lower protein concentrations. Therefore, the samples for MST might contain both trimers and tetramers. Moreover, as serial dilutions of A46(6M1-T83) were used for MST, the trimer to tetramer ratio might not be the same in all samples. For optimal K_D calculations, the oligomeric state of A46(6M1-T83) at several concentrations should be determined in the MST buffer. Nevertheless, the calculated K_D assuming a trimeric state (~ 4 µM) differs only slightly from the calculated K_D assuming a tetrameric state (~ 5 µM). In addition, the calculated K_D was about three to four times higher when a laser power of 60 % instead of 80 % was used. The Monolith NT.115 user manual states that the lowest possible MST power should be used. Hence, it is reasonable to assume that the measurements performed at 60 % laser power resemble the biological state better than the measurements performed at 80 % laser power as a higher laser power might have destructive effects on the proteins. Nonetheless, although we cannot be certain about the affinity, an interaction between MyD88(146-296) and A46(6M1-T83) was clearly observed. The N-terminal part of A46 might therefore add specificity to the interactions of A46 with TLR

adapter proteins. This is in line with the observation that the C-terminal part alone can interact with MyD88 but with a lower affinity than the full-length A46. However, as we did not observe any interactions between A46(6M1-T83) and TRAM or MAL, we cannot explain the different affinity of A46(N87-T229) to MAL compared to the full-length protein that was observed by Fedosyuk et al. (2014). Nonetheless, the N-terminal domain of A46 might strengthen the interactions between the C-terminus of A46 and TRAM or MAL by stabilizing a tetrameric conformation of the full-length protein.

4.3 Expression and Purification of MyD88 variants

The expression of human and murine MyD88 TIR domains, ranging from amino acids 156 to 296, proved to be more difficult than the expression of A46 N-terminal variants. The first expression test in E. coli BL21(DE3) in LB medium at 25 °C over-night showed that most of the protein of interest was insoluble. Attempts to improve the solubility by the variation of several parameters, for example the strain of E. coli that was used for expression, the expression temperature and duration as well as the composition of the resuspension buffer, were unsuccessful. When the recombinant proteins were expressed in E. coli BL21(DE3) Codon Plus at 16 °C over-night following a cold-shock on ice, no protein of correct size was detected. Instead, a protein corresponding to the size of the TRX-tag alone was expressed. This was not the case when the recombinant proteins were expressed in E. coli BL21(DE3) at 25 °C over-night without cold-shock prior to induction. The only difference between E. coli BL21(DE3) and E. coli BL21(DE3) Codon Plus is that the Codon Plus strain codes for three additional tRNAs to ensure rapid translation of codons not common in E. coli. This strain should therefore be more suitable for the expression of recombinant viral proteins. In subsequent expressions at 25 °C, the expression and solubility of the proteins did not differ between the two strains. Therefore, the use of E. coli BL21(DE3) Codon Plus cannot explain the expression of the TRX-tag alone instead of the recombinant protein. Premature stop codons in the plasmids were ruled out by sequencing. Moreover, the same plasmids were successfully translated into the recombinant proteins in later expressions. Therefore, the cold shock and expression at 16 °C seems to be responsible for the premature stop of translation. This is unexptected as lower expression temperatures tend to enhance the solubility of recombinant proteins (Rosano & Ceccarelli, 2014). It was possible to purify the soluble proteins with a yield of about 0.5 mg protein per liter expression culture if they were expressed in E. coli BL21(DE3) at 25 °C over-night. Expressions were performed in 12 L LB medium to obtain enough protein for MST experiments. Further expression conditions should be tested to avoid losing the majority of expressed protein of interest.

It was not possible to purify full-length human MyD88. Although the solubility could be slightly enhanced by using buffers of low ionic strength during the purification process, the protein precipitated during concentration for SEC. For future purifications, the solution should not be higher concentrated than absolutely necessary for SEC. Moreover, further conditions and different solubility tags should be tested for their influence on solubility. Alternatively, it might be worth purifying the protein without cleaving off the tag.

4.4 Conclusion

The most important findings of this thesis are summarized in Fig. 38. We showed that, in contrast to the observations of Stack and Bowie (2012), an intact BB loop in TRAM is not necessary for the interaction with A46, as the triple mutant TIR/TRAM F112A P116H C117H interacted with A46(N87-T229) (Fig. 38A). Moreover, we successfully expressed and purified the N-terminal domain of A46, covering amino acids 1 to 83 (Fig. 38B). We showed that this construct can form tetramers and might therefore facilitate tetramerization of full-length A46. Another role of the A46 N-terminal domain might be to facilitate binding of the full-length protein to MyD88, as it specifically interacts with this protein but neither TRAM nor MAL. Additionally, A46(6M1-T83) could form crystals and was used to solve the structure of the A46 N-terminus (Fig. 38D) (Fedosyuk et al., unpublished data).

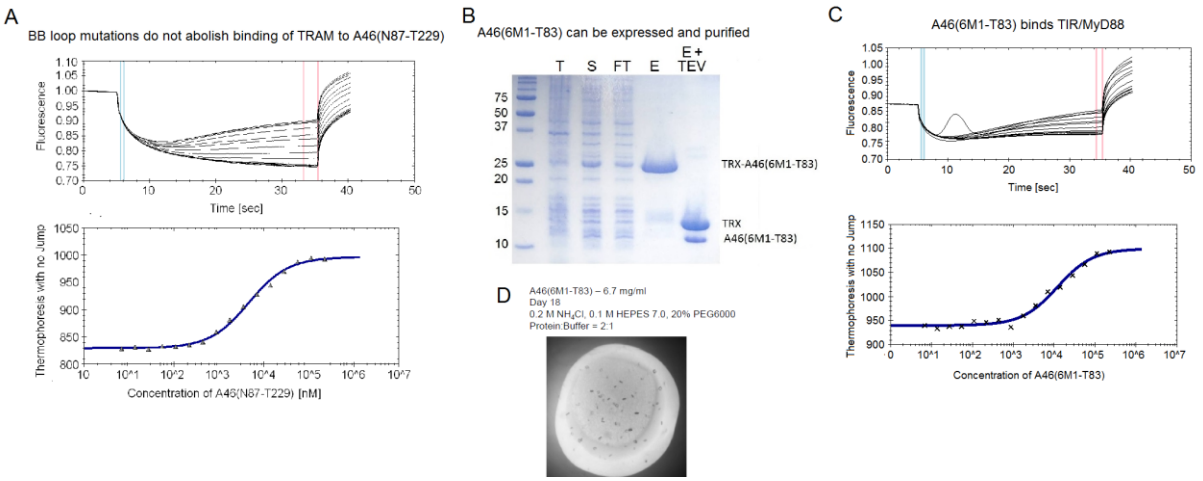

Fig. 38: Summary of this work. (A) MST measurement of TRAM F112A P116H C117H with A46(N87-T229) shows that the BB loop mutations do not abolish interactions between those proteins (see chapter 3.1). (B) A46(6M1-T83) could be expressed in E. coli BL21 and was purified by Ni-NTA chromatography. The TRX tag was efficiently cleaved off by TEV protease (see chapter 3.2.1.2). (C) A46(6M1-T83) binds TIR/MyD88 (see chapter 3.2.3.2). (D) The purified protein formed crystals (Fedosyuk et al., unpublished data).

5 Appendix

5.1 Amino acids

1-letter-code	3-letter-code	amino acid
A	Ala	Alanine
C	Cys	Cysteine
D	Asp	Aspartic acid
E	Glu	Glutamic acid
F	Phe	Phenylalanine
G	Gly	Glycine
H	His	Histidine
I	Ile	Isoleucine
K	Lys	Lysine
L	Leu	Leucine
M	Met	Methionine
N	Asn	Asparagine
P	Pro	Proline
Q	Gln	Glutamine
R	Arg	Arginine
S	Ser	Serine
T	Thr	Threonine
V	Val	Valine
W	Trp	Tryptophan
Y	Tyr	Tyrosine

5.2 Abbreviations

General abbreviations	
°C	degrees Celsius
2-5A	pppA2'p5'A2'p5'A
Amp	ampicillin
APS	ammonium persulfate
ATP	adenosine triphosphate
BLAST	basic local alignment search tool
CAM	chloramphenicol
CARD	caspase activation and recruitment domain
Da	Dalton
DC	dendritic cell
ddH_2O	double-distilled water
DNA	deoxyribonucleic acid
dNTP	deoxynucleotide triphosphate
ds	double-stranded
DTT	dithiothreitole
EDTA	ethylenediaminetetraacetic acid
ER	endoplasmic reticulum
EV	extracellular virus
FMDV	foot-and-mouth disease virus
FPLC	fast protein liquid chromatography
g	gram
GAS	gamma-IFN activation site
GSH	glutathione, reduced
IFN	interferon
IL	interleukin
IPTG	isopropyl-β-D1-thiogalactypyranoside
ISG	IFN-stimulated gene
ISRE	IFN-stimulated response element
IV	immature virus

KAc	potassium acetate
Kan	kanamycine
kbp	kilo base pairs
kDa	kilo Dalton
L	liter
LB	lysogeny broth
LPS	lipopolysaccharide
M	molar
MALLS	multi angle laser light scattering
mg	milligram
min	minute(s)
ml	milliliter
mM	millimolar
MQ H_2O	Milli-Q H_2O
mRNA	messenger RNA
MST	microscale thermophoresis
MV	mature virus
MVA	modified vaccinia Ankara
ng	nanogram
Ni-NTA	nickel-nitrolotriacetic acid
NK cells	natural killer cells
nm	nanometer
o/n	over-night
OD600	optical density at 600 nm
PAMP	pathogen-associated molecular pattern
PBS	phosphate-buffered saline
PBS-T	phosphate-buffered saline Tween-20
PCR	polymerase chain reaction
pI	isoelectric point
poly(A)	poly-adenosine monophosphates
PRR	pattern-recognition receptor

RLR	RIG-I-like receptor
RNA	ribonucleic acid
rpm	revolutions per minute
RT	room temperature
SDS	sodium dodecyl sulfate
SDS-PAGE	sodium dodecyl sulfate-polyacrylamide gel electrophoresis
SEC	size exclusion chromatography
sec.	second(s)
ss	single-stranded
TAE	Tris-acetate-EDTA
TB	terrific broth
TEMED	tetramethylethylenediamine
TEV	tobacco etch virus
TIR	Toll/interleukin-1 receptor
TIR/	TIR domain of
TLR	Toll-like receptor
TY medium	tryptone-yeast extract medium
UV	ultraviolet
V	Volt
VACV	vaccinia virus
VARV	variola virus
VIPER	viral inhibitory peptide of TLR4
WHO	World Health Organization
wt	wild-type
µg	microgram
µl	microliter
µM	micromolar
Protein names	
AF-1	accessory factor 1
Bcl-2	B-cell lymphoma 2
CREB	cyclic AMP response element-binding protein

DUBA	deubiquitinating enzyme A
eIF-2α	eukaryotic initiation factor 2α
G3BP	Ras-GTPase-activating protein SH3 domain-binding protein
GST	glutathione S-transferase
h/mTRAM(x-y)	human/murine TRAM, amino acids x to y
hMAL(x-y)	human MAL, amino acids x to y
hMyD88(x-y)	human MyD88, amino acids x to y
hnRNP	heterogeneous ribonucleoprotein particle
IFN-αR	IFN-α/β receptor
IFN-γR	IFN-γ receptor
IKK	IκB kinase
IL-1R	IL-1 receptor
IPS-1	interferon β-promoter stimulator
IRAK	IL-1R-associated kinase
IRF	interferon regulatory factor
ISGF 3	IFN-stimulated gene factor 3
IκB	inhibitor of NF-κB
JAK	Janus kinase
LGP2	laboratory of genetics and physiology 2
MAL	MyD88-adapter-like
MAP	mitogen-activated protein
MAPK	MAP kinase
MAVS	mitochondrial antiviral signaling
MBP	maltose-binding protein
MDA5	melanoma differentiation-associated protein 5
MKK	MAPK kinase
MyD88	myeloid differentiation primary response 88
NF-κB	nuclear factor κ-light-chain-enhancer of activated B cells
OAS	2’-5’ oligoadenylate synthetase
PI3K	phosphatidylinositol 3-kinase
PKR	protein kinase R

RIG-I	retinoic acid inducible gene I
RIP	receptor interacting protein
RMB3	RNA-binding protein 3
RNase	ribonuclease
RNF125	RING finger protein 125
SARM	sterile-alpha and Armadillo motif containing protein
SPI-3	serine protease inhibitor 3
STAT	signal transducer and activator of transcription
TAB	TAK binding protein
TAK1	transforming growth factor-β-activated kinase 1
TANK	TRAF family member-associated NF-κB activator
TBK1	TANK binding kinase 1
TFIIS	transcription elongation factor SII
TICAM	TIR-containing adapter molecule
TIRAP	TIR domain containing adapter protein
TRAF	tumour necrosis factor receptor-associated factor
TRAM	TRIF-related adapter molecule
TRIF	TIR domain-containing adapter inducing IFN-β
TRX	thioredoxin
Tyk2	tyrosine kinase 2
VETF	vaccinia virus early transcription factor
VITF	vaccinia virus intermediate transcription factor
VLTF	vaccinia virus late transcription factor

References

Aguet, M., Dembic, Z., Merlin, G., 1988: Molecular cloning and expression of the human interferon-gamma receptor. Cell 55, 273 – 280.

Ahn, B. Y., Gershon, P. D., Jones, E. V., Moss, B., 1990a: Identification of rpo30, a vaccinia virus RNA polymerase gene with structural similarity to a eukaryotic transcription elongation factor. Mol. Cell. Biol. 10, 5433 – 5441.

Ahn, B. Y., Gershon, P. D., Moss, B., 1994: RNA polymerase-associated protein Rap94 confers promoter specificity for initiating transcription of vaccinia virus early genes. J. Biol. Chem. 269, 7552 – 7557.

Ahn, B. Y., Jones, E. V., Moss, B., 1990b: Identification of the vaccinia virus gene encoding an 18-kilodalton subunit of RNA polymerase and demonstration of a 5' poly(A) leader on its early transcript. J. Virol. 64, 3019 – 3024.

Ahn, B. Y., Moss, B., 1992: RNA polymerase-associated transcription specificity factor encoded by vaccinia virus. Proc. Natl. Acad. Sci. U. S. A. 89, 3536 – 3540.

Akira, S., Uematsu, S., Takeuchi, O., 2006: Pathogen recognition and innate immunity. Cell 124, 783 – 801.

Alcamí, A., Smith, G. L., 1995: Vaccinia, cowpox, and camelpox viruses encode soluble gamma interferon receptors with novel broad species specificity. J. Virol. 69, 4633 – 4639.

Alcamí, A., Smith, G. L., 1996: Soluble interferon-gamma receptors encoded by poxviruses. Comp. Immunol. Microbiol. Infect. Dis. 19, 305 – 317.

Alcamí, A., Symons, J. A., Smith, G. L., 2000: The vaccinia virus soluble alpha/beta interferon (IFN) receptor binds to the cell surface and protects cells from the antiviral effects of IFN. J. Virol. 74, 11230 – 11239.

Alexopoulou, L., Holt, A. C., Medzhitov, R., Flavell, R. A., 2001: Recognition of double-stranded RNA and activation of NF-kappaB by Toll-like receptor 3. Nature 413, 732 – 738.

Amegadzie, B. Y., Ahn, B. Y., Moss, B., 1991a: Identification, sequence, and expression of the gene encoding a Mr 35,000 subunit of the vaccinia virus DNA-dependent RNA polymerase. J. Biol. Chem. 266, 13712 – 13718.

Amegadzie, B. Y., Ahn, B. Y., Moss, B., 1992: Characterization of a 7-kilodalton subunit of vaccinia virus DNA-dependent RNA polymerase with structural similarities to the smallest subunit of eukaryotic RNA polymerase II. J. Virol. 66, 3003 – 3010.

Amegadzie, B. Y., Holmes, M. H., Cole, N. B., Jones, E. V., Earl, P. L., Moss, B., 1991b: Identification, sequence, and expression of the gene encoding the second-largest subunit of the vaccinia virus DNA-dependent RNA polymerase. Virology 180, 88 – 98.

Anderson, K. V., Jürgens, G., Nüsslein-Volhard, C., 1985: Establishment of dorsal-ventral polarity in the Drosophila embryo: genetic studies on the role of the Toll gene product. Cell 42, 779 – 789.

Aoyagi, M., Zhai, D., Jin, C., Aleshin, A. E., Stec, B., Reed, J. C., Liddington, R. C., 2007: Vaccinia virus N1L protein resembles a B cell lymphoma-2 (Bcl-2) family protein. Protein Sci. 16, 118 – 124.

Appleyard, G., Hapel, A. J., Boulter, E. A 1971: An antigenic difference between intracellular and extracellular rabbitpox virus. J. Gen. Virol. 13, 9 – 17.

Arimoto, K., Takahashi, H., Hishiki, T., Konishi, H., Fujita, T., Shimotohno, K., 2007: Negative regulation of the RIG-I signaling by the ubiquitin ligase RNF125. Proc. Natl. Acad. Sci. U. S. A. 104, 7500 – 7505.

Armstrong, J. A., Metz, D. H., Young, M. R., 1973: The mode of entry of vaccinia virus into L cells. J. Gen. Virol. 21, 533 – 537.

Assarsson, E., Greenbaum, J. A., Sundström, M., Schaffer, L., Hammond, J. A., Pasquetto, V., Oseroff, C., Hendrickson, R. C., Lefkowitz, E. J., Tscharke, D. V., Sidney, J., Grey, H. M., Head, S. R., Peters, B., Sette, A., 2007: Kinetic analysis of a complete poxvirus transcriptome reveals an immediate-early class of genes. PNAS 105, 2140 – 2145.

Bach, E. A., Tanner, J. W., Marsters, S., Ashkenazi, A., Aquet, M., Shaw, A. S., Schreiber, R. D., 1996: Ligand-induced assembly and activation of the gamma interferon receptor in intact cells. Ml. Cell. Biol. 16, 3214 – 3221.

Baglioni, C., Minks, M. A., Maroney, P. A., 1978: Interferon action may be mediated by activation of a nucleare by pppA2'p5'A2'p5'A. Nature 273, 684 – 687.

Ball, L. A., White, C. N., 1978: Oligonucleotide inhibitor of protein synthesis made in extracts of interferon-treated chick embryo cells: Comparison with the mouse low molecular weight inhibitor. Proc. Natl. Acad. Sci. U. S. A. 75, 1167 – 1171.

Ballard, D. W., Walker, W. H., Doerre, S., Sista, P., Molitor, J. A., Dixon, E. P., Peffer, N. J., Hannink, M., Greene, W. C., 1990: The v-*rel* oncogene encodes a κB enhancer binding protein that inhibits NF-κB function. Cell 63, 803 – 814.

Baroudy, B. M., Moss, B., 1980: Purification and characterization of a DNA-dependent RNA polymerase from vaccinia virions. J. Biol. Chem. 255, 4372 – 4380.

Bartfai, T., Behrens, M. M., Gaidarova, S., Pemberton, J., Shivanyuk, A., Rebek, Jr., J., 2003: A low molecular weight mimic of the Toll/IL-1 receptor/resistance domain inhibits IL-1 receptor-mediated responses. Proc. Natl. Acad. Sci. U. S. A. 100, 7971 – 7976.

Barton, G. M., Kagan, J. C., Medzhitov, R., 2005: Intracellular localization of Toll-like receptor 9 prevents recognition of self DNA but facilitates access to viral DNA. Nat. Immunol. 7, 49 – 56.

Beard, P. M., Griffiths, S. J., Gonzales, O., Haga, I. R., Pechenick Jowers, T., Reynolds, D. K., Wildenhain, J., Tekotte, H., Auer, M., Tyers, M., Ghazal, P., Zimmer, R., Haas, J., 2014: A loss of function analysis of host factors influencing vaccinia virus replication by RNA interference. PLoS One 9: e98431.

Beattie, E., Paoletti, E., Tartaglia, J., 1995: Distinct patterns of IFN sensitivity observed in cells infected with vaccinia K3L- and E3L-mutant viruses. Virology 210, 254 – 263.

Beg, A. A., Ruben, S. M., Scheinman, R. I., Haskill, S., Rosen, C. A., Baldwin, Jr., A. S., 1992: I kappa B interacts with the nuclear localization sequence of the subunits of NF-kappa B: mechanism for cytoplasmic retention. Genes Dev. 6, 1899 – 1913.

Benech, P., Merlin, G., Revel, M., Chebath, J., 1985b: 3' end structure of the human (2'-5') oligo A synthetase gene: prediction of two distinct proteins with cell type-specific expression. Nucleci Acids Res. 13, 1267 – 1281.

Benech, P., Mory, Y., Revel, M., Chebath, J., 1985a: Structure of two forms of the interferon-induced (2'-5') oligo A synthetase of human cells based on cDNAs and gene sequences. EMBO J. 4, 2249 – 2256.

Bisht, H., Weisberg, A. S., Moss, B., 2008: Vaccinia virus I1 protein is required for cell entry and membrane fusion. J. Virol. 82, 8687 – 8694.

Bisht, H., Weisberg, A. S., Szajner, P., Moss, B., 2009: Assembly and disassembly of the capsid-like external scaffold of immature virions during vaccinia virus morphogenesis. J. Virol. 83, 9140 – 9150.

Boulter, E. A., 1969: Protection against poxviruses. Proc. R. Soc. Med. 62, 295 – 297.

Boulter, E. A., Zwartouw, H. T., Titmuss, D. H., Maber, H. B., 1971: The nature of the immune state produced by inactivated vaccinia virus in rabbits. Am. J. Epidemiol. 94, 612 – 620.

Boyd, O., Turner, P. C., Moyer, R. W., Condit, R. C., Moussatche, N., 2010: The E6 protein from vaccinia virus is required for the formation of immature virions. Virology 399, 201 – 211.

Brakel, C., Kates, J. R., 1974: Poly(A) polymerase from vaccinia virus-infected cells. I. Partial purification and characterization. J. Virol. 14, 715 – 723.

Branca, A. A., Baglioni, C., 1981: Evidence that types I and II interferons have different receptors. Nature 294, 268 – 770.

Broyles, S. S., 2003: Vaccinia virus transcription. J. Gen. Virol. 84, 2293 – 2303.

Broyles, S. S., Fesler, B. S., 1990: Vaccinia virus gene encoding a component of the viral early transcription factor. J. Virol. 64, 1523 – 1529.

Broyles, S. S., Moss, B., 1986: Homology between RNA polymerases of poxviruses, prokaryotes, and eukaryotes: nucleotide sequence and transcriptional analysis of vaccinia virus genes encoding 147-kDa and 22-kDa subunits. Proc. Natl. Acad. Sci. U. S. A. 83, 3141 – 3145.

Broyles, S. S., Moss, B., 1988: DNA-dependent ATPase activity associated with vaccinia virus early transcription factor. J. Biol. Chem. 263, 10761 – 10765.

Broyles, S. S., Pennington, M. J., 1990: Vaccinia virus gene encoding a 30-kilodalton subunit of the viral DNA-dependent RNA polymerase. J. Virol. 64, 5376 – 5382.

Broyles, S. S., Yuen, L., Shuman, S., Moss, B., 1988: Purification of a factor required for transcription of vaccinia virus early genes. J. Biol. Chem. 263, 10754 – 10760.

Cairns, J., 1960: The initiation of vaccinia infection. Virology 11, 603 – 623.

Carroll, K., Elroy-Stein, O., Moss, B., Jagus, R., 1993: Recombinant vaccinia virus K3L gene product prevents activation of double-stranded RNA-dependent, initiation factor 2 alpha-specific protein kinase. J. Biol. Chem. 268, 12837 – 12842.

Carter, G. C., Law, M., Hollinshead, M., Smith, G. L., 2005: Entry of the vaccinia virus intracellular mature virion and its interactions with glycosaminoglycans.

Carty, M., Goodbody, R., Schröder, M., Stack, J., Moynagh, P. N., Bowie, A. G., 2006: The human adaptor SARM negatively regulates adaptor protein TRIF-dependent Toll-like receptor signaling. Nat. Immunol. 7, 1074 – 1081.

Challberg, M. D., Englund, P. T., 1979: Purification and properties of the deoxyribonucleic acid polymerase induced by vaccinia virus. J. Biol. Chem. 254, 7812 – 7819.

Chang, A., Metz, D. H., 1976: Further investigations on the mode of entry of vaccinia virus into cells. J. Gen. Virol. 32, 275 – 282.

Chang, H. W., Watson, J. C., Jacobs, B. L., 1992: The E3L gene of vaccinia virus encodes an inhibitor of the interferon-induced, double-stranded RNA-dependent protein kinase. Proc. Natl. Acad. Sci. U. S. A. 89, 4825 – 4829.

Chebath, J., Benech, P., Hovanessian, A., Galabru, J., Revel, M., 1987: Four different forms of interferon-induced 2',5'-oligo(A) synthetase identified by immunoblotting in human cells. J. Biol. Chem. 262, 3852 – 3857.

Chen, R. A., Ryzhakov, G., Cooray, S., Randow, F., Smigh, G. L., 2008: Inhibition of IkappB kinase by vaccinia virulence factor B14. PLoS Pathog. 4: e22.

Chen, Z., Hagler, J., Palombella, V. J., Melandri, F., Scherer, D., Ballard, D., Maniatis, T., 1995: Signal-induced site-specific phosphorylation targets I kappa B alpha to the ubiquitin-proteasome pathway. Genes Dev. 9, 1586 – 1597.

Chiu, W.-L., Lin, C.-L., Yang, M.-H., Tzou, D.-L. M., Chang, W., 2007: Vaccinia virus 4c (A26L) protein on intracellular mature virus binds to the extracellular cellular matrix laminin. J. Virol. 81, 2149 – 2157.

Chlanda, P., Carbajal, M. A., Cyrklaff, M., Griffiths, G., Krijnse-Locker, J., 2009: Membrane rupture generates single open membrane sheets during vaccinia virus assembly. Cell Host Microbe 6, 81 – 90.

Chong, K. L., Feng, L., Schappert, K., Meurs, E., Donahue, T. F., Friesen, J. D., Hovanessian, A. G., Williams, B. R., 1992: Human p68 kinase exhibits growth suppression in yeast and homology to the translational regulator GCN2. EMBO J. 11, 1553 – 1562.

Chung, C. S., Chen, C. H., Ho, M. Y., Huang, C. Y., Liao, C. L., Chang, W., 2006: Vaccinia virus proteome: identification of proteins in vaccinia virus intracellular mature virion particles. J. Virol. 80, 2127 – 2140.

Chung, C. S., Hsiao, J. C., Chang, Y. S., Chang, W, 1998: A27L protein mediates vaccinia virus interaction with cell surface heparan sulfate. J. Virol. 72, 1577 – 15785.

Citarella, R. V., Muller, R., Schlabach, A., Weissbach, A., 1972: Studies on vaccinia virus-directed deoxyribonucleic acid polymerase. J. Virol. 10, 721 – 729.

Clemens, M. J., Williams, B. R. G., 1978: Inhibition of cell-free protein synthesis by $pppA^{2'}p^{5'}A^{2'}p^{5'}A$: a novel oligonucleotide synthesized by interferon-treated L cell extracts. Cell 13, 565 – 572.

Cohen, B., Novick, D., Barak, S., Rubinstein, M., 1995: Ligand-induced association of the type I interferon receptor components. Mol. Cell. Biol. 15, 4208 – 4214.

Colamonici, O. R., D'Alessandro, F., Diaz, M. O., Gregory, S. A., Neckers, L. M., Nordan, R., 1990: Characterization of three monoclonal antibodies that recognize the interferon alpha 2 receptor. PNAS 87, 7230 – 7234.

Colamonici, O. R., Platania, L. C., Domanski, P., Handa, R., Gilmour, K. C., Diaz, M. O., Reich, N., Pitha-Rowe, P., 1995: Transmembrane signaling by the alpha subunit of the type I interferon receptor is essential for activation of the JAK kinases and the transcriptional factor ISGF3. J. Biol. Chem. 270, 8188 – 8193.

Colinas, R. J., Goebel, S. J., Davis, S. W., Johnson, G. P., Norton, E. K., Poletti, E., 1990: A DNA ligase gene in the Copenhagen strain of vaccinia virus is nonessential for viral replication and recombination. Virology 179, 267 – 275.

Cooper, J. A., Moss, B., 1979: *In vitro* translation of immediate early, early, and late classes of RNA from vaccinia virus-infected cells. Virology 96, 368 – 380.

Cooray, S., Bahar, M. W., Abrescia, N. G., McVey, C. E., Bartlett, N. W., Chen, R. A., Stuart, D. I., Grimes, J. M., Smith, G. L., 2007: Functional and structural studies of the vaccinia virus virulence factor N1 reveal a Bcl-2-like anti-apoptotic protein. J. Gen. Virol. 88, 1656 – 1666.

Dales, S., Mosbach, E. H., 1968: Vaccinia as a model for membrane biogenesis. Virol. 35, 564 – 583.

Dales, S., Siminovitch, L., 1961: The development of vaccinia virus in Earle's L strain cells as examined by electron microscopy. JCB 10, 475 – 503.

David, M., Larner, A. C., 1992: Activation of transcription by interferon-alpha in a cell-free system. Science 257, 813 – 815.

De Silva, F. S., Lewis, W., Berglund, P., Koonin, E. V., Moss, B., 2007: Poxvirus DNA primase. Proc. Natl. Acad. Sci. U. S. A. 104, 18724 – 18729.

De Silva, F. S:, Moss, B., 2003: Vaccinia virus uracil DNA glycosylase has an essential role in DNA synthesis that is independent of its glycosylase activity: catalytic site mutations reduce virulence but not virus replication in cultured cells. J. Virol. 77, 159 – 166.

De Silva, F. S., Moss, B., 2005: Origin-independent plasmid replication occurs in vaccinia virus cytoplasmic factories and requires all five known poxvirus replication factors. Virol. J. 22, 2 – 23.

Decker, T., Lew, D. J., Mirkovitch, J., Darnell, Jr., J. E., 1991: Cytoplasmic avtivation of GAF, an IFN-gamma-regulated DNA-binding factor. EMBO J. 10, 927 – 932.

DeHaven, B. C., Gupta, K., Isaacs, S. N., 2011: The vaccinia virus A56 protein: a multifunctional transmembrane glycoprotein that anchors two secreted viral proteins. J. Gen. Virol. 92, 1971 – 1980.

DeLange, A. M., McFadden, G., 1986: Sequence-nonspecific replication of transfected plasmid DNA in poxvirus-infected cells. Proc. Natl. Acad. Sci. U. S. A. 83, 614 – 618.

Dellis, S., Strickland, K. C., McCrary, W. J., Patel, A., Stocum, E., Wright, C. F., 2004: Protein interactions among the vaccinia virus late transcription factors. Virology 329, 328 – 336.

Di Tommaso, P., Moretti, S., Xenarios, I., Orobitg, M., Montanyola, A., Chang, J. M., Taly, J. F., Notredame, C., 2011: T-Coffee: a web server for the multiple sequence alignment of protein and RNA sequences using structural information and homology extension. Nucleic Acids Res. 39: W13 – 17.

Diebold, S. S., Kaisho, T., Hemmi, H., Akira, S., Reis e Sousa, C., 2004: Innate antiviral responses by means of TLR7-mediated recognition of single-stranded RNA. Science 303, 1529 – 1531.

DiPerna, G., Stack, J., Bowie, A. G., Boyd, A., Kotwal, G., Zhang, Z., Arvikar, S., Latz, E., Fitzgerald, K. A., Marshall, W. L., 2004: Poxvirus protein N1L targets the I-kappaB kinase complex, inhibits signaling to NF-kappaB by the tumor necrosis factor superfamily of receptors, and inhibits NF-kappaB and IRF3 signaling by toll-like receptors. J. Biol. Chem. 279, 36570 – 36578.

Doceul, V., Hollinshead, M., van der Linden, L., Smith, G. L., 2010: Repulsion of superinfecting virions: a mechanism for rapid virus spread. Science 327, 873 – 876.

Domanski, P., Witte, M., Kellum, M., Rubinstein, M., Hackett, R., Pitha, P., Colamonici, O. R., 1995: Cloning and expression of a long form of the β subunit of the interferon αβ receptor that is required for signaling. J. Biol. Chem. 270, 21606 – 21611.

Dong, B., Silverman, R. H., 1995: 2-5A-dependent Rnase molecules dimerize during activation by 2-5A. J. Biol. Chem. 270, 4133 – 4137.

Du, Q., Jiang, L., Wang, Y., Wang, M., She, F., Chen, Y., 2014: Tumor necrosis factor-α promotes the lymphangiogenesis of gallbladder carcinoma through nuclear factor-κB-mediated upregulation of vascular endothelial growth factor-C. Cancer Sci. 105, 1261 – 1271.

Dubochet, J., Adrian, M., Richter, K., Garces, J., Wittek, R., 1994: Structure of intracellular mature vaccinia virus observed by cryoelectron microscopy. J. Virol. 68, 1935 – 1941.

Duncan, S. A., Smith, G. L., 1992: Identification and characterization of an extracellular envelope glycoprotein affecting vaccinia virus egress. J. Virol. 66, 1610 – 1621

Dunne, A., Ejdebäck, M., Ludidi, P. L., O'Neill, L. A. J., Gay, N. J., 2003: Toll-like receptors and the adaptors Mal and MyD88. J. Biol. Chem. 278, 41443 – 41451.

Earl, P. L., Jones, E. V., Moss, B., 1986: Homology between DNA polymerases of poxviruses, herpesviruses, and adenoviruses: nucleotide sequence of the vaccinia virus DNA polymerase gene. Proc. Natl. Acad. Sci. U. S. A. 83, 3659 – 3663.

Edelmann, K. H., Richardson-Burns, S., Alexopoulou, L., Tyler, K. L., Flavell, R. A., Oldstone, M. B., 2004: Does Toll-like receptor 3 play a biological role in virus infections? Virology 322, 231 – 238.

Elkord, E., Dangoor, A., Burt, D. J., Southgate, T. D., Daayana, S., Harrop, R., Drijfhout, J. W., Sherlock, D., Hawkins, R. E., Stern, P. L., 2009: Immune evasion mechanisms in colorectal cancer liver metastasis patients vaccinated with TroVax (MVA-5T4). Cancer Immunol. Immunother. 58, 1657 – 1667.

Engelstad, M., Howard, S. T., Smith, G. L., 1992: A constitutively expressed vaccinia gene encodes a 42-kDa glycoprotein related to complement control factors that forms part of the extracellular virus envelope. Virology 188, 801 – 810.

Evans, E., Klemperer, N., Ghosh, R., Traktman, P., 1995: The vaccinia virus D5 protein, which is required for DNA replication, is a nucleic acid-independent nucleoside triphosphatase. J. Virol. 69, 5353 – 5361.

Evans, E., Traktman, P., 1987: Molecular genetic analysis of a vaccinia virus gene with an essential role in DNA replication. J. Virol. 61, 3152 – 3162.

Evans, E., Traktman, P., 1992: Characterization of vaccinia virus DNA replication mutants with lesions in the D5 gene. Chromosoma 102, S. 72 – 82.

Farrell, P. J., Balkow, K., Hunt, T., Jackson, R. J., Trachsel, H., 1977: Phosphorylation of initiation factor eIF-2 and the control of reticulocyte protein synthesis. Cell 11, 187 – 200.

Fenner, F., Henderson, D. A., Arita, I., Ježek, Z., Ladnyi, I. D., 1988: Smallpox and its eradication. History of international public health, No 6. World Health Organization, Geneva.

Fitzgerald, K. A., McWhirter, S. M., Faia, K. L., Rowe, D. C., Latz, E., Golenbock, D. T., Coyle, A. J., Liao, S. M., Maniatis, T., 2003: IKKε and TBK1 are essential components of the IRF3 signaling pathway. Nat. Immunol. 4, 491 – 496.

Fitzgerald, K. A., Palsson-McDermott, E. M., Bowie, A. G., Jefferies, C. A., Mansell, A. S., Brady, G., Brint, E., Dunne, A., Gray, P., Harte, M. T., McMurray, D., Smith, D. E., Sims, J. E., Bird, T. A., O'Neill, L. A., 2001: Mal (MyD88-adapter-like) is required for Toll-like receptor-4 signal transduction. Nature 413, 78 – 83.

Foo, C. H., Lou, H., Whitbeck, J. C., Ponce-de-Le#on, M., Atanasiu, D., Eisenberg, R. J., Cohen, G. H., 2009: Vaccinia virus L1 binds to cell surfaces and blocks virus entry independently of glycosaminoglycans. Virology 385, 368 – 382.

Forsbach, A., Nemorin, J. G., Montino, C., Müller, C., Samulowitz, U., Vicari, A. P., Jurk, M., Mutwiri, G. K., Krieg, A. M., Lipford, G. B., Vollmer, J., 2008: Identification of RNA sequence motifs stimulating sequence-specific TLR8-dependent immune responses. J. Immunol. 180, 3729 – 3738.

Fountoulakis, M., Juranville, J. F., Stüber, D., Weibel, E. K., Garotta, G., 1990: Purification and biochemical characterization of a soluble human interferon gamma receptor expressed in Escherichia coli. J. Biol. Chem. 265, 13268 – 13275.

Franklin, E., Khan, A. R., 2013: Poxvirus antagonism of innate immunity by Bcl-2 fold proteins. J. Struc. Biol. 181, 1 – 10.

Fu, X.-Y., Kessler, D. S., Veals, S. A., Levy, D. E., Darnell, Jr., J. E., 1990: ISGF3, the transcriptional activator induced by interferon α, consists of multiple interacting polypeptide chains. Proc. Natl. Acad. Sci. U. S. A. 87, 8555 – 8559.

Gack, M. U., Shin, Y. C., Joo, C. H., Urano, T., Liang, C., Sun, L., Takeuchi, O., Akira, S., Chen, Z., Inoue, S., Jung, J. U., 2007: TRIM25 RING-finger E3 ubiquitin ligase is essential for RIG-I-mediated antiviral activity. Nature 446, 916 – 920.

Gadina, M., Hilton, D., Johnston, J. A., Morinobu, A., Lighvani, A., Zhou, Y.-J., Visconti, R., O'Shea, J. J., 2001: Signaling by type I and II cytokine receptors: ten years after. Curr. Opin. Immunol. 13, 363 – 373.

Garcia, A. D., Aravind, L., Koonin, E. V., Moss, B., 2000: Bacterial-type DNA holliday junction resolvases in eukaryotic viruses. Proc. Natl. Acad. Sci. U. S. A. 97, 8926 – 8931.

Garcia, A. D., Moss, B., 2001: Repression of vaccinia virus Holliday junction resolvase inhibits processing of viral DNA into unit-length genomes. J. Virol. 75, 6460 – 6471.

Garon, C. F., Barbose, E., Moss, B., 1978: Visualization of an inverted terminal repetition in vaccinia virus DNA. Proc. Natl. Acad. Sci. U. S. A. 75, 4863 – 4867.

Geisler, R., Bergmann, A., Hiromi, Y., Nüsslein-Volhard, C., 1992: cactus, a gene involved in dorsoventral pattern formation of Drosophila, is related to the I kappa B gene family of vertebrates. Cell 71, 613 – 621.

Georgel, P., Jiang, Z., Kunz, S., Janssen, E., Mols, J., Hoebe, K., Bahram, S., Oldstone, M. B., Beutler, B., 2007: Vesicular stomatitis virus glycoprotein G activates a specific antiviral Toll-like receptor 4-dependent pathway. Virology 362, 304 – 313.

Gershon, P. D., Moss, B., 1990: Early transcription factor subunits are encoded by vaccinia virus late genes. Proc. Natl. Acad. Sci. U. S. A. 87, 4401 – 4405.

Geshelin, P., Berns, K. I., 1974: Characterization and localization of the naturally occuring cross-links in vaccinia virus DNA. J. Mol. Biol. 88, 785 – 788.

Ghosh, S., Baltimore, D., 1990: Activation in vitro of NF-kappa B by phosphorylation of its inhibitor I kappa B. Nature 344, 678 – 682.

Ghosh, S., Gifford, A. M., Riviere, L. R., Tempst, P., Nolan, G. P., Baltimore, D., 1990: Cloning of the p50 DNA binding subunit of NF-kappa B: homology to rel and dorsal. Cell 62, 1019 – 1029.

Gibbs, V. C., Williams, S. R., Gray, P. W., Schreiber, R. D., Pennica, D., Rice, G., Goeddel, D. V., 1991: The extracellular domain of the human interferon gamma receptor interacts with a species-specific signal transducer. Mol. Cell. Biol. 11, 5860 – 5866.

Gil, J., Alcamí, J., Esteban, M., 2000a: Activation of NF-κB by the dsRNA-dependent protein kinase, PKR involves the IκB kinase complex. Oncogene 19, 1369 – 1378.

Gil, J., García, M. A., Gomez-Puertas, P., Guerra, S., Rullas, J., Nakano, H., Alcamí, J., Esteban, M., 2004b: TRAF family proteins link PKR with NF-kappa B activation. Mol. Cell Biol. 24, 4502 – 4512.

Gitlin, L., Barchet, W., Gilfillan, S., Cella, M., Beutler, B., Flavell, R. A., Diamond, M. S., Colonna, M., 2006: Essential role of mda-5 in type I IFN responses to polyriboinosinic:polyribocytidylic acid and encephalomyocarditis picornavirus. Proc. Natl. Acad. Sci. U. S: A: 103, 8459 – 8464.

Goebel, S. J., Johnson, G. P., Perkus, M. E., Davis, S. W., Winslow, J. P., Paoletti, E., 1990: The complete DNA sequence of vaccinia virus. Virology 179, 247 – 266.

Gohda, J., Matsummura, T., Inoue, J., 2004: Cutting edge: TNFR-associated factor (TRAF) 6 is essential for MyD88-dependent pathway but not toll/IL-1 receptor domain-containing adaptor-inducing IFN-beta (TRIF)-dependent pathway in TLR signaling. J. Immunol. 173, 2913 – 2917.

González, J. M., Esteban, M., 2010: A poxvirus Bcl-2-like gene family involved in regulation of host immune response: sequence similarity and evolutionary history. Virol. J. 7: 59.

Graham, S. C., Bahar, M. W., Cooray, S., Chen, R. A., Whalen, D. M., Abrescia, N. G., Alderton, D., Owens, R. J., Stuart, D. I., Smith, G. L., Grimes, J. M., 2008: Vaccinia virus proteins A52 and B14 share a Bcl-2-like fold but have evolved to inhibit NF-kappaB rather than apoptosis. PLoS Pathog. 4: e1000128.

Gray, P. W., Goeddel, D. V., 1982: Structure of the human immune interferon gene. Nature 298, 869 – 863

Greenlund, A. C., Farrar, M. A., Viviano, B. L., Schreiber, R. D., 1994: Ligand-induced IFN gamma receptor tyrosine phosphorylation couples the receptor to its signal transduction system (p91). EMBO J., 13, 1591 – 1600.

Guiducci, C., Ghirelli, C., Marloie-Provost, M. A., Matray, T., Coffman, R. L., Liu, Y., J., Barrat, F. J., Soumelis, V., 2008: PI3K is critical for the nuclear translocation of IRF-7 and type I IFN production by human plasmacytoid predendritic cells in response to TLR activation. J. Exp. Med. 205, 315 – 322.

Häcker, H., Redecke, V., Blagoev, B., Kratchmarova, I., Hsu, L.-C., Wang, G. G., Kamps, M. P., Raz, E., Wagner, H., Häcker, G., Mann, M., Karin, M., 2005: Specificity in Toll-like receptor signalling through distinct effector functions of TRAF3 and TRAF6. Nature 439, 204 – 207.

Haeberle, H. A., Takizawa, R., Casola, A., Brasier, A. R., Dieterich, H. J., van Rooijen, N., Gatalica, Z., Garofalo, R: P., 2002: Respiratory syncytial virus-induced activation of nuclear factor-kappaB in the lung involves alveolar macrophages and toll-like receptor 4-dependent pathways. J. Infect. Dis. 186, 1199 – 1206.

Harrop, R., Connolly, N., Redchenko, I., Valle, J., Saunders, M., Ryan, M. G., Myers, K. A., Drury, N., Kingsman, S. M., Hawkins, R. E., Carroll, M. W., 2006: Vaccination of colorectal cancer patients with motified vaccinia Ankara delivering the tumor antigen 5T4 (TroVax) induces immune responses which correlate with disease control: a phase I/II trial. Clin. Cancer Res. 12, 3416 – 3424.

Harte, M. T., Haga, I. R., Maloney, G., Gray, P., Reading, P. C., Bartlett, N. W., Smith, G. L., Bowie, A., O'Neill, L. A., 2003: The poxvirus A52R targets Toll-like receptor signaling complexes to suppress host defense. J. Exp. Med. 197, 343 – 351.

Hayashi, F., Smith, K. D., Ozinsky, A., Hawn, T. R., Yi, E. C., Goodlett, D. R., Eng, J. K., Akira, S., Underhill, D. M., Aderem, A., 2001: The innate immune response to bacterial flagellin is mediated by Toll-like receptor 5. Nature 410, 1099 – 1103.

Heil, F., Hemmi, H., Hochrein, H., Ampenberger, F., Kirschning, C., Akira, S., Lipford, G., Wagner, H., Bauer, S., 2004: Species-specific recognition of single-stranded RNA via Toll-like receptor 7 and 8. Science 303, 1526 – 1529.

Hemmi, H., Kaisho, T., Takeuchi, O., Sato, S., Sanjo, H., Hoshino, K., Horiuchi, T., Tomizawa, H., Takeda, K., Akira, S., 2002: Small anti-viral compounds activate immune cells via the TLR7 MyD88-dependent signaling pathway. Nat. Immunol. 3, 196 – 200.

Hemmi, H., Takeuchi, O., Kawai, T., Kaisho, T., Sato, S., Sanjo, H., Matsumoto, M., Hoshino, K., Wagner, H., Takeda, K., Akira, S., 2000: A Toll-like receptor recognizes bacterial DNA. Nature 408, 740 – 745.

Hemmi, H., Takeuchi, O., Sato, S., Yamamoto, M., Kaisho, T., Sanjo, H., Kawai, T., Hoshino, K., Takeda, K., Akira, S., 2004: The roles of two IκB kinase-related kinases in lipopolysaccharide and double stranded RNA signaling and viral infection. JEM 199, 1641 – 1650.

Heuser, J., 2005: Deep-etch EM reveals that the early poxvirus envelope is a single membrane bilayer stabilized by a geodetic “honeycomb” surface coat. J. Cell Biol. 169, 269 – 283.

Hiller, G., Weber, K., 1985: Golgi-derived membranes that contain an acylated viral polypeptide are used for vaccinia virus envelopment. J. Virol. 55, 651 – 659.

Hirschfeld, M., Kirschning, C. J., Schwandner, R., Wesche, H., Weis, J. H., Wooten, R. M., Weis, J. J., 1999: Cutting edge: inflammatory signaling by Borrelia burgdorferi lipoproteins is mediated by toll-like receptor 2. J. Immunol. 163, 2382 – 2386.

Hiscott, J., Marois, J., Garoufalis, J., D’Addario, M., Roulston, A., Kwan, I., Pepin, N., Lacoste, J., Nguyen, H., Bensi, G., et al., 1993: Characterization of a functional NF-kappa B site in the human interleukin 1 beta promoter: evidence for a positive autoregulatory loop. Mol. Cell. Biol. 13, 6231 – 6240.

Hole, N., Stern, P. L., 1988: A 72 kD trophoblast glycoprotein defined by a monoclonal antibody. Br. J. Cancer 57, 239 – 246.

Hollinshead, M., Rodger, G., van Eijl, H., Law, M., Hollinshead, R., Vaux, D. J., Smith, G. L., 2001: Vaccinia virus utilizes microtubules for movement to the cell surface. J. Cell. Biol. 154, 389 – 402.

Hollinshead, M., Vanderplasschen, A., Smith, G. L., Vaux, D. J., 1999: Vaccinia virus intracellular mature virions contain only one lipid membrane. J. Virol. 73, 1503 – 1517.

Honda, K., Yanai, H., Mizutani, T., Negishi, H., Shimada, N., Suzuki, N., Ohba, Y., Takaoka, A., Yeh, W.-C., Taniguchi, T., 2004: Role of a transductional-transcriptional processor complex involving MyD88 and IRF-7 in Toll-like receptor signaling. Proc. Natl. Acad. Sci. U. S. A. 101, 15416 – 15421.

Honda, K., Yanai, H., Negishi, H., Asagiri, M., Sato, M., Mizutani, T., Shimada, N., Ohba, Y., Takaoka, A., Yoshida, N., Taniguchi, T., 2005: IRF-7 is the master regulator of type-I interferon-dependent immune responses. Nature 434, 772 – 777.

Horng, T., Barton, G. M., Flavell, R. A., Medzhitov, R., 2002: The adaptor molecule TIRAP provides signalling specificity for Toll-like receptors. Nature 420, 329 – 333.

Horng, T., Barton, G. M., Medzhitov, R., 2001: TIRAP: an adapter molecule in the Toll signaling pathway. Nat. Immunol. 2, 835 – 841.

Hornung, V., Ellegast, J., Kim, S., Brzóka, K., Jung, A., Kato, H., Poeck, H., Akira, S., Conzelmann, K. K., Schlee, M., Endres, S., Hartmann, G., 2006: 5‘-Triphosphate RNA is the ligand for RIG-I. Science 314, 994 – 997.

Hoshino, K., Sugiyama, T., Matsumoto, M., Tanaka, T., Saito, M., Hemmi, H., Ohara, O., Akira, S., Kaisho, T., 2006: IκB kinase-α is critical for interferon-α production induced by Toll-like receptors 7 and 9. Nature 440, 949 – 953.

Hoshino, K., Takeuchi, O., Kawai, T., Sanjo, H., Ogawa, T., Takeda, Y., Takeda, K., Akira, S., 1999: Cutting edge: Toll-like receptor 4 (TLR4)-deficient mice are hyporesponsive to lipopolysaccharide: evidence for TLR4 as the Lps gene product. J. Immunol. 162, 3749 – 3752.

Hovanessian, A. G., Brown, R. E., Kerr, I. M., 1977: Synthesis of low molecular weight inhibitor of protein synthesis with enzyme from interferon-treated cells. Nature 268, 537 – 540.

Hovanessian, A. G., Svab, J., Marié, I., Robert, N., Chamaret, S., Larent, A. G., 1988: Characterization of 69- and 100-kDa forms of 2-5A-synthetase from interferon-treated human cells. J. Biol. Chem. 263, 4945 – 4949.

Howard, S. T., Smith, G. L., 1989: Two early vaccinia virus genes encode polypeptides related to protein kinases. J. Gen. Virol. 70, 3187 – 3201.

Hoyos, B., Ballard, D. W., Böhnlein, E., Siekevitz, M., Greene, W. C., 1989: Kappa B-specific DNA binding proteins: role in the regulation of human interleukin-2 gene expression. Science 244, 457 – 460.

Hsiao, J. C., Chung, C. S., Chang, W., 1998: Cell surface proteoglycans are necessary for A27L protein-mediated cell fusion: identification of the N-terminal region of A27L protein as the glycosaminoglycan-binding domain.

Hsiao, J. C., Chung, C. S., Chang, W., 1999: Vaccinia virus envelope D8L protein binds to cell surface chondroitin sulfate and mediates the adsorption of intracellular mature virions to cells. J. Virol. 73. 8750 – 8761.

http://blast.ncbi.nlm.nih.gov/Blast.cgi

http://www.embl.de/pepcore/pepcore_services/protein_purification/chromatography/hiload16-60_superdex75/GF75_16.pdf

Huang, C.-Y-, Lu, T.-Y., Bair, C.-H., Chang, Y.-S., Jwo, J.-K., Chang, W., 2008: A novel cellular protein, VPEF, facilitates vaccinia virus penetration into HeLa cells through fluid phase endocytosis. J. Virol. 82, 7988 – 7999.

Hubbs, A. E., Wright, C. F., 1996: The A2L intermediate gene product is required for in vitro transcription from a vaccinia virus late promoter. J. Virol. 70, 327 – 331.

Husain, M., Moss, B., 2005: Role of receptor-mediated endocytosis in the formation of vaccinia virus extracellular envelope particles. J. Virol. 79, 4080 – 4089.

Hutchens, M. A., Luker, K. E., Sonstein, J., Núñez, G., Curtis, J. L., Luker, G. D., 2008: Protective effect of Toll-like receptor 4 in pulmonary vaccinia infection. PLoS Pathog. 4: e1000153.

Igarashi, K., Garotta, G., Ozmen, L., Ziemiecki, A., Wilks, A. F., Harpur, A. G., Larner, A. C., Finbloom, D. S., 1994: Interferon-γ induces tyrosine phosphorylation of interferon-γ receptor and regulated association of protein tyrosine kinases, Jak1 and Jak2, with its receptor. J. Biol. Chem. 269, 14333 – 14336.

Isaacs, A., Lindenmann, J., 1957: Virus interference. I. The interferon. Proc. R. Soc. Lond. B. Biol. Sci. 147, 258 – 267.

Isaacs, S. N., Wolffe, E. J., Payne, L. G., Moss, B., 1992: Characterization of a vaccinia virus-encoded 42-kilodalton class I membrane glycoprotein component of the extracellular virus envelope. J. Virol. 66, 7217 – 72214.

Ishii, K., Moss, B., 2002: Mapping interaction sites of the A20R protein component of the vaccinia virus DNA replication complex. Virology, 303, 232 – 239.

Izmailyan, R., Hsao, J. C., Chung, C. S., Chen, C. H., Hsu, P. W., Liao, C. L., Chang, W., 2012: Integrin β1 mediates vaccinia virus entry through activation of PI3K/Akt signaling. J. Virol. 86, 6677 – 6687.

Jacobsen, H., Czarniecki, C. W., Krause, D., Friedman, R. M., Silverman, R. H., 1983: Interferon-induced synthesis of 2-5A-dependent Rnase in mouse JLS-V9R cells. Virology 125, 496 – 501.

Jerabek-Willemnsen, M., Wienken, C. J., Braun, D., Baaske, P., Duhr, S., 2011: Molecular interaction studies using microscale thermophoresis. Assay Drug Dev. Technol. 9, 342 – 353.

Jones, E. V., Moss, B., 1984: Mapping of the vaccinia virus DNA polymerase gene by marker rescue and cell-free translation of selected RNA. J. Virol. 49, 72 – 77.

Jones, E. V., Puckett, C., Moss, B., 1987: DNA-dependent RNA polymerase subunits encoded within the vaccinia virus genome. J. Virol. 61, 1765 – 1771.

Jungwirth, C., Joklik, W. K., 1965: Studies on „early“ enzymes in HeLa cells infected with vaccinia. Virology 27, 80 – 93.

Kalverad, A. P., Thompson, G. S., Vogel, A., Schröder, M., Bowie, A. G., Khan, A. R., Homans, S. W:, 2009: Poxvirus K7 protein adopts a Bcl-2 fold: biochemical mapping of its interactions with human DEAD box RNA helicase DDX3. J. Mol. Biol. 385, 843 – 853.

Kates, J. R., McAuslan, B. R., 1967a: Poxvirus DNA-dependend RNA polymerase. Proc. Natl. Acad. Sci. U. S. A. 58, 134 – 141.

Kates, J. R., McAuslan, B. R., 1967b: Messenger RNA synthesis by a „coated“ viral genome. Proc. Natl. Acad. Sci. U. S. A. 57, 314 – 320.

Kates, J., Beeson, J., 1970: Ribonucleic acid synthesis in vaccinia virus: I. The mechanism of synthesis and release of RNA in vaccinia cores. J. Mol. Biol. 50, 1 – 18.

Kato, H., Sato, S., Yoneyama, M., Yamamoto, M., Uematsu, S., Matsui, K., Tsujimura, T., Takeda, K., Fujita, T., Takeuchi, O., Akira, S., 2005: Cell type-specific involvement of RIG-I in antiviral response. Immunity 23, 19 – 28.

Kato, H., Takeuchi, O., Sato, S., Yoneyama, M., Yamamoto, M., Matsui, K., Uemtasu, S., Jung, A., Kawai, T., Ishii, K. J., Yamaguchi, O., Otsu, K., Tsujimura, T., Koh, C. S., Reis e Sousa, C:, Matsuura, Y., Fujita, T., Akira, S., 2006: Differential roles of MDA5 and RIG-I helicases in the recognition of RNA viruses. Nature 441, 101 – 105.

Katsafanas, G. C., Moss, B., 2004: Vaccinia virus intermediate stage transcription is complemented by Ras-GTPase-activating protein SH3 domain-binding protein (G3BP) and cytoplasmic activation/proliferation-associated protein (p137) individually or as a heterodimer. J. Biol. Chem. 279, 52210 – 52217.

Kawai, T., Adachi, O., Ogawa, T., Takeda, K., Akira, S., 1999: Unresponsiveness of MyD88-deficient mice to endotoxin. Immunity 11, 115 – 122.

Kawai, T., Akira, S., 2007: TLR signalling. Semin. Immunol. 19, 24 – 32.

Kawai, T., Akira, S., 2008: Toll-like receptor and RIG-I-like receptor signaling. Ann. N. Y. Acad. Sci. 1143, 1 – 20.

Kawai, T., Sato, S., Ishii, K. J., Coban, C., Hemmi, H., Masahiro, Y., Terai, K., Matsuda, M., Inoue, J.-i., Uematsu, S., Takeuchi, O., Akira, S., 2004: Interferon-α induction through Toll-like receptors involves a direct interaction of IRF7 with MyD88 and TRAF6. Nat. Immunol. 5, 1061 – 1068.

Kawai, T., Takahashi, K., Sato, S:, Coban, C., Kumar, H., Kato, H., Ishii, K. J., Takeuchi, O., Akira, S., 2005: IPS-1, an adaptor triggering RIG-I- and Mda5-mediated type I interferon induction. Nat. Immunol. 6, 981 – 988.

Kayagaki, N., Phung, Q., Chan, S., Chaudhari, R., Quan, C., O'Rourke, K. M., Eby, M., Pietras, E., Cheng, G., Bazan, J. F., Zhang, Z., Arnott, D., Dixit, V. M., 2007: DUBA: a deubiquitinase that regulates type I interferon production. Science 318, 1628 – 1632.

Keck, J. G., Baldick Jr., C. J., Moss, B., 1990: Role of DNA replication in vaccinia virus gene expression: A naked template is required for transcription of three late *trans*-activator genes. Cell 61, 801 – 809.

Keck, J. G., Kovacs, G. R., Moss, B., 1993: Overexpression, purification, and late transcription factor activity of the 17-kilodalton protein encoded by the vaccinia virus A1L gene. J. Virol. 67, 5740 – 5748.

Kelly, J. M., Gilbert, C. S., Stark, G. R., Kerr, I. M., 1985: Differential regulation of interferon-induced mRNAs and c-myc mRNA by alpha- and gamma-interferons. Eur. J. Biochem. 153, 367 – 371.

Kerr, I. M., Brown, R. E., 1978: pppA2'p5'A2'p5'A: an inhibitor of protein synthesis synthesized with an enzyme fraction from interferon-treated cells. Proc. Natl. Acad. Sci. U. S. A. 75, 256 – 260.

Kerr, I. M., Brown, R. E., Ball, L. A., 1974: Increased sensitivity of cell-free protein synthesis to double-stranded RNA after interferon treatment. Nature 250, 57 – 59.

Kerr, S. M., Smith, G. L., 1989: Vaccinia virus encodes a polypeptide with DNA ligase activity. Nuclic Acids. Res. 17, 9039 – 9050.

Kidd, S., 1992: Characterization of the Drosophila cactus locus and analysis of interactions between cactus and dorsal proteins. Cell 71, 623 – 635.

Kim, D. W., Krishnamurthy, V., Bines, S. D:, Kaufman, H. L., 2010: TroVax, a recombinant modified vaccinia Ankara virus encoding 5T4: lessons learned and future development. Hum. Vaccin. 6, 784 – 791.

Kim, S. H., Cohen, B., Novick, D., Rubinstein, M., 1997: Mammalian type I interferon receptors consists of two subunits: IFNaR1 and IFNaR2. Gene 196, 279 – 286.

Kim, Y., Lee, H., Heo, L., Seok, C., Choe, J., 2014: Structure of vaccinia virus A46, an inhibitor of TLR4 signaling pathway, shows the conformation of VIPER motif. Protein Sci. 23, 906 – 914.

King, A. M. Q., Lefkowitz, E., Adams, M. J., Carstens, E: B. (ed), 2011: Poxviridae. In: Virus Taxonomy: Ninth report of the international committee on taxonomy of viruses. San Diego: Elsevier.

Klemperer, N., McDonald, W. Boyle, K., Unger, B., Traktman, P., 2001: The A20R protein is a stoichiometric component of the processive form of vaccinia virus DNA polymerase. J. Virol. 75, 12298 – 12307.

Kotenko, S. V., Izotova, L. S., Pollack, B. P., Mariano, T. M., Donnelly, R. J., Muthukumaran, G., Cook, J. R., Garotta, G., Silvennoinen, O., Ihle, J. N., et al., 1995: Interaction between the components of the interferon gamma receptor complex. J. Biol. Chem. 270, 20915 – 20921.

Kovacs, G. R., Moss, B., 1996: The vaccinia virus H5R gene encodes late gene transcription factor 4: purification, cloning, and overexpression. J. Virol. 70, 6796 – 6802.

Kovacs, G. R., Rosales, R., Keck, J. G., Moss, B., 1994: Modification of the cascade model for regulation of vaccinia virus gene expression: purification of a prereplicative, late-stage-specific transcription factor. J. Virol. 68, 3443 – 3447.

Kreijtz, J. H. C. M., Suezer, Y., van Amerongen, G., de Mutsert, G., Schnierle, B. S., Wood, J. M., Kuiken, T., Fouchier, R. A. M., Löwer, R. A. M., Osterhaus, A. D. M. E., Sutter, G., Rimmelzwaan, G. F., 2007: Recombinant modified vaccinia virus Ankara-based vaccine induces protective immunity in mice against infection with influenza virus H5N1. J. Infect. Dis. 195, 1598 – 1606.

Kumar, A., Haque, J., Lacoste, J., Hiscott, J., Williams, B. R., 1994: Double-stranded RNA-dependent protein kinase activates transcription factor NF-kappa B by phosphorylating I kappa B. Proc. Natl. Acad. Sci. U. S. A. 91, 6288 – 6292.

Kumar, H., Kawai, T., Kato, H., Sato, S., Takahashi, K., Coban, C., Yamamoto, M., Uematsu, S., Ishii, K. J., Takeuchi, O., Akira, S., 2006: Essential role of IPS-1 in innate immune responses against RNA viruses. J. Exp. Med. 203, 1795 – 1803.

Kuznetsov, Y., Gershon, P. D., McPherson, A., 2008: Atomic force microscopy investigation of vaccinia virus structure. J. Virol. 82, 7551 – 7566.

Kvansakul, M., Hinds, M. G., 2013: Structural biology of the Bcl-2 family and its mimicry by viral proteins. Cell Death Dis. 4: e909.

Kvansakul, M., Yang, H., Fairlie, W. D., Czabotar, P. E., Fischer, S. F., Perugini, M. A., Huang, D. C., Colman, P. M., 2008: Vaccinia virus anti-apoptotic F1L is a novel Bcl-2-like domain-swapped dimer that binds a highly selective subset of BH3-containing death ligands. Cell Death Differ. 15, 1564 – 1571.

Law, M., Carter, G. C., Roberts, K. L., Hollinshead, M., Smith, G. L., 2006: Ligand-induced and nonfusogenic dissolution of a viral membrane. Proc. Natl. Acad. Sci. U. S. A. 103, 5989 – 5994.

Le Goffic, R., Balloy, V., Lagranderie, M., Alexopoulou, L., Escriou, N., Flavell, R., Chignard, M., Si-Tahar, M., 2006: Detrimental contribution of the Toll-like receptor (TLR)3 to influenza A virus-induced acute pneumonia. PLoS Pathog. 2: e53.

Lebleu, B., Sen, G. C., Shaila, S., Cabrer, B., Lengyel, P., 1976: Interferon, double-stranded RNA, and protein phosphorylation. Proc. Natl. Acad. Sci. U. S. A. 73, 3107 – 3111.

Lemaitre, B., Nicolas, E., Michaut, L., Reichhart, J.-M., Hoffmann, J. A., 1996: The dorsoventral regulatory gene cassette spätzle/Toll/cactus controls the potent antifungal response in Drosophila adults. Cell 1996, 973 – 983.

Levy, D. E., Kessler, D. S., Pine, R., Reich, N., Darnell, Jr., J. E., 1988: Interferon-induced nuclear factors that bind a shared promoter element correlate with positive and negative transcriptional control. Genes Dev. 2, 383 – 393.

Li, X., Commane, M., Burns, C., Vithalani, K., Cao, Z., Stark, G. R., 1999: Mutant cells that do not respond to interleukin-1 (IL-1) reveal a novel role for IL-1 receptor-associated kinase. Mol. Cell. Biol. 19, 4643 – 4652.

Libermann, T. A., Baltimore, D., 1990: Activation of interleukin-6 gene expression through NF-kappa B transcription factor. Mol. Cell. Biol. 10, 2327 – 2334.

Lin, C. L., Chung, C. S., Heine, H. G., Chang, W., 2000: Vaccinia virus envelope H3L protein binds to cell surface heparan sulfate and is important for intracellular mature virion morphogenesis and virus infection in vitro and in vivo. J. Virol. 74, 3353 – 3365.

Lin, R., Heylbroeck, C., Pitha, P. M., Hiscott, J., 1998: Virus-dependent phosphorylation of the IRF-3 transcription factor regulates nuclear translocation, transactivation potential, and proteasome-mediated degradation. Mol. Cell. Biol. 18, 2986 – 2996.

Lin, S., Broyles, S. S., 1994: Vaccinia protein kinase 2: a second essential serine/threonine protein kinase encoded by vaccinia virus. Proc. Natl. Acad. Sci. U. S. A. 91, 7653 – 7657.

Lindahl, T., 1993: Instability and decay of the primary structure of DNA. Nature 362, 709 – 715.

Liu, L., Cooper, T., Howley, P. M., Hayball, J. D., 2014: From crescent to mature virion: vaccinia virus assembly and maturation. Viruses 6, 3787 – 3808.

Locker, K. J., Kuehn, A., Schleich, S., Rutter, G., Hohenberg, H., Wepf, R., Griffiths, G., 2000: Entry of the two infectious forms of vaccinia virus at the plasma membrane is signaling-dependent for the IMV but not the EEV. Mol. Biol. Cell 11, 2497 – 2511.

Loiarro, M., Capolunghi, F., Fantó, N., Gallo, G., Campo, S., Arseni, B., Carsetti, R., Carminati, P., De Santis, R., Ruggiero, V., Sette, C., 2007: Pivotal advance: Inhibition of MyD88 dimerization and recruitment of IRAK1 and IRAK4 by a novel peptidomimetic compound. J. Leukoc. Biol. 82, 801 – 810.

Lysakova-Devine, T., Keogh, B., Harrington, B., Nagpal, K., Halle, A., Golenbock, D. T., Monie, T., Bowie, A. G. 2010: Viral inhibitory peptide of TLR4, a peptide derived from vaccinia protein A46,

specifically inhibits TLR4 by directly targeting MyD88 adaptor-like and TRIF-related adaptor molecule. J. Immunol. 185, 4261 – 4271.

Mahy, B. W. J., 2003: An overview on the use of a viral pathogen as a bioterrorism agent: why smallpox? Antiviral Res. 57, 1 – 5.

Mallardo, M., Leithe, E., Schleich, S., Roos, N., Doglio, L., Krijnse Locker, J., 2002: Relationship between vaccinia virus intracellular cores, early mRNAs, and DNA replication sites. J. Virol. 76, 5167 – 5183.

Mallardo, M., Schleich, S., Kirjnse Locker, J., 2001: Microtubule-dependent organization of vaccinia virus core-derived early mRNAs into distinct cytoplasmic structures. Mol. Biol. Cell 12, 3875 – 3891.

Maloney, G., Schröder, M., Bowie, A. G., 2005: Vaccinia virus protein A52R activates p38 mitogen-activated protein kinase and potentiates lipopolysaccharide-induced interleukin-10. J. Biol. Chem. 280, 30838 – 30844.

Mansur, D. S., Maluquer de Motes, C., Unterholzner, L., Sumner, R. P., Ferguson, B. J., Ren, H., Stmadova, P., Bowie, A. G., Smith, G. L., 2013: Poxvirus targeting of E3 ligase β-TrCP by molecular mimicry: a mechanism to inhibit NF-κB activation and promote immune evasion and virulence. PLoS Pathog. 9: e1003183.

Marié, I., Blanco, J., Rebouillat, D., Hovanessian, A. G., 1997: 69-kDa and 100-kDa isoforms of interferon-induced (2'-5')oligoadenylate synthetase exhibit differential catalytic parameters. Eur. J. Biochem. 248, 558 – 566.

Marié, I., Hovanessian, A. G., 1992: The 69-kDa 2-5A synthetase is composed of two homologous and adjacent functional domains. J. Biol. Chem. 267, 9933 – 9939.

Maruri-Avidal L., Weisberg, A. S., Bisht, H., Moss, B., 2013a: Analysis of viral membranes formed in cells infected by a vaccinia virus L2-deletion mutant suggests their origin from the endoplasmic reticulum. J. Virol. 87, 1861 – 1871.

Maruri-Avidal, L., Domi, A., Weisberg, A. S., Moss, B., 2011a: Participation of vaccinia virus L2 protein in the formation of crescent membranes and immature virions. J. Virol. 85, 2504 – 2511.

Maruri-Avidal, L., Weisberg, A. S., Moss, B., 2011b: Vaccinia virus L2 protein associates with the endoplasmic reticulum near the growing edge of crescent precursors of immature virions and stabilizes a subset of viral membrane proteins. J. Virol. 85, 12431 – 12441.

Maruri-Avidal, L., Weisberg, A. S., Moss, B., 2013b: Direct formation of vaccinia virus membranes from the endoplasmic reticulum in the absence of the newly characterized L2-interacting protein A30.5. J. Virol. 87, 12313 – 12326.

Matsui, K., Kumagai, Y., Kato, H., Sato, S., Kawagoe, T., Uematsu, S., Takeuchi, O., Akira, S., 2006: Cutting edge: Role of TANK-binding kinase 1 and inducible IkappaB kinase in IFN responses against viruses in innate immune cells. J. Immunol. 177, 5785 – 5789.

Maylan, E., Burns, K., Hofmann, K., Blancheteau, V., Martinon, F., Kelliher, M., Tschopp, J., 2004. RIP1 is an essential mediator of Toll-like receptor 3-induced NF-kappa B activation. Nat. Immunol. 5, 503 – 507.

McConkey, S. J., Reece, W. H., Moorthy, V. S., Webster, D., Dunachie, S., Butcher, G., Vuola, J. M., Blanchard, T. J., Gothard, P., Watkins, K., Hannan, C. M., Everaere, S., Brown, K., Kester, K. E., Cummings, J., Williams, J., Heppner, D. G., Pathan, A., Flanagan, K., Arulanantham, N., Roberts, M. T., Roy, M., Smith, G. L., Schneider, J., Peto, T., Sinden, R. E., Gilbert, S. C., Hill, A. V., 2003: Enhanced T-cell immunogenicity of plasmid DNA vaccines boosted by recombinant modified vaccinia virus Ankara in humans. Nat. Med. 9, 729 – 735.

McCraith, S., Holtzman, T., Moss, B., Fields, S., 2000: Genome-wide analysis of vaccinia virus protein-protein interactions. Proc. Natl. Acad. Sci. U. S. A. 97, 4879 – 4884.

McDonald, W. F., Klemperer, N., Traktman, P., 1997: Characterization of a processive form of the vaccinia virus DNA polymerase. Virology 234, 168 – 175.

McDonald, W. F., Traktman, P., 1994a: Overexpression and purification of the vaccinia virus DNA polymerase. Protein Expr. Purif. 5, 409 – 421.

McDonald, W. F., Traktman, P., 1994b: Vaccinia virus DNA polymerase. In vitro analysis of parameters affecting processivity. J. Biol. Chem. 269, 31190 – 31197.

McGettrick, A. F., Brint, E. K., Palsson-McDermott, E. M., Rowe, D. C., Golenbock, D: T., Gay, N. J., Fitzgerald, K. A., O'Neill, L. A., 2006: Trif-related adapter molecule is phosphorylated by PKCε during Toll-like receptor 4 signaling. PNAS 103, 9196 – 9201.

McNulty, S., Bornmann, W., Schriewer, J., Werner, C., Smith, S. K., Olson, V. A., Damon, I. K., Buller, R. M., Heuser, J., Kalma, D., 2010: Multiple phosphatidylinositol 3-kinases regulate vaccinia virus morphogenesis. PLoS One 5: e10884.

McShane, H., Pathan, A. A., Sander, C. R., Keating, S. M., Gilbert, S. C., Huygen, K., Fletcher, H. A., Hill, A. V. S., 2004: Recombinant modified vaccinia virus Ankara expressing antigen 85A boosts BCG-primed and naturally acquired antimycobacterial immunity in humans. Nat. Med. 10, 1240 – 1244.

Melchjorsen, J., Jensen, S. B., Malmgaard, L., Rasmussen, S. B., Weber, F., Bowie, A. G., Matikainen, S., Paludan, S. R., 2005: Activation of innate defense against a paramyxovirus is mediated by RIG-I and TLR7 and TLR8 in a cell-type specific manner. J. Virol. 79, 12944 – 12951.

Mercer, J., Helenius, A., 2009: Virus entry by macropinocytosis. Nat. Cell Biol. 11: 510 – 520.

Mercer, J., Helenius, A., 2010: Apoptotic mimicry: phosphatidylserine-mediated macropinocytosis of vaccinia virus. Ann. N. Y. Acad. Sci. 1209, 49 – 55.

Merchlinsky, M., 1990: Mutational analysis of the resolution sequence of vaccinia virus DNA: essential sequence consists of two separate AT-rich regions highly conserved among poxviruses. J. Virol. 64, 5029 – 5035.

Metz, D. H., Esteban, M., Danielescu, G., 1975: The formation of virus polyribosomes in L cells infected with vaccinia virus. J. Gen. Virol. 27, 181 – 195.

Meylan, E., Curran, J., Hormann, K., Moradpour, D., Binder, M., Bartenschlager, R:, Tschopp, J., 2005: Cardif is an adaptor protein in the RIG-I antiviral pathway and is targeted by hepatitis C virus. Nature 437, 1167 – 1172.

Miguel, R: N., Wong, J., Westoll, J. F., Brooks, H. J., O'Neill, L. A: J., Gay, N. J., Bryant, C. E., Monie, T. P., 2007: A dimer of the Toll-like receptor 4 cytoplasmic domain provides a specific scaffold for the recruitment of signalling adaptor proteins. PLoS One 2: e788.

Millns, A. K., Carpenter, M. S., DeLange, A. M., 1994: The vaccinia virus-encoded uracil DNA glycosylase has an essential role in viral DNA replication. Virology 198, 504 – 513.

Montanuy, I., Alejo, A., Alcamí, A., 2011: Glycosaminoglycans mediate retention of the poxvirus type I interferon binding protein at the cell surface to locally block interferon antiviral responses. FASEB J. 25, 1960 – 1971.

Moore, K. W., de Waal Malefyt, R., Coffman, R. L., O'Garra, A., 2001: Interleukin-10 and the interleukin-10 receptor. Annu Rev. Immunol. 19: 683 – 765.

Moretti, S., Armougom, F., Wallace, I. M., Higgins, D. G., Jongeneel, C. V., Notredame, C., 2007: The M-Coffee web server: a meta-method for computing multiple sequence alignments by combining alternative alignment methods. Nucleic Acids Res. 35: W645 – 648.

Morgan, J. R., Cohen, L. K., Roberts, B. E., 1984: Identification of the DNA sequences encoding the large subunit of the mRNA-capping enzyme of vaccinia virus. J. Virol. 52, 206 – 214.

Mori, N., Prager, D., 1996: Transactivation of the interleukin-1alpha promoter by human T-cell leukemia virus type I and type II Tax proteins. Blood 87, 3410 – 3417.

Moss, B., 2001: Poxviridae: the viruses and their replication. In: Fields Virology, 4th edn., p. 2905 – 2975. Edited by D. M. Knipe & P. M. Howley. Philadelphia, PA: Lippincott Williams & Wilkins.

Moss, B., 2006: Poxvirus entry and membrane fusion. Virology 344, 48 – 54.

Moss, B., Smith, G. L., Gerin, J. L., Purcell, R. H., 1984: Live recombinant vaccinia virus protects chimpanzees against hepatitis B. Nature 311, 67 – 69.

Mulryan, K., Ryan, M. G., Myers, K. A., Shaw, D., Wang, W., Kingsman, S. M., Stern, P. L., Carroll, M. W., 2002: Attenuated recombinant vaccinia virus expressing oncofetal antigen (tumor-associated antigen) 5T4 induces active therapy of established tumors. Mol. Cancer Ther. 1, 1129 – 1137.

Munyon, W., Paoletti, E., Grace, Jr., J. T., 1967: RNA polymerase activity in purified infectious vaccinia virus. Proc. Natl. Acad. Sci. U. S. A. 58, 2280 – 2287.

Nafez, S., Oikawa, K., Odero, G. L., Sproule, M., Ge, N., Schapansky, J., Abrenica, B., Hatherell, A., Cadonic, C., Zhang, S., Song, X., Kauppinen, T., Glazner, G. W., Grilli, M., Czubryt, M. P., Eisenstat, D. D., Albensi, B. C., 2014: Early growth response 2 (Egr-2) expression is triggered by NF-κB activation. Mol. Cell. Neurosci. 64C, 95 – 103.

Negri, A., 1906: Über Filtration des Vaccinevirus. Zeitschrift für Hygiene und Infektionskrankheiten 54, 327 – 346.

Nevins, J. R., Joklik, W. K., 1977a: Isolation and properties of the vaccinia virus DNA-dependent RNA polymerase. J. Biol. Chem. 252, 6930 – 6983.

Nevins, J. R., Joklik, W. K., 1977b: Isolation and partial characterization of the poly(A) polymerases from HeLa cells infected with vaccinia virus. J. Biol. Chem. 252, 6939 – 6947.

Niles, E. G., Lee-Chen, G. J., Shuman, S., Moss, B., Broyles, S. S., 1989: Vaccinia virus gene D12L encodes the small subunit of the viral mRNA capping enzyme. Virology 172, 513 – 522.

Notredame, C., Higgins, D. G., Heringa, J., 2000: T-Coffee: A novel method for fast and accurate multiple sequence alignment. J. Mol. Biol. 302, 205 – 217.

Oda, S.-i., Franklin, E:, Khan, A. R., 2011: Poxvirus A46 protein binds to TIR domain-containing Mal/TIRAP via an α-helical sub-domain. Mol. Immunol. 48, 2144 – 2150.

Oganesyan, G., Saha, S. K., Guo, B., He, J. Q., Shahangian, A., Zarnegar, B., Perry, A., Cheng, G., 2006: Critical role of TRAF3 in the Toll-like receptor-dependent and –independent antiviral response. Nature 439, 208 – 211.

Ohnishi, H., Tochio, H., Kato, Z., Orii, K. E., Li, A., Kimura, T., Hiroaki, H., Kondo, N., Shirakawa, M., 2009: Structural basis for the multiple interactions of the MyD88 TIR domain in TLR4 signaling. Proc. Natl. Acad. Sci. U. S. A. 106, 10260 – 10265.

Ojeda, S., Senkevich, T. G., Moss, B., 2006: Entry of vaccinia virus and cell-cell fusion require a highly conserved cysteine-rich membrane protein encoded by the A16L Gene. J. Virol. 80, 51 – 61.

Oshiumi, H., Matsumoto, M., Funami, K., Akazawa, T., Seya, T., 2003: TICAM-1, an adaptor molecole that participates in Toll-like receptor 3-mediated interferon-beta induction. Nat. Immunol. 4, 161 – 167.

Ozinsky, A., Underhill, D. M., Fontenot, J. D., Hajjar, A. M., Smith, K. D., Wilson, C. B., Schroeder, L., Aderem, A., 2000: The repertoire for pattern recognition of pathogens by the innate immune system is defined by cooperation between toll-like receptors. Proc. Natl. Acad. Sci. U. S. A. 97, 13766 – 13771.

Paoletti, E., Lipinskas, B. R., Samsonoff, C., Mercer, S., Panicali, D., 1984: Construction of live vaccines using genetically engineered poxviruses: biological activity of vaccinia virus recombinants expressing the hepatatis B virus surface antigen and the herpes simplex virus glycoprotein D. Proc. Natl. Acad. Sci. U. S. A. 81, 193 – 197.

Paran, N., De Silva, F. S., Senkevich, T. G., Moss, B., 2009: Cellular DNA ligase I is recruited to cytoplasmic vaccinia virus factories and masks the role of the vaccinia ligase in viral DNA replication. Cell Host Microbe 6, 563 – 569.

Passarelli, A. L., Kovacs, G. R., Moss, B., 1996: Transcription of a vaccinia virus late promoter template: requirement for the product of the A2L intermediate-stage gene. J. Virol. 70, 4444- 4450.

Patel, D. D., Pickup, D. J., 1989: The second-largest subunit of the poxvirus RNA polymerase is similar to the corresponding subunits of prokaryotic and eukaryotic RNA polymerases. J. Virol. 63, 1076 – 1086.

Payne, L. G., 1979: Identification of the vaccinia hemagglutinin polypeptide from a cell system yielding large amounts of extracellular enveloped virus. J. Virol. 31, 147 – 155.

Payne, L. G., 1980: Significance of extracellular enveloped virus in the in vitro and *in vivo* dissemination of vaccinia. J. gen. Virol. 50, 89 – 100.

Payne, L. G., Kristenson, K., 1979: Mechanism of vaccinia virus release and its specific inhibition by N_1-isonicotinoyl-N_2-3-methyl-4-chlorobenzoylhydrazine. J. Virol. 32, 614 – 622.

Payne, L. G., Norrby, E., 1976: Presence of haemagglutinin in the envelope of extracellular vaccinia virus particles. J. Gen. Virol. 32, 63 – 72.

Peters, R. T., Liao, S.-M., L., Maniatis, T., 2000: IKKε is part of a novel PMA-inducible IκB kinase complex. Mol. Cell 5, 513 – 522.

Pichlmair, A., Schulz, O., Tan, C. P., Näslund, T. I., Liljeström, P., Weber, F., Reis e Sousa, C., 2006: RIG-I-mediated antiviral responses to single-stranded RNA bearing 5'-phosphates. Science 314, 997 – 1001.

Platanias, L. C., 2005: Mechanisms of type-I- and type-II-interferon-mediated signaling. Nat. Rev. Immunol. 5, 375 – 386.

Poltorak, A., He, X., Smirnova, I., Liu, M. Y., van Huffel, C., Du, X., Birdwell, D., Alejos, E., Silva, M., Galanos, C., Freudenberg, M., Ricciardi-Castagnoli, P., Layton, B., Beutler, B., 1998a: Defective LPS signaling in C3H/HeJ and C57BL/10ScCr mice: mutations in Tlr4 gene. Science 282, 2085 – 2088.

Poltorak, A., Smirnova, I., He, X., Liu, M. Y., van Huffel, C., McNally, O., Birdwell, D., Alejos, E., Silva, M., Du, X., Thompson, P., Chan, E. K., Ledesma, J., Roe, B., Clifton, S., Vogel, S. N., Beutler, B., 1998b: Genetic and physical mapping of the Lps locus: identification of the toll-4 receptor as a candidate gene in the critical region. Blood Cells Mol. Dis. 24, 340 – 355.

Quick, S. D., Broyles, S. S., 1990: Vaccinia virus gene D7R encodes a 20,000 dalton subunit of the viral DNA-dependent RNA polymerase. Virology 178, 603 – 605.

Rebouillat, D., Hovnanian, A., Marié, I., Hovanessian, A. G., 1999: The 100-kDa 2',5'-oligoadenylate synthetase catalyzing preferentially the synthesis of dimeric pppA2'p5'A molecules is composed of three homologous domains. J. Biol. Chem. 274, 1557 – 1565.

Rempel, R. E., Anderson, M. K., Evans, E., Traktman, P., 1990: Temperature-sensitive vaccinia virus mutants identify a gene with an essential role in viral replication. J. Virol. 64, 574 – 583.

Rempel, R. E., Traktman, P., 1992: Vaccinia virus B1 kinase: phenotypic analysis of temperature-sensitive mutants and enzymatic characterization of recombinant proteins. J. Virol. 66, 4413 – 4426.

Resch, W., Hixson, K. K., Moore, R. J., Lipton, M. S., Moss, B., 2007: Protein composition of the vaccinia virus mature virion. Virology 358, 233 – 247.

Riedel, S., 2005: Edward Jenner and the history of smallpox and vaccination. Proc. (Bayl. Univ. Med. Cent.) 18, 21 – 25.

Rietdorf, J., Ploubidou, A., Reckmann, I., Holmström, A., Frischknecht, F., Zettl, M., Zimmermann, T., Way, M., 2001: Kinesin-dependent movement on microtubules precedes actin-based motility of vaccinia virus. Nat. Cell. Biol. 3, 992 – 1000.

Roberts, W. K., Hovanessian, A., Brown, R. E., Clemens, M. J., Kerr, I. M., 1976: Interferon-mediated protein kinase and low-molecular-weight inhibitor of protein synthesis. Nature 264, 477 – 480.

Rochester, S. C., Traktman, P., 1998: Characterization of the single-stranded DNA binding protein encoded by the vaccinia I3 gene. J. Virol. 72, 2917 – 2926.

Ronni, T., Agarwal, V., Haykinson, M., Haberland, M. E., Cheng, G., Smale, S. T., 2003: Common interaction surfaces of the Toll-like receptor 4 cytoplasmic domain stimulate multiple nuclear targets. Mol. Cell. Biol. 23, 2543 – 2555.

Roper, R. L., Payne, L. G., Moss, B., 1996: Extracellular vaccinia virus envelope glycoprotein encoded by the A33R gene. J. Virol. 70, 3753 – 3762.

Rosales, R., Harris, N., Ahn, B. Y., Moss, B., 1994a: Purification and identification of a vaccinia virus-encoded intermediate stage promoter-specific transcription factor that has homology to eukaryotic transcription factor SII (TFIIS) and an additional role as a viral RNA polymerase subunit. J. Biol. Chem. 269, 14260 – 14267.

Rosales, R., Sutter, G., Moss, B., 1994b: A cellular factor is required for transcription of vaccinia viral intermediate-stage genes. Proc. Natl. Acad. Sci. U. S. A. 91, 3794 – 3798.

Rosano, G. L., Ceccarelli, E. A., 2014: Recombinant protein expression in Escherichia coli: advances and challenges. Front. Microbiol. 5: 172.

Saha, S. K., Pietras, E. M., He, J. Q., Kang, J. R., Liu, S. Y., Oganesyan, G., Shahangian, A., Zarnegar, B., Shiba, T. L., Wang, Y., Cheng, G., 2006: Regulation of antiviral responses by a direct and specific interaction between TRAF3 and Cardif. EMBO J. 25, 3257 – 3263.

Samuel, C. E., Duncan, R., Knutson, G. S., Hershey, J. W., 1984: Mechanism of interferon action. Increased phosphorylation of protein synthesis initiation factor eIF-2 alpha in interferon-treated, reovirus-infected mouse L929 fibroblasts in vitro and in vivo. J. Biol. Chem. 259, 13451 – 13457.

Sanderson, C. M., Hollinshead, M., Smith, G. L., 2000: The vaccinia virus A27L protein is needed for the microtubule-dependent transport of intracellular mature virus particles. J. Gen. Virol. 81, 47 – 58.

Sanz, P., Moss, B., 1998: A new vaccinia virus intermediate transcription factor. J. Virol. 72, 6880 – 6883.

Sato, S., Sugiyama, M., Yamamoto, M., Watanabe, Y., Kawai, T., Takeda, K., Akira, S., 2003: Toll/IL-1 receptor domain-containing adaptor inducing IFN-beta (TRIF) associates with TNF receptor-associated factor 6 and TANK-binding kinase 1, and activates two distinct transcription factors, NF-kappa B and IFN-regulatory factor-3, in the Toll-like receptor signalling. J. Immunol. 171, 4304 – 4310.

Saunders, M. E., Gewert, D. R., Tugwell, M. E., McMahon, M., Williams, B. R., 1985: Human 2-5A synthetase: characterization of a novel cDNA and corresponding gene structure. EMBO J. 4, 1761 – 1768.

Schmelz, M., Sodeik, B., Ericsson, M., Wolffe, E. J., Shida, H., Hiller, G., Griffiths, G., 1994: Assembly of vaccinia virus: the second wrapping cisterna is derived from the trans Golgi network. J. Virol. 68, 130 – 147.

Schmidt, F. I., Bleck, C. K., Helenius, A., Mercer, J., 2011: Vaccinia extracellular virions enter cells by macropinocytosis and acid-activated membrane rupture. EMBO J., 30, 3647 – 3661.

Schnierle, B. S., Gershon, P. D., Moss, B., 1992: Cap-specific mRNA (nucleoside-O2'-)-methyltransferase and poly(A) polymerase stimulatory activities of vaccinia virus are mediated by a single protein. Proc. Natl. Acad. Sci. U. S. A. 89, 2897 – 2910.

Schröder, M., Baran, M., Bowie, A. G., 2008: Viral targeting of DEAD box protein 3 reveals its role in TBK1/IKKepsilon-mediated IRF activation. EMBO J. 27, 2147 – 2157.

Seet, B. T., Johnston, J. B., Brunetti, C. R., Barrett, J. W., Everett, H., Cameron, C., Sypula, J., Nazarian, S. H., Lucas, A., McFadden, G., 2003: Poxviruses and immune evasion. Annu. Rev. Immunol. 21, 377 – 423.

Sen, G. C., Lengyel, P., 1992: The interferon system. A bird's eye view of its biochemistry. J. Biol. Chem. 267, 5017 – 5020.

Senkevich, T. G., Moss, B., 2005: Vaccinia virus H2 protein is an essential component of a complex involved in virus entry and cell-cell fusion. J. Virol. 79, 4744 – 4754.

Senkevich, T. G., Ojeda, S., Townsley, A., Nelson, G. E., Moss, B., 2005: Poxvirus multiprotein entry-fusion complex. PNAS 102, 18572 – 18577.

Senkevich, T. G., Ward, B. M., Moss, B., 2004: Vaccinia virus entry into cells is dependent on a virion surface protein encoded by the A28L gene. J. Virol. 78, 2357 – 2366.

Seth, R. B., Sun, L., Ea, C. K., Chen, Z. J., 2005: Identification and characterization of MAVS, a mitochondrial antiviral signaling protein that activates NF-kappaB and IRF 3. Cell 122, 669 – 682.

Sharma, S., tenOever, B. R., Grandvaux, N., Zhou, G. P., Lin, R., Hiscott, J., 2003: Triggering the interferon antiviral response through an IKK-related pathway. Science 300, 1148 – 1151.

Shimada, T., Kawai, T., Takeda, K., Matsumoto, M., Inoue, J.-i., Tatsumi, Y., Kanamaru, A., Akira, S., 1999: IKK-ι, a novel lipopolysaccharide-inducible kinase that is related to IκB kinases. Int. Immunol. 11, 1357 – 1362.

Shinohara, M.L., Lu, L., Bu, J., Werneck, M. B., Kobayashi, K. S:, Glimcher, L. H., Cantor, H., 2006: Osteopontin expression is essential for interferon-alpha production by plasmacytoid dendritic cells. Nat. Immunol. 7, 498 – 506.

Shitbeck, J. C., Foo, C. H., Ponce de Leon, M., Eisenberg, R. J., Cohen, G. H., 2009: Vaccinia virus exhibits cell-type-dependent entry characteristics. Virology 385, 383 – 391.

Sica, A., Dorman, L., Viggiano, V., Cippitelli, M., Ghosh, P., Rice, N., Young, H. A., 1997: Interaction of NF-kappaB and NFAT with the interferon-gamma promoter. J. Biol. Chem. 272, 30412 – 30420.

Silva, A. M., Whitmore, M., Xu, Z., Jiang, Z., Li, X., Williams, B. R. G., 2004: Protein kinase R (PKR) interacts with and activates mitogen-activated protein kinase kinase 6 (MKK6) in response to double-stranded RNA stimulation. J. Biol. Chem. 279, 37670 – 37676.

Silvennoinen, O., Ihle, J. N., Schlessinger, J., Levy, D. E., 1993: Interferon-induced nuclear signalling by Jak protein tyrosine kinases. Nature 366, 583 – 585.

Smith, G. L., Godson, G. N., Nussenzweig, V., Nussenzweig, R. S., Barnwell, J., Moss, B., 1984: Plasmodium knowlesi sporozoite antigen: expression by infectious recombinant vaccinia virus. Science 224, 397 – 399.

Smith, G. L., Mackett, M., Moss, B., 1983a: Infectious vaccinia virus recombinants that express hepatitis B virus surface antigen. Nature 302, 490 – 495.

Smith, G. L., Murphy, B. R., Moss, B., 1983b: Construction and characterization of an infectious vaccinia virus recombinant that expresses the influenza hemagglutinin gene and induces resistance to influenza virus infection in hamsters. Proc. Natl. Acad. Sci. U. S. A. 80, 7155 – 7159.

Sodeik, B., Doms, R. W., Ericsson, M., Hiller, G., Machamer, C. E., van`t Hof, W. van Meer, G., Moss, B., Griffiths, G., 1993: Assembly of vaccinia virus: role of the intermediate compartment between the endoplasmic reticulum and the Golgi stacks.

Son, Y. H., Jeong, Y. T., Lee, K. A., Choi, K. H., Kim, S. M., Rhim, B. Y., Kim, K., 2008: Roles of MAPK and NF-kappaB in interleukin-6 induction by lipopolysaccharide in vascular smooth muscle cells. J. Cardiovasc. Pharacol. 51, 71 – 77.

Spencer, E., Shuman, S., Hurwitz, J., 1980: Purification and properties of vaccinia virus DNA-dependent RNA polymerase. J. Biol. Chem. 255, 5388 – 5395.

Stack, J., Bowie, A. G., 2012: Poxviral protein A46 antagonizes Toll-like receptor 4 signaling by targeting BB loop motifs in Toll-IL-1 receptor adaptor proteins to disrupt receptor:adaptor interactions. J. Biol. Chem. 287, 22672 – 22682.

Stack, J., Haga, I. R., Schröder, M., Bartlett, N. W., Maloney, G., Reading, P. C., Fitzgerald, K. A., Smith, G. L., Bowie, A. G., 2005: Vaccinia virus protein A46R targets multiple Toll-like-interleukin-1 receptor adaptors and contributes to virulence. J. Exp. Med. 201, 1007 – 1018.

Stack, J., Hurst, T. P., Flannery, S. M., Brennan, K., Rupp, S., Oda, S.-i. Khan, A. R., Bowie, A. G., 2013: Poxviral protein A52 stimulates p38 mitogen-activated protein kinase (MAPK) activation by causing tumor necrosis factor receptor-associated factor 6 (TRAF6) self-association leading to transforming growth factor β-activated kinase 1 (TAK1) recruitment. J. Biol. Chem. 288, 33642 – 33653.

Stanitsa, E. S., Arps, L., Traktman, P., 2006: Vaccinia virus uracil DNA glycosylase interacts with the A20 protein to form a heterodimeric processivity factor for the viral DNA polymerase. J. Biol. Chem. 281, 3439 – 3451.

Steward, R., 1987: Dorsal, an embryonic polarity gene in Drosophila, is homologous to the vertebrate-oncogene, c-rel. Science 238, 692 – 694.

Sutter, G., Moss, B., 1992: Nonreplicating vaccinia vector efficiently expresses recombinant genes. Proc. Natl. Acad. Sci. U. S. A. 89, 10847 – 10851.

Symons, J. A., Alcamí, A., Smith, G. L., 1995: Vaccinia virus encodes a soluble type I interferon receptor of novel structure and broad species specificity. Cell 81, 551 – 560.

Szajner, P., Jaffe, H., Weisberg, A. S., Moss, B., 2003: Vaccinia virus G7L protein interacts with the A30L protein and is required for association of viral membranes with dense viroplasm to form immature virions. J. Virol. 77, 3418 – 3429.

Szajner, P., Jaffe, H., Weisberg, A. S., Moss, B., 2004a: A complex of seven vaccinia virus proteins conserved in all chordopoxviruses is required for the association of membranes and viroplasm to form immature virions. Virology 330, 447 – 459.

Szajner, P., Weisberg, A. S., Lebowitz, J., Heuser, J., Moss, B., 2005: External scaffold of spherical immature poxvirus particles is made of protein trimers, forming a honeycomb lattice. J. Cell. Biol. 170, 971 – 981.

Szajner, P., Weisberg, A. S., Moss, B., 2004b: Evidence for an essential catalytic role of the F10 protein kinase in vaccinia virus morphogenesis. J. Virol. 78, 257 – 265.

Szajner, P., Weisberg, A. S., Moss, B., 2004c: Physical and functional interactions between vaccinia virus F10 protein kinase and virion assembly proteins A30 and G7. J. Virol. 78, 266 – 274.

Takeuchi, O., Hoshino, K., Kawai, T., Sanjo, H., Takada, H., Ogawa, T., Takeda, K., Akira, S., 1999: Differential roles of TLR2 and TLR4 in recognition of gram-negative and gram-positive bacterial cell wall components. Immunity 11, 443 – 451.

Takeuchi, O., Kawai, T., Mühlradt, P. F., Morr, M., Radolf, J. D., Zychlinsky, A., Takeda, K., Akira, S., 2001: Discrimination of bacterial lipoproteins by Toll-like receptor 6. Int. Immunol. 13, 933 – 9340.

Tartaglia, J., Perkus, M. E., Taylor, J., Norton, E. K., Audonnet, J. C., Cox, W. I., Davis, S. W., van der Hoeven, J., Meignier, B., Riviere, M., et al., 1992: NYVAC: a highly attenuated strain of vaccinia virus. Virology 188, 217 – 232.

Teale, A., Campbell, S., Van Buuren, N., Magee, W. C., Watmough, K., Couturier, B., Shipclark, R., Barry, M., 2009: Orthopoxviruses require a functional ubiquitin-proteasome system for productive replication.

Thiel, D. J., le Du, M.-H., Walter, R. L., D'Arcy, A., Chéne, C., Fountoulakis, M., Garotta, G., Winkler, F. K., Ealick, S. E., 2000: Observation of an unexpected third receptor molecule in the crystal structure of human interferon-γ receptor complex. Structure 8, 927 – 936.

Tolonen, N., Doglio, L., Schleich, S., Krijnse Locker, J., 2001: Vaccinia virus DNA replication occurs in endoplasmic reticulum-enclosed cytoplasmic mini-nuclei. Mol. Biol. Cell. 12, 2031 – 2046.

Tooze, J., Hollinshead, M., Reis, B., Radsak, K., Kern, H., 1993: Progeny vaccinia and human cytomegalovirus particles utilize early endosomal cisternae for their envelopes. Eur. J. Cell Biol. 60, 163 – 178

Townsley, A. C., Moss, B., 2007: Two distinct low-pH steps promote entry of vaccinia virus. J. Virol. 81, 8613 – 8620.

Townsley, A. C., Senkevich, T. G., Moss, B., 2005a: The product of the vaccinia virus L5R gene is a fourth membrane protein encoded by all poxviruses that is required for cell entry and cell-cell fusion. J. Virol. 79, 10988 – 10998.

Townsley, A. C., Senkevich, T. G., Moss, B., 2005b: Vaccinia virus A21 virion membrane protein is required for cell entry and fusion. J. Virol. 79, 9458 – 9469.

Townsley, A. C., Weisberg, A. S., Wagenaar, T. R., Moss, B., 2006: Vaccinia virus entry into cells via low-pH-dependent endosomal pathway. J. Virol. 80, 8899 – 8908.

Traktman, P., Anderson, M. K., Rempel, R. E., 1989: Vaccinia virus encodes an essential gene with strong homology to protein kinases. J. Biol. Chem. 264, 21458 – 21461.

Traktman, P., Caligiuri, A., Jesty, S. A., Liu, K., 1995: Temperature-sensitive mutants with lesions in the vaccinia virus F10 kinase undergo arrest at the earliest stage of virion morphogenesis. J. Virol. 69, 6581 – 6587.

Traktman, P., Sridhar, P., Condit, R. C., Roberts, B. E., 1984: Transcriptional mapping of the DNA polymerase gene of vaccinia virus. J. Virol. 49, 125 – 131.

Tsujimura, H., Tamura, T., Kong, H. J., Nishiyama, A., Ishii, K. J., Klinman, D. M., Ozato, K., 2004: Toll-like receptor 9 signaling activates NF-kappaB through IFN regulatory factor 8/IFN consensus sequence binding protein in dendritic cells. J. Immunol. 172, 6820 – 6827.

Turner, G. S., Squires, E. J., 1971: Inactivated smallpox vaccine: immunogenicity of inactivated intracellular and extracellular vaccinia virus. J. Gen. Virol. 13, 19 – 25.

Turner, P. C., Moyer, R. W., 2008: The vaccinia virus fusion inhibitor proteins SPI-3 (K2) and HA (A56) expressed by infected cells reduce the entry of superinfecting virus. Virology 380, 226 – 233.

Uematsu, S., Sato, S., Yamamato, M., Hirotani, T., Kato, H., Takeshita, F., Matsuda, M., Coban, C., Ishii, K. J., Kawai, T., Takeuchi, O., Akira, S., 2005: Interleukin-1 receptor-associated kinase-1 plays an essential role for Toll-like receptor (TLR)7- and TLR9-mediated interferon-α induction. J. Exp. Med. 201, 915 – 923.

Unterholzner, L., Sumner, R. P., Baran, M., Ren, H., Mansur, D. S., Bourke, N. M., Randow, F., Smith, G. L., Bowie, A. G., 2011: Vaccinia virus protein C6 is a virulence factor that binds TBK-1 adaptor proteins and inhibits activation of IRF3 and IRF7. PLoS Pathog. 7: e1002247.

Upton, C., Stuart, D. T., McFadden, 1993: Identification of a poxvirus gene encoding a uracil DNA glycosylase. Proc. Natl. Acad. Sci. U. S. A. 90, 4518 – 4522.

Uzé, G., Lutfalla, G., Gresser, I., 1990: Genetic transfer of a functional human interferon α receptor into mouse cells: Cloning and expression of its c-DNA. Cell 60, 225 – 234.

van Eijl, H., Hollinshead, M., Rodger, G., Zhang, W. H., Smith, G. L., 2002: The vaccinia virus F12L protein is associated with intracellular enveloped virus particles and is required for their egress to the cell surface. J. Gen. Virol. 83, 195 – 207.

Vanderplasschen, A., Hollinshead, M., Smith, G. L., 1998: Intracellular and extracellular vaccinia virions enter cells by different mechanisms. J. Gen. Virol. 79, 877 – 887.

Vanderplasschen, A., Smith, G. L., 1997: A novel virus binding assay using confocal microscopy: demonstration that the intracellular and extracellular vaccinia virions bind to different cellular receptors. J. Virol. 71, 4032 – 4041.

Vázquez, M. I., Esteban, M., 1999: Identification of functional domains in the 14-kilodalton envelope protein (A27L) of vaccinia virus. J. Virol. 73, 9098 – 9109.

Velazquez, L., Fellous, M., Stark, G. R., Pellegrini, S., 1992: A protein tyrosine kinase in the interferon α/β signaling pathway. Cell 70, 313 – 322.

Verardi, P. H., Titong, A., Hagen, C. J., 2012: A vaccinia virus renaissance: New vaccine and immunotherapeutic uses after smallpox eradication. Hum. Vaccin. Immunother. 8, 961 – 970.

Verstak, B., Arnot, C. J., Gay, N. J., 2013: An alanine-to-proline mutation in the BB-loop of TLR3 Toll/IL-1R domain switches signaling adaptor specificity from TRIF to MyD88. J. Immunol. 191, 6101 – 6109.

Vos, J. C., Sasker, M., Stunnenberg, H. G., 1991: Vaccinia virus capping enzyme is a transcription initiation factor. EMBO J. 10, 2553 – 2558.

Vos, J. C., Stunnenberg, H. G., 1988: Derepression of a novel class of vaccinia virus genes upon DNA replication. EMBO J. 7, 3487 – 3492.

Wagenaar, T. R., Moss, B., 2007: Association of vaccinia virus fusion regulatory proteins with the multicomponent entry/fusion complex. J. Virol. 81, 6286 – 6293.

Wagenaar, T. R., Moss, B., 2009: Expression of the A56 and K2 proteins is sufficient to inhibit vaccinia virus entry and cell fusion. J. Virol. 83, 1546 – 1554.

Wagenaar, T. R., Ojeda, S., Moss, B., 2008: Vaccinia virus A56/K2 fusion regulatory protein interacts with the A16 and G9 subunits of the entry fusion complex. J. Virol. 82, 5153 – 5160.

Wallace, I. M., O'Sullivan, O., Higgins, D. G., Notredame, C., 2006: M-Coffee: combining multiple sequence alignment methods with T-Coffee. Nucleic Acids Res. 34: 1692 – 1699.

Wang, S., Shuman, S., 1995: Vaccinia virus morphogenesis is blocked by temperature-sensitive mutations in the F10 gene, which encodes protein kinase 2. J. Virol. 69, 6376 – 6388.

Wang, T., Town, T., Alexopoulou, L., Anderson, J. F., Fikrig, E., Flavell, R. A., 2004: Toll-like receptor 3 mediates West Nile virus entry into the brain causing lethal encephalitis. Nat. Med. 10, 1366 – 1373.

Ward, B. M., Moss, B., 2001: Visualization of intracellular movement of vaccinia virus virions containing a green fluorescent protein-B5R membrane protein chimera. J. Vriol. 75, 4802 – 4813.

Wasilenko, S. T., Stewart, T. L., Meyers, A. F., Barry, M., 2003: Vaccinia virus encodes a previously uncharacterized mitochondrial-associated inhibitor of apoptosis. Proc. Natl. Acad. Sci. U. S. A. 100, 14345 – 14350.

Wathelet, M., Moutschen, S., Cravador, A., DeWit, L., Defilippi, P., Huez, G., Content, J., 1986: Full-length sequence and expression of the 42 kDa 2-5A synthetase induced by human interferon. FEBS Lett 196, 113 – 120.

Watling, D., Guschin, D., Müller, M., Silvennoinen, O., Witthuhn, B. A., Quelle, F. W., Rogers, N. C., Schindler, C., Stark, G. R., Ihle, J. N., et al. 1993: Complementation by the protein tyrosine kinase JAK2 of a mutant cell line defective in the interferon-γ signal transduction pathway. Nature 366, 166 – 170.

Wei, C. M., Moss, B., 1975: Methylated nucleotides block 5'-terminus of vaccinia virus messenger RNA. Proc. Natl. Acad. Sci. U. S. A. 72, 318 – 322.

Wesche, H., Henzel, W. J., Shillinglaw, W., Li, S., Cao, Z., 1997: MyD88: an adapter that recruits IRAK to the IL-1 receptor complex. Immunity 7, 837 – 847.

Williams, B. R. G., 2001: Signal integration via PKR. Sci. STKE 2001, re2

Willis, N. J., 1997: Edward Jenner and the eradication of smallpox. Scott. Med. J. 42, 118 . 21.

Wittek, R., Menna, A., Müller, H. K., Schümperli, D., Boseley, P. G., Wyler, R., 1978: Inverted terminal repeats in rabbit poxvirus and vaccinia virus DNA. J. Virol. 28, 171 – 181.

Woods, A. M., Wang, W. W., Shaw, D. M., Ward, C. M., Carroll, M. W., Rees, B. R., Stern, P. L., 2002: Characterization of the murine 5T4 oncofetal antigen: a target for immunotherapy in cancer.

World Health Organization: The global eradication of smallpox. Final report of the global commission for the certification of smallpox eradication. In: History of International Public Health No. 4. Geneva, World Health Organization, 1980.

Wright, C. F., Keck, J. G., Tsai, M. M., Moss, B., 1991: A transcription factor for expression of vaccinia virus late genes is encoded by an intermediate gene. J. Virol. 65, 3715 – 3720.

Wright, C. F., Oswald, B. W., Dellis, S., 2001: Vaccinia virus late transcription is activated in vitro by cellular heterogeneous nuclear ribonucleoproteins. J. Biol. Chem. 276, 40680 – 40686.

Wrigth, C. F., Coroneos, A. M., 1993: Purification of the late transcription system of vaccinia virus: identification of a novel transcription factor. J. Virol. 67, 7264 – 7270.

Xu, L. G., Wang, Y. Y:, Han, K. J., Li, L. Y., Zhai, Z., Shu, H. B., 2005: VISA is an adapter protein required for virus-triggered IFN-beta signaling. Mol. Cell 19, 727 – 740.

Xu, Y., Tao, X., Shen, B., Horng, T., Medzhitov, R., Manley, J. L., Tong, L., 2000: Structural basis for signal transduction by the Toll/interleukin-1 receptor domains. Nature 408, 111 – 115.

Yamamoto, M., Sato, S., Hemmi, H., Hoshino, K., Kaisho, T., Sanjo, H., Takeuchi, O., Sugiyama, M., Okabe, M., Takeda, K., Akira, S., 2003a: Role of adaptor TRIF in the MyD88-independent toll-like receptor signaling pathway. Science 301, 640 – 643.

Yamamoto, M., Sato, S., Hemmi, H., Sanjo, H., Uematsu, S., Kaisho, T., Hoshino, K., Takeuchi, O., Kobayashi, M., Fujita, T., Takeda, K., Akira, S., 2002a: Essential role for TIRAP in activation of the signalling cascade shared by TLR2 and TLR4. Nature 420, 324 – 329.

Yamamoto, M., Sato, S., Hemmi, H., Uematsu, S., Hoshino, K., Kaisho, T., Takeuchi, O., Takeda, K., Akira, S., 2003b: TRAM is specifically involved in the Toll-like receptor 4-mediated MyD88-independent signaling pathway. Nat. Immunol. 4, 1144 – 1150.

Yamamoto, M., Sato, S., Mori, K., Hoshino, K., Takeuchi, O., Takeda, K., Akira, S., 2002b: Cutting edge: a novel Toll/IL-1 receptor domain-containing adapter that preferentially activates IFN-beta promoter in the Toll-like receptor signalling. J. Immunol. 169, 6668 – 6672.

Yoneyama, M., Kikuchi, M., Natsukawa, T., Shinobu, N., Imaizumi, T., Miyagishi, M., Taira, K., Akira, S., Fujita, T., 2004: The RNA helicase RIG-I has an essential function in double-stranded RNA-induced innate antiviral responses. Nat. Immunol. 5, 730 – 737.

Yoneyama, M., Suhara, W., Fukuhara, Y., Fukuda, M., Nishida, E., Fujita, T., 1998: Direct triggering of the type I interferon system by virus infection: activation of a transcription factor complex containing IRF-3 and CBP/p300. EMBO J. 17, 1087 – 1095.

Zamanian-Daryoush, M., Mogensen, T. H., DiDonato, J. A., Williams, B. R. G., 2000: NF-κB activation by double-stranded-RNA-activated protein kinase (PKR) is mediated through NF-κB-inducing kinase and IκB kinase. Mol. Cell Biol. 20, 1278 – 1290.

Zhang, B., Li, M., Chen, L., Yang, K., Shan, Y., Zhu, L., Sun, S., Li, L., Wang, C., 2009: The TAK1-JNK cascade is required for IRF3 function in the innate immune response. Cell Res. 19, 412 – 428.

Zhang, Q., Tian, M., Feng, Y., Zhao, K., Xu, J., Liu, Y., Shao, Y., 2013: Genomic sequence and virulence of clonal isolates of vaccinia virus Tiantan, the Chinese smallpox vaccine strain. PLoS One 8: e60557.

Zhang, S. Y., Jouanguy, E., Ugolini, S., Smahi, A., Elain, G., Romero, P., Segal, D., Sancho-Shimizu, V., Lorenzo, L., Puel, A., Picard, C., Chapgier, A., Plancoulaine, S., Titeux, M., Cognet, C., von Bernuth, H., Ku, C. L., Casrouge, A., Zhang, X. X., Barriero, L., Leonard, J., Hamilton, C., Lebon, P., Héron, B., Vallée, L., Quintana-Murcí, L., Hovnanian, A., Rozenberg, F., Vivier, E., Geissmann, F., Tardieu, M., Abel, L., Casanova, J. L., 2007: TLR3 deficiency in patients with herpes simplex encephalitis. Science 317, 1522 – 1527.

Zhang, Y., Keck, J. G., Moss, B., 1992: Transcription of viral late genes is dependent on expression of the viral intermediate gene G8R in cells infected with an inducible conditional-lethal mutant vaccinia virus. J. Virol. 66, 6470 – 6479.

Zhu, Y. X., Kang, L. Y., Luo, W., Li, C. C., Yang, L., Yang, Y. C., 1996: Multiple transcription factors are required for activation of human interleukin 9 gene in T cells. J. Biol. Chem. 271, 15815 – 15822.

Zilberstein, A., Kimchi, A., Schmidt, A., Revel, M., 1978: Isolation of two interferon-induced translational inhibitors: a protein kinase and an oligo-isoadenylate synthetase. Proc. Natl. Acad. Sci. U. S. A. 75, 4734 – 4738.

Curriculum Vitae

Katharina Radakovics

Education

Oct. 2012 – present	Master Molecular Microbiology and Immunobiology University of Vienna
Oct. 2009 – Jun. 2012	Bachelor Biology University of Vienna
Sep. 2001 – Jun. 2009	High School Aufbau- und Realgymnasium Hollabrunn

Work Experience

Jan. 2014 – Dec. 2014	Master thesis Max F. Perutz Laboratories, Vienna (Group Prof. Skern)
Sep. 2013 – Dec. 2013	Internship University of Bristol, Bristol (Group Dr. Morgan)
Jul. 2012 – Sep. 2012	Internship Novartis Institutes of Biomedical Research, Basel (Group Dr. Billich) ´
Jul. 2008	GEN-AU SummerSchool Institute of Molecular Biotechnology Austria (Group J. A. Pospisili

Language Skills

Mother tongue	German
Other languages	English, fluent

Scientific Skills

Molecular biologic techniques

PCR, electrophoresis, transformation, protein expression and purification (ÄKTA FPLC), protein-protein interaction studies (Microscale Thermophoresis), cell culture (RAW264.7), isolation of neutrophils, ELISA

Presenting scientific data

Participation in the poster session of the symposium *Crossing Frontiers in Life Sciences*

Explaining complex topics

Tutoring of school children (in chemistry and math), supervision of trainees

Lebenslauf

Katharina Radakovics

Ausbildung

Seit Okt. 2012	Master Molekulare Mikrobiologie und Immunbiologie Universität Wien
Okt. 2009 – Jun. 2012	Bachelor Biologie Universität Wien
Sep. 2001 – Jun. 2009	Allgemeinbildende Höhere Schule Aufbau- und Realgymnasium Hollabrunn

Berufserfahrung

Jan. 2014 – Dez. 2014	Masterarbeit Max F. Perutz Laboratories, Wien (Gruppe Prof. Skern)
Sep. 2013 – Dez. 2013	Auslandspraktikum University of Bristol, Bristol (Gruppe Dr. Morgan)
Jul. 2012 – Sep. 2012	Auslandspraktikum Novartis Institutes of Biomedical Research, Basel (Gruppe Dr. Billich)
Jul. 2008	GEN-AU SummerSchool Institute of Molecular Biotechnology Austria (Gruppe J. A. Pospisilik)

Sprachkenntnisse

Muttersprache	Deutsch
Weitere Sprachen	Englisch, fließend

Wissenschaftliche Fähigkeiten

Molekularbiologische Techniken

PCR, Elektrophorese, Transformation, Protein-Expression und –Aufreinigung (ÄKTA FPLC), Protein-Protein-Interaktionsstudien (Microscale Thermophoresis), Zellkulture (RAW264.7), Isolation von Neutrophilen, ELISA

Präsentation wissenschaftlicher Daten

Poster-Präsentation im Zuge des Symposiums *Crossing Frontiers in Life Sciences*

Erklärung komplexer Sachverhalte

Erfahrung als Nachhilfelehrerin (Chemie und Mathematik) und in der Betreuung von Laborpraktikanten